Check for updates

ADVANCED FUNCTIONAL MATERIALS
www.afm-journal.de

A Roadmap Review of Thermally Conductive Polymer Composites: Critical Factors, Progress, and Prospects

Zhengfang Wang, Zijian Wu, Ling Weng, Shengbo Ge,* Dawei Jiang, Mina Huang, Daniel M. Mulvihill, Qingguo Chen, Zhanhu Guo, Abdullatif Jazzar, Ximin He,* Xuehua Zhang, and Ben Bin Xu**

Recently, the need for miniaturization and high integration have steered a strong technical wave in developing (micro-)electronic devices. However, excessive amounts of heat may be generated during operation/charging, severely affecting device performance and leading to life/property loss. Benefiting from their low density, easy processing and low manufacturing cost, thermally conductive polymer composites have become a research hotspot to mitigate the disadvantage of excessive heat, with potential applications in 5G communication, electronic packaging and energy transmission. By far, the reported thermal conductivity coefficient (λ) of thermally conductive polymer composite is far from expectation. Deeper understanding of heat transfer mechanism is desired for developing next generation thermally conductive composites. This review holistically scopes current advances in this field, while giving special attention to critical factors that affect thermal conductivity in polymer composites as well as the thermal conduction mechanisms on how to enhance the λ value. This review covers critical factors such as interfacial thermal resistance, chain structure of polymer, intrinsic λ value of different thermally conductive fillers, orientation/configuration of nanoparticles, 3D interconnected networks, processing technology, etc. The applications of thermally conductive polymer composites in electronic devices are summarized. The existing problems are also discussed, new challenges and opportunities are prospected.

1. Introduction

With the arrival of 5G era, electronics achieve unprecedented developments in the direction of integration, miniaturization, and precision.[1–3] Due to the drastic reduction while maintaining high power density requirements, the increasing density of heat flow generated in these devices often leads to more and more prominent heat dissipation problems.[4–6] If this heat cannot bedischarged in time, the reliability and stability of electronic devices during operation will be negatively impacted, and their lifespan will also be seriously threatened.[7,8] Studies have shown that for an increase of every 2 °C, the performance of electronic devices decreases by 10%.[9,10] To ensure the long-term, safe, and reliable operation of electronic devices, research and development of new thermally conductive materials has become a top priority for next-generation electronics.[11–13]

The heat transfer between the equipment and the heat sink plays a decisive role in the heat dissipation process. Introducing composite materials with highly thermal conductivity between the electronic components and the heat sink is critical to tackle these heat dissipation issues.[14] Thermal interface materials (TIMs) are materials used to dissipate and improve the transfer of heat out of electronics devices. Generally, the TIMs are placed between the heat-generating chip and/or component and the heat spreading substrate or dissipating device as shown in **Figure 1**.[15–18] TIMs can not only improve the interfacial thermal transfer, but also provide mechanical support and electromagnetic shielding.[19–21]

Z. Wang, Z. Wu, L. Weng, Q. Chen
Department of Material Science and Technology
Harbin University of Science and Technology
Harbin 150040, China
E-mail: zijian.wu@hrbust.edu.cn

Z. Wu, L. Weng, Q. Chen
Key Laboratory of Engineering Dielectric and Its Application Technology of Ministry of Education
Harbin University of Science and Technology
Harbin 150040, China

S. Ge
Jiangsu Co-Innovation Center of Efficient Processing and Utilization of Forest Resources
International Innovation Center for Forest Chemicals and Materials
College of Materials Science and Engineering
Nanjing Forestry University
Nanjing, Jiangsu 210037, China
E-mail: geshengbo@njfu.edu.cn

The ORCID identification number(s) for the author(s) of this article can be found under https://doi.org/10.1002/adfm.202301549

DOI: 10.1002/adfm.202301549

 © 2023 Wiley-VCH GmbH

The ideal characteristics of TIMs include low bond line thickness, high thermal conductivity, and low contact thermal resistance. Presently, TIMs are mainly polymer matrix composite because they are easy to prepare and inexpensive. In order to minimize the influence of thermally conductive particles on the properties of polymers, advanced polymeric-based TIMs can be prepared using a preconstructed thermally-conductive architecture to ensure a favorable-particle distribution and the formation of an interconnected network in the polymer matrix.[18,22–30] The electrical insulation, mechanical strength, long-term stability, and the flame resistance of TIMs also need to be considered for their practical applications.[31]

Benefiting from the merits of good flexibility, low density, excellent insulation, low cost, corrosion resistance, and ease of processing, polymer composites have been widely applied as thermal management materials in a variety of applications.[32–35] However, the intrinsic low λ value of polymer matrices due to their amorphous arrangement and vibrations of the molecular chains limits their application in thermal management to a certain extent.[36–39] For most polymers, phonon thermal conduction is the dominant thermal conduction pathway. As the amorphous structure and vibrations of the macromolecular chains in polymers can induce massive phonon scattering, the vast majority of neat polymers are heat insulators or relatively poor heat conductors (λ values of 0.1–0.5 W m^{-1} K^{-1}).[40–44]

Currently, two strategies have been implemented to enhance their thermal conduction capability: i) Improving the orientation and crystallinity of polymer chains by designing and changing the structures of molecules and chain links[45] and ii) compounding with thermally conductive fillers. Strategies i) and ii) are called the intrinsic thermally conductive polymers and filled thermally conductive polymers, respectively. Strategy i) is relatively complicated and time-consuming,[46,47] whereas strategy ii) is considered as a more efficient and convenient approach.[48,49]

Owing to the advantages of easy processing, low cost, and easy to industrialize, thermally conductive polymer composites have been widely used in industrial fields, including energy, electronic packaging, electrical equipment, and aerospace.[34,50–52] Nevertheless, the fundamental understanding of heat conduction and the macro/micro-regulation strategy of heat conduction remain relatively under-developed. Interfacial thermal resistance is the additional resistance to heat flow when the heat flows through the contact interface of two phases, and it plays a dominant role in the overall heat transport capacity of the composite.[53,54] The research on interfacial thermal resistance is mainly developed based on the continuous medium theory and atomic theory. The main ones developed based on the continuous medium theory include the acoustic mismatch model (AMM) and the diffusive mismatch model (DMM), which ignore the actual structure of atoms and are only applicable to the solid-solid interface at temperatures less than 30 K.[55] The theories developed based on atomic theory are derived from various simulations with full consideration of the microstructure of atoms, and mainly include Lattice dynamics, Green's function approach, Molecular dynamics simulation (subdivided into nonequilibrium molecular dynamics (NEMD) and equilibrium molecular dynamics (EMD) simulations), The Boltzmann transport equation and the Monte Carlo method.[56] Current techniques for measuring ITR mainly include steady-state measurements (including the traditional heater-sensor method and electron-beam self-heating method) and transient measurements (including differential 3 ω methods and pump-probe thermoreflectance technique).[57–59]

Various means have been applied to facilitate a high λ in polymer composite by reducing the interfacial thermal resistance, e.g., the synergistic effect between different fillers, surface functionalization of fillers, building a 3D interconnected framework structure, the orientation of thermal conductive fillers and the bonding-enhanced interfacial thermal transport. As heat conduction processes are influenced by multiple variables, depth understanding of the synergistic impact of multiple factors on the heat conduction process is significant for improving thermally conductive polymer composites. However, the comprehensive reviews of factors critical to thermal conductivity of polymer composites are relatively scarce.

Compared with previous related reviews, this review provides a comprehensive summary of the heat conduction mechanism of materials from the macroscopic to the microscopic level, which is beneficial to the reader for a deeper understanding of the internal thermal conductivity mechanism of materials. Second, the paper also provides comprehensive coverage of the factors affecting the λ value of polymer composites, which provides an effective reference for the preparation of composites with excellent thermal conductivity. The challenges and trends in the development of high thermal conductivity and electrical insulation materials are also scoped from more than 300 research papers in the past seven years, to profile the roadmap. The summary of thermally conductive fillers and the processing method of polymer composite are systematic and comprehensive, along with a few engineering applications. In addition, the latest research hotspots (e.g. the establishment of 3D thermal conductivity networks) are emphasized.

D. Jiang
Heilongjiang Key Laboratory of Molecular Design and Preparation of Flame Retarded Materials
Northeast Forestry University
Harbin 150040, China

M. Huang
College of Materials Science and Engineering
Taiyuan University of Science and Technology
Taiyuan 030024, China

D. M. Mulvihill
Materials and Manufacturing Research Group
James Watt School of Engineering
University of Glasgow
Glasgow G12 8QQ, UK

Z. Guo, B. B. Xu
Mechanical and Construction Engineering
Faculty of Engineering and Environment
Northumbria University
Newcastle Upon Tyne NE1 8ST, UK
E-mail: ben.xu@northumbria.ac.uk

A. Jazzar, X. He
Department of Materials Science and Engineering
University of California
Los Angeles (UCLA)
Los Angeles, CA 90095, USA
E-mail: ximinhe@ucla.edu

X. Zhang
Department of Chemical and Materials Engineering
University of Alberta
Edmonton, Alberta T6G 1H9, Canada

© 2023 Wiley-VCH GmbH

16163028, 0, Downloaded from https://onlinelibrary.wiley.com/doi/10.1002/adfm.202301549 by University of California - Los Ange, Wiley Online Library on [16/06/2023]. See the Terms and Conditions (https://onlinelibrary.wiley.com/terms-and-conditions) on Wiley Online Library for rules of use; OA articles are governed by the applicable Creative Commons License

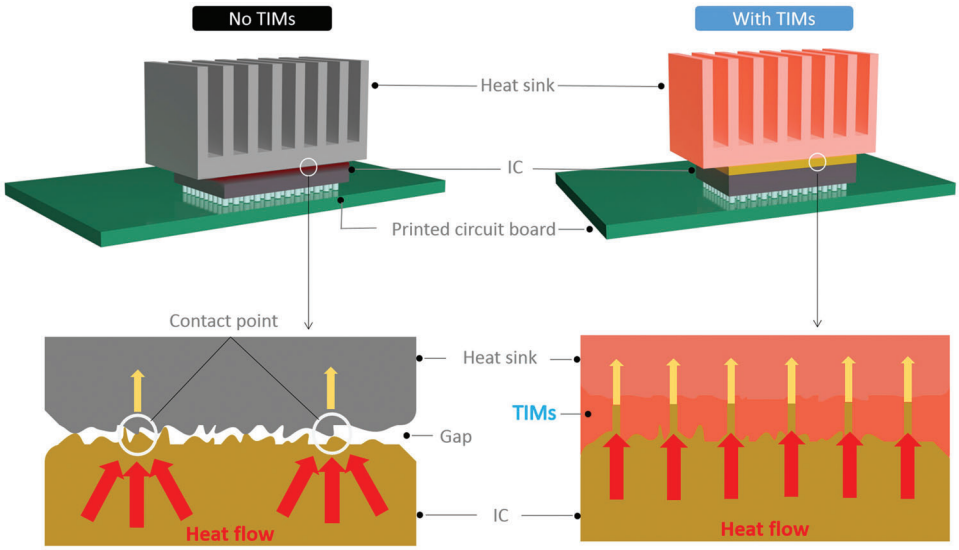

Figure 1. Schematic illustration of working mechanism of a Thermal interface material (TIM).

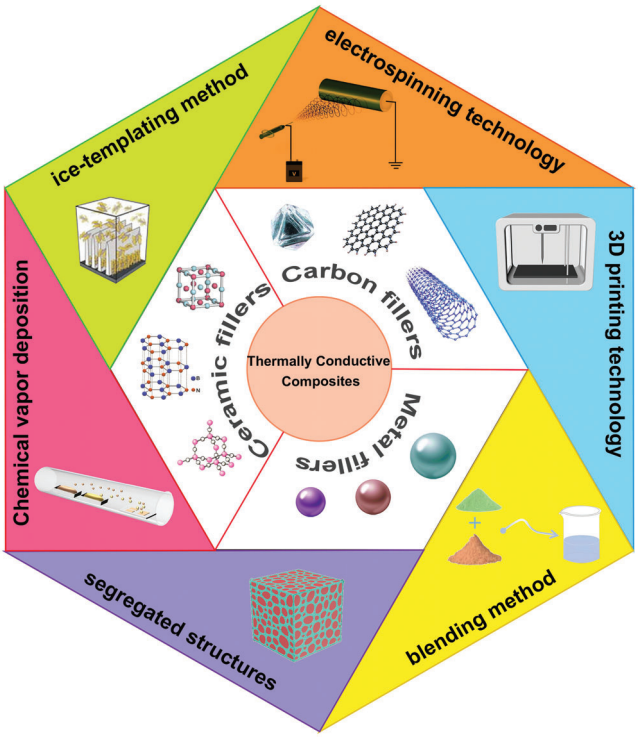

Figure 2. A landscape view of the reviewed technical points in this review.

A brief overview of thermally conductive polymer composite is shown in **Figure 2**.

2. Thermal Conduction Mechanisms

Electrons, phonons, and photons are the main carriers of thermal conduction in solids. The thermal conduction of matter results from the collisions and interactions of these particles.[38] Polymer-based thermally conductive materials are usually used at relatively low temperatures, so the contribution of photons to the thermal conductivity of the material is minimal and in general, the electrons and phonons are mainly considered.[60] A phonon is a quantum of the vibrational energy of a crystal dot matrix, corresponding to the smallest unit of energy of a sound wave vibration. It is a wave packet composed of acoustic waves that behave like a quasiparticle with energy $h\nu$, momentum h/λ, and zero mass (ν is the frequency of vibration, λ is the wavelength, and h is Planck's constant).[61] Insulators are heat-transferring by phonons, and the magnitude of their thermal conductivity depends on the phonon mean free paths.[62,63]

Phonon scattering determines the transport behavior of phonons.[64] Phonon scattering in solid materials mainly includes phonon-phonon scattering, phonon scattering due to lattice defects, phonon scattering due to mass differences of isotope atoms, and phonon boundary scattering.[65,66] Phonon–phonon scattering includes three-phonon scattering and multiphonon scattering.[67,68] A three-phonon scattering process is a process in which two phonons merge to form a new phonon or a phonon splits into two phonons. Depending on whether the momentum of the phonons is conserved during the scattering process, the three-phonon scattering process is divided into an inverse process and a regular process.[69] Regular scattering occurs when the scattering process satisfies both conservations of momentum and conservation of energy (generally occurs at lower temperatures), and inverse scattering occurs when it satisfies conservation of energy but not conservation of momentum (generally occurs at higher temperatures), and inverse scattering produces thermal resistance due to the loss of phonon momentum.[70] Multiphonon scattering mainly refers to four-phonon scattering and is not considered in general.[71] Among these phonon scatterings, phonon scattering can be subdivided into three categories, namely boundary scattering, regular scattering, and damped scattering, depending on whether momentum is conserved during phonon scattering and the region in which phonon scattering occurs. Damped

© 2023 Wiley-VCH GmbH

16163028, 0, Downloaded from https://onlinelibrary.wiley.com/doi/10.1002/adfm.202301549 by University of California - Los Ange, Wiley Online Library on [16/06/2023]. See the Terms and Conditions (https://onlinelibrary.wiley.com/terms-and-conditions) on Wiley Online Library for rules of use; OA articles are governed by the applicable Creative Commons License

scattering includes the inverse process of three-phonon scattering, defect scattering, isotope scattering, and phonon-boundary scattering.

The transport behavior of phonons is closely related to the dimensionality of system, and the transport properties of phonons change significantly from the 3D macroscopic material system to the low-dimensional nanomaterial system.[72] In bulk materials, the phonon mean free path is much smaller than the characteristic dimensions of material, when phonon scattering is almost isotropic and the heat transport phenomenon is diffusive thermal transport. Where the component and temperature of material are determined, the thermal conductivity is only related to the intrinsic properties of material and not to its dimensions, when the distribution of equilibrium phonons converges to a Planck distribution and the dominant scattering mode is damped scattering.[70] At a micro/nanoscale, the phonon mean free path is greater than or close to the characteristic size of the material, so that the phonon can propagate from the high-temperature end to the low-temperature end before it has been scattered, resulting in ballistic transport, which can be described by the Landau transport equation.[72] When regular scattering dominates, the mode of heat transport is phonon hydrodynamic heat conduction, where the total energy and momentum of phonons in the crystal are conserved and the distribution of equilibrium phonons obeys the Drift Planck Distribution. The macroscopic drift velocity of phonons is the collective behavior of phonons in crystals, which under certain conditions has properties similar to those of fluid microclusters, showing viscous and hydrodynamic phenomena (including phonon Poiseuille flow and Second Sound). Most phonon hydrodynamic phenomena currently observed are at low temperatures.[73–75]

Physical models describing phonon thermal conductivity can be broadly classified into three categories, namely macroscopic, microscopic, and mesoscopic models. The microscopic model is a direct study of the motion of microscopic particles such as atoms or molecules by modeling the interaction between atoms, using statistical methods to obtain macroscopic quantities from the microscopic information of particles. The model focuses mainly on simple thermal conductivity systems at the nanoscale because it is more computationally intensive and inefficient when the number of microscopic particles is too large or when the system under study is large.[76] The microscopic models mainly include molecular dynamics methods (based on Newton's equations in classical mechanics), first-principles calculations, and non-equilibrium Green's function methods (both based on Schrödinger's equation in quantum mechanics).[77,78]

The macroscopic model is a top-down modeling idea by considering more microscopic physical processes based on the Fourier equations and describing the non-Fourier effects of heat transfer at the micro-nanoscale by building the corresponding mathematical models.[79] The macroscopic model with its relatively simple mathematical description and clear physical connotations is computationally very efficient in solving practical heat transfer problems. However, due to the large amount of microscopic information that is ignored, the model contains mostly empirical parameters that need to be obtained by fitting experimental data or through other means. Macroscopic models (generally referred to as generalized Fourier laws) include the Phonon Hydrodynamic Model, the Dual-Phase-Lag Model, the Ballistic-Diffusive Model, the Thermon Gas Model, and the Viscous Heat Model.[80,81]

The mesoscopic model (based on the phonon Boltzmann equation) ignores the fluctuating effects in the phonon transport process, draws on the theory of gas transport mechanisms, and uses the phonon distribution function to describe the distribution of different phonon modes, thus establishing a dynamic theoretical framework for describing phonon transport.[79] Compared to the other two types of models, the phonon Boltzmann equation is a reasonable choice after considering the accuracy of the model and the complexity of the calculation.[82] On the one hand, the macroscopic models describing phonon thermal conductivity can all be derived from the phonon transport Boltzmann equation under certain approximation conditions, and on the other hand, the direct tracking of microscopic particle motion is replaced by modeling the phonon number density distribution, which reduces the computational effort to a large extent. Although this simplification discards a large amount of microscopic information, the phonon Boltzmann equation also accurately captures the laws of heat transfer at the micro-nano scale when the system under study is much larger than the atomic scale.[83,84] The phonon properties (e.g., phonon dispersion relation, heat capacity spectra, the density of states, relaxation time, etc.) are first obtained using microscopic methods, and then used as input parameters for the phonon Boltzmann equation, and finally, the phonon Boltzmann equation is solved, which is the mainstream idea for solving phonon transport problems in finite size micro and nanostructures.[85]

Like other solid materials, metals have a component of heat conduction associated with lattice vibrations, i.e., phonon heat conduction. Also, a unique feature of metals is the presence of carriers, especially electrons. These point-charged entities are responsible not only for the transport of charge (i.e., electric current) but also for the transport of heat. In crystals, the interaction between electrons and phonons is present everywhere, even in perfect metals, where there is a certain resistance at high temperatures.[86] This is because heat causes distortions in the lattice, and phonons play the role of scattering centers in this process, i.e. electrons are scattered by the absorption and emission of phonons.[87] The first studies to investigate electron-phonon coupling were to investigate the temperature dependence of the resistance of metals. The most common method of calculating the electroacoustic coupling coefficient uses the McMillan formula modified by Allen and Dynes, and the specific procedure has been implemented by Quantum Espresso.[88,89] It is well known that an electron is a kind of fermion, obeying Fermi-Dirac statistics, and its motion law can be obtained by density functional theory (DFT). This theory is a quantum mechanical method to study the electronic structure of a multielectron system, which is based on the Thomas-Fermi model and uses the charge density instead of the wave function as the fundamental variable to describe the system.[65,90]

At the atomic scale, heat is transferred through waves formed by the vibrations of atoms on the lattice, so heat transfer at the microscale can be analyzed by probing the thermal vibrational changes of atoms. The phonon density of states is the power spectrum of atomic vibrations obtained by Fourier transforming the velocity autocorrelation function of a specified group of atoms, which is proportional to the result after Fourier transforming the

© 2023 Wiley-VCH GmbH

16163028, 0, Downloaded from https://onlinelibrary.wiley.com/doi/10.1002/adfm.202301549 by University of California - Los Ange, Wiley Online Library on [16/06/2023]. See the Terms and Conditions (https://onlinelibrary.wiley.com/terms-and-conditions) on Wiley Online Library for rules of use; OA articles are governed by the applicable Creative Commons License

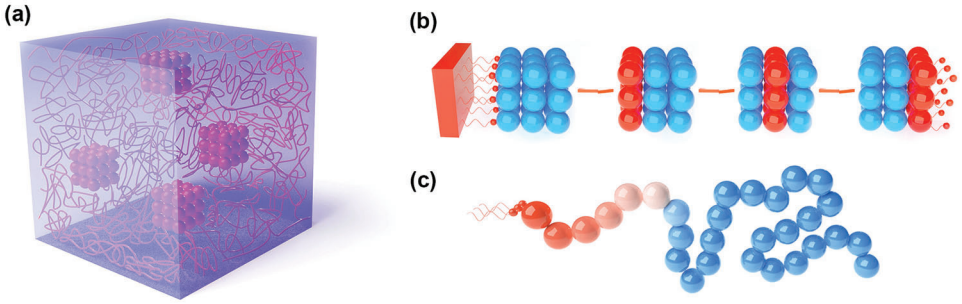

Figure 3. Schematic diagram of the microstructure of the polymer. a) Schematic diagram of the internal structure of polymer. b) Crystalline regions in polymers. c) Amorphous regions in polymers.

velocity autocorrelation function.[91,92] When heat is transferred between different types of atoms, differences in atomic masses, intrinsic vibrational frequencies, and temperatures will result in a vibrational mismatch between the atoms, i.e., a mismatch in phonon mode frequencies. The match between phonon mode frequencies determines the mutual heat transfer efficiency, therefore a parameter expressing the vibrational match between atoms is needed to quantify the efficiency of energy transfer between phonons. To further analyze the heat transfer mechanism, the overlap energy is used to quantify the level of vibrational matching between two atomic groups.[93] A deeper understanding of different types of phonon thermal transport at multiple scales and temperature intervals is of great significance for the study of high-performance thermal management materials, for which the current theory still has many shortcomings and needs further refinement.

Due to the random entanglement of polymer chains, the higher molecular mass of the polymer and the polydispersity mean that the polymer is difficult to form complete crystals.[94] Semicrystalline polymers contain a small number of crystalline regions where atoms are tightly connected, where heat transfer is achieved by vibrations of the crystal lattice. In establishing long-range ordering in a polymer, vibrations of the crystal lattice can allow rapid heat transfer along molecular chains (**Figure 3**b).[95] In non-crystalline regions, on the other hand, thermal conduction is achieved by the thermal vibration of irregular molecules around a fixed location, and the thermal energy is transmitted to adjacent molecules in sequence (Figure 3c).[43,96,97] Because of the low crystallinity of polymers, presence of defects, nonharmonic vibrations of molecular chains and crystal lattices, and so on, phonon propagation is highly hindered in polymers, resulting in a generally low λ value.[98] The internal structure of polymer is schematically shown in Figure 3a.

For filled polymer composites, the increase in thermal conductivity is mainly due to the addition of high thermally conductive fillers.[99–101] Thermal conductivity mechanism of the filled thermally conductive composite is explained by three different theories: thermal conduction path theory, thermal percolation theory, and thermoelastic coefficient theory. Among them, thermal conduction path theory is the most widely accepted mechanism. The schematic diagram of thermal conduction path theory, thermal percolation theory, and thermoelastic coefficient theory are shown in **Figure 4**.

2.1. Thermal Conduction Path Theory

Thermal conductivity paths are established by connecting the thermally conductive fillers in the polymer matrix. When the filler concentration is relatively low in polymer matrix, the particles are isolated from each other. The interfacial thermal resistance between fillers and matrix and the λ value of the matrix are crucial factors in determining the thermal conductivity of material (Figure 4a).[96] Hence, the thermal conductivity of polymer composites remains low. When the filler concentration continuously increases, the particles contact each other and form thermally conductive networks, allowing a better path for heat flow (Figure 4b).[102] In the case that the direction of heat flow is parallel to the thermally conductive network, the thermal conductivity of the composite is significantly improved. Conversely, failure to establish a thermal conductivity network in the direction of heat flow results in a considerable thermal resistance. The λ value of composite material cannot be significantly improved.[103,104]

2.2. Thermal Percolation Theory

Percolation theory was initially developed to explain the conductive phenomenon of conductive composites. With a low filler loading, the fillers are uniformly dispersed in the polymer matrix to form a "sea-island structure" without forming a continuous network, so that the conductivity of the composite increases slowly with higher filler content. As the conductive filler increases and the filler content arrives at the percolation threshold, the conductive fillers interconnect to form a "sea-sea structure", which increases the conductivity dramatically. In the field of thermally conductive composites, percolation theory can also explain the thermal conductivity behavior of composites. However, it is still controversial whether it can fully describe this behavior. Within a wide range of filler dosage, the percolation point has not been observed in some polymer composites, with almost no sudden change in λ values.[105,106] Many researchers believe that thermally conductive fillers must have a sufficiently high λ value to produce thermal percolation.[107,108] Therefore, only for particles with high λ values, such as CNTs and graphene nanosheets, can the phenomenon of thermal conduction percolation similar to the conduction behavior be observed (Figure 4c).[109] However, the overall λ value is still very low. The above results are due to

© 2023 Wiley-VCH GmbH

16163028, 0, Downloaded from https://onlinelibrary.wiley.com/doi/10.1002/adfm.202301549 by University of California - Los Ange, Wiley Online Library on [16/06/2023]. See the Terms and Conditions (https://onlinelibrary.wiley.com/terms-and-conditions) on Wiley Online Library for rules of use; OA articles are governed by the applicable Creative Commons License

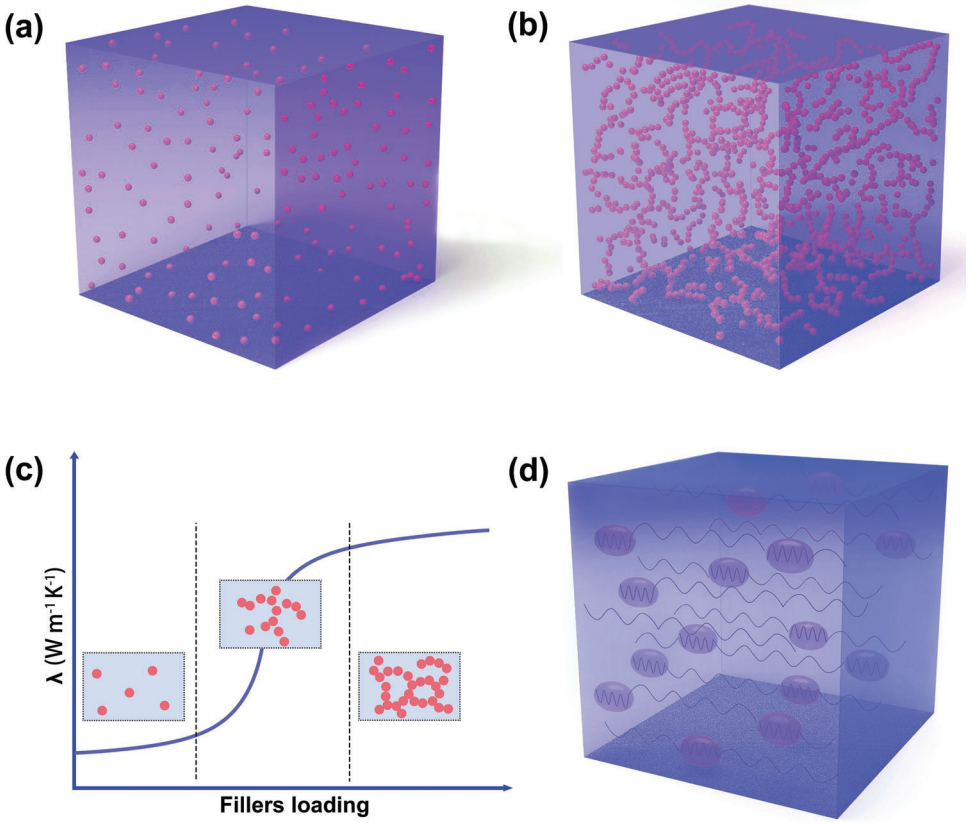

Figure 4. Thermal conductivity mechanism of composite materials. a) Isolated state at low filler content. b) Thermal conduction paths at high filler content. c) Thermal percolation theory. d) Thermoelastic coefficient theory.

the fact that phonons, as the main heat conduction carriers, do not have tunneling effects like electrons, which leads to severe phonon scattering at interfaces, resulting in more considerable interfacial thermal resistance.[110] Therefore, the thermal conductivity of the system is still very low even if the amount of heat-conducting particles is above the percolation threshold.

2.3. Thermoelastic Coefficient Theory

Unlike the mentioned thermal path theory (taking the matrix and the filler as two parts), the thermoelastic theory considers the composite material as a whole, and the corresponding thermal conductivity depending on the macroscopic properties of the entire material. The variation pattern of λ values is akin to elastic coefficient and modulus in classical vibration and elastic mechanics. Therefore, the thermal conductivity of material can be regarded as the thermal elastic coefficient in the phonon propagation process (thermal vibration). Higher the thermal elastic coefficient and faster phonon transfer efficiency mean higher thermal conductivity. The increase in thermal conductivity can be regarded as the combined enhancement of the high thermal conductivity filler to the polymer (Figure 4d).[52] The λ value of composite gradually increases with the increase of particle content

3. Critical Factors for the Thermal Conductivity of Polymers Composites

The factors that lead to the low λ values of intrinsic polymers are mainly related to the molecular structure.[32,111] The intrinsic thermal conductivity of a polymer depends mainly on the orientation and crystallinity of the polymer. If the chain structure of the material is ordered, heat will be rapidly transferred along the molecular chain direction, leading to a higher thermal conductivity in this direction.[112,113] Zhu et al. found an increase in λ value from 21 W m^{-1} K^{-1} (unstretched) to 51 W m^{-1} K^{-1} by heat-stretching Spectra S-900 ultrahigh-molecular-weight polyethylene (UHMWPE) microfiber. It was found, using X-ray diffraction, that the crystallinity of UHMWPE decreased from 92% to 83% after stretching, while the crystallite size and crystallite orientation did not change. The result from polarization Raman spectroscopy showed that the amorphous structure became more aligned after stretching, suggesting that the significant increase in the thermal conductivity of polymer was attributed to the enhanced alignment of the amorphous chains.[114] Crystallinity is also an essential factor in the λ value of polymers. When the polymer has a higher crystallinity, it will generally possess a better thermal conductivity.[114]

In addition, the number of polar groups contained in polymers and the degree of polarization of polar groups also affect the

© 2023 Wiley-VCH GmbH

16163028, 0, Downloaded from https://onlinelibrary.wiley.com/doi/10.1002/adfm.202301549 by University of California - Los Ange, Wiley Online Library on [16/06/2023]. See the Terms and Conditions (https://onlinelibrary.wiley.com/terms-and-conditions) on Wiley Online Library for rules of use; OA articles are governed by the applicable Creative Commons License

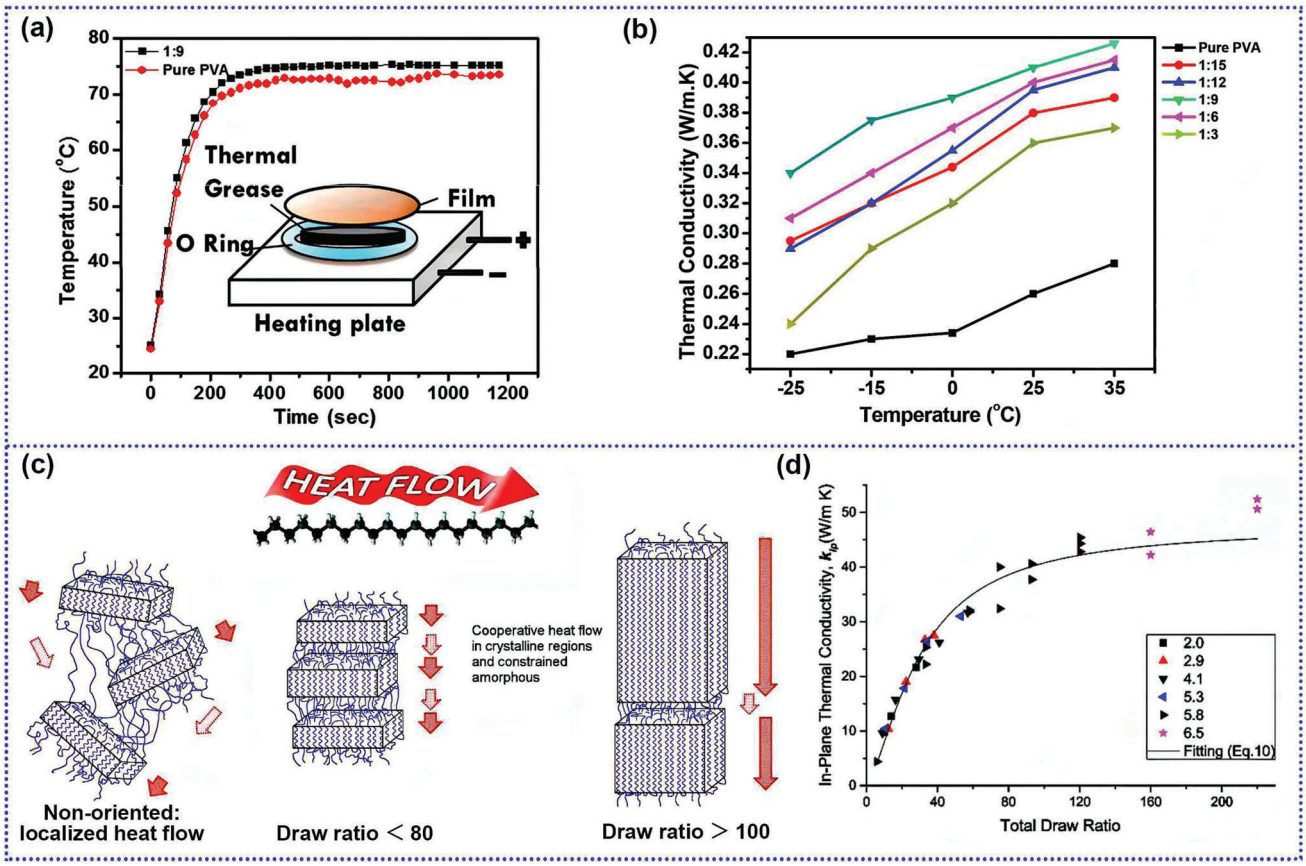

Figure 5. Factors affecting the thermal conductivity of polymers. a) Temperature–time profile of polymer films. Insert is the schematic of experimental setup. b) Thermal conductivity versus temperature plot of pure PVA and PEG-PVA films. Reproduced with permission.[118] Copyright 2017, Elsevier. c) Increasing thermal conductivity of material at different stretching ratios (crystal orientation for draw ratios lower than 80, followed by increase in crystal size at higher stretching). d) In-plane thermal conductivity as a function of total draw ratio. Reproduced with permission.[124] Copyright 2017, Elsevier.

thermal conductivity of polymers, which is higher when it contains more polar groups and these polar groups are more easily polarized. Intramolecular interactions are another essential factor, where strong covalent bonds can provide effective paths for phonon transport in polymers, thus increasing the λ value.[115,116]

In contrast, hydrogen bonds and van der Waals forces (two main types of typical noncovalent bonds) can improve thermal conductivity by restricting the twisting motion of molecular chains and the formation of disordered structures, thus improving polymer crystallinity.[103,117] It has been shown that the increase in the number and strength of hydrogen bonds affects the final thermal conductivity of polymers. Mehra et al. reported the introduction of short-chain poly (ethylene glycol) (PEG) into long-chain poly (vinyl alcohol) (PVA) to improve the λ value of the polymer by forming new thermal conduction pathways through hydrogen bonding interactions between the two polymers. The number of thermal bridges increases with the continuous addition of PEG molecules, and at optimum loading (1:9 for PVA: PEG), a well-established thermal conductivity path is formed in the polymer, and the λ value of the PEG–PVA sample is enhanced to 1.6 times that of pure PVA films. The addition of PEG breaks the random intermolecular attraction of the PVA polymer chain, thus establishing ordered and homogenously distributed hydrogen bonds and reducing phonon scattering, promoting thermal conductivity within the polymer (**Figure 5**a,b).[118]

Most polymeric materials contain surface chain folding layers and intermediate uncharacterized regions. In addition to the polymer chain structure and intermolecular interactions between the chains, the polymer chain configuration on the surface of a bulk polymer plays an important role in its thermal conductivity.[119] The surface chain folding layer of the polymer is formed during the growth of the polymer, and the variation of adjacent chain folding limits the thickness of polymer. For layered polymers, the effect of chain-folded layers on the polymer material cannot be ignored because of the limited film thickness and the large surface-to-volume ratio.[120] Using molecular dynamics simulations, Ouyang et al. explored the effect of chain folding on the thermal conductivity of lamellar amorphous polyethylene (LAPE) with different chain lengths (L0). After analysis, it was found that the thermal conductivity of short-chain LAPE without boundary chain folding was uniform along the chain length, and the thermal conductivity increased with the increase of the average chain length. When the average chain length increases to a certain degree, chain folding starts to occur at the bound-

 © 2023 Wiley-VCH GmbH

16163028, 0, Downloaded from https://onlinelibrary.wiley.com/doi/10.1002/adfm.202301549 by University of California - Los Ange, Wiley Online Library on [16/06/2023]. See the Terms and Conditions (https://onlinelibrary.wiley.com/terms-and-conditions) on Wiley Online Library for rules of use; OA articles are governed by the applicable Creative Commons License

ary, which leads to the local thermal conductivity of the boundary being significantly lower than that of the central region. The morphological analysis of the chains shows that the folding of the boundary chains leads to the reduction of the orientation order parameter and the radius of gyration along the heat flow direction, and further vibrational spectral analysis shows that the folding of the boundary chains shifts the vibrational spectrum to lower frequencies and suppresses the transmission coefficients of the C–C and C–H vibrations, which reveal the physical origin of the non-uniform local thermal conduction and help to understand the fundamental heat transport behavior of the lamellar amorphous polymer.[121]

The thermal conductivity of bulk crystalline polymers is also closely related to their molecular structure. Due to the intrinsic presence of bending phonon modes, crystalline polymers can provide a platform for the study of phonon hydrodynamics, and at the same time, phonon hydrodynamics can also provide a theoretical basis for the study of the thermal conductivity of crystalline polymers. Phonon scattering is an important factor affecting thermal conductivity at the micro and nanoscale. Hydrodynamic phonon transport is not negligible in the study of the thermal conductivity of highly thermally conductive materials.[122,123] Zhang et al. investigated hydrodynamic phonon transport in polyacene $(-C_4H_2-)n$ (PA-I), polyacetylene $(-C_2H_2-)n$ (PA-II), and polyethylene $(-C_2H_4-)\underline{n}$ (PE) crystalline polymers based on the Boltzmann transport equation. Hydrodynamic phonon transport in PA-I and PA-II appeared in the low-temperature range below 50 K, while the hydrodynamic phonon transport of PE appeared in the intermediate temperature range around 120 K (which is not consistent with the value predicted by Guyer's criterion). They propose a modified criterion based on spectral thermal conductivity, which is found to work well in all three polymer crystals, showing agreement with both the thermal conductivity results and the predicted results for the phonon drifting component. This study provides a physical basis for hydrodynamic phonon transport in polymer systems and a reliable criterion for the study of hydrodynamic phonon transport in complex systems.[73]

Intrinsically thermally conductive polymers can be synthesized and molded to improve their thermal conductivity by changing the structure of molecules and chains to obtain a special physical structure.[45] Commonly used methods are highly stretching, electrospinning, and templating.[113] Ronca et al. first reported that the thermal conductivity of UHMWPE reached 18.4 W m^{-1} K^{-1} by solid-state biaxial stretching. Thermal diffusivity of polymers with different molecular weights was measured by in-plane laser flash thermal analysis, and a strong correlation was found between the stretching ratio and the resulting in-plane thermal conductivity. Higher λ values were found in UHMWPE with higher molecular weights and smaller numbers of chain ends (Figure 5c,d).[124]

For the particle-filled thermally conductive polymer material, the thermal conductivity is much lower than that of the theoretical prediction, this is mainly due to the poor interfacial compatibility and high interfacial thermal resistance between the matrix and fillers.[125–128] Therefore, a series of factors such as filler type, size, shape, loading, distribution, and the mutual effect between polymer and filler would all produce a strong impact on the ultimate λ value of the composites.[129–131] The type of thermally conductive filler will significantly affect the thermal conductivity of the composite.[132,133]

Table 1. Thermal conductivity of common thermally conductive fillers.

Fillers	λ [W m^{-1} K^{-1}]	Refs.	Fillers	λ [W m^{-1} K^{-1}]	Refs.
Ag	450	[62]	Si	200	[62]
Cu	483	[62]	GO	1000	[63]
Au	345	[62]	SiC	80–120	[62]
Al	204	[62]	BN	170	[95]
Fe	80	[60]	Si_3N4	180	[62]
Graphene	5000 ($\lambda\|\|$)	[108]	AlN	200	[62]
CNT	3000($\lambda\|\|$)	[108]	Al_2O_3	20-29	[62]
Diamond	2000	[62]	SiO_2	1-10	[62]
Graphite	1500 ($\lambda\|\|$)	[95]	BeO	260	[18]
CF	8-70	[62]			

3.1. Type of Thermally Conductive Fillers

Commonly used thermally conductive fillers are metals, ceramics, and carbon materials. The λ values of common thermally conductive fillers are listed in **Table 1**. Although metals have a high intrinsic λ value and excellent operating performance, their disadvantages are easy oxidation at high temperatures and high coefficients of thermal expansion (CTE).[52,62,134,135] In addition, the density will increase when adding a large amount of metal to the polymer, thus restricting applications where being lightweight is required.[47,136] In recent years, the application of metal fillers in thermal interface materials is gradually decreasing. Therefore, this review will not introduce more about the properties and applications of metals.

3.1.1. Ceramics

Ceramic fillers have high thermal conductivity; however, their electrical conductivity is low enough to be used for applications requiring electrical insulation,[11,17,137] mainly including carbides, oxides, and nitrides. The carbides often used as thermally conductive fillers mainly include silicon carbide (SiC) and MXenes. Silicon carbide has high hardness, high thermal conductivity (≈120 W m^{-1} K^{-1}), high-temperature resistance, chemical corrosion resistance, low CTE, and stable chemical properties.[138–141] However, its application in insulation is somewhat restricted due to its poor insulating properties. Yao et al. utilized the freeze-casting method to achieve vertically aligned and interconnected SiC nanowires networks, which provide a channel for heat transfer and achieve a high through-plane thermal conductivity of 1.67 W m^{-1} K^{-1} at a low filler loading of 2.17 vol % (**Figure 6**a–c).[142]

MXenes (Ti_3C_2) are new type of 2D transition metal carbides, mainly prepared by etching the aluminum atom layers of MAX (Ti_3AlC_2) with hydrofluoric acid or a mixture of hydrochloric acid and fluoride solution.[143,144] It has excellent thermal and electrical conductivity, a high specific surface area, and hydrophilicity, and is widely used.[145–148] Guo et al. prepared 3D carbon fiber

© 2023 Wiley-VCH GmbH

16163028, 0, Downloaded from https://onlinelibrary.wiley.com/doi/10.1002/adfm.202301549 by University of California - Los Ange, Wiley Online Library on [16/06/2023]. See the Terms and Conditions (https://onlinelibrary.wiley.com/terms-and-conditions) on Wiley Online Library for rules of use; OA articles are governed by the applicable Creative Commons License

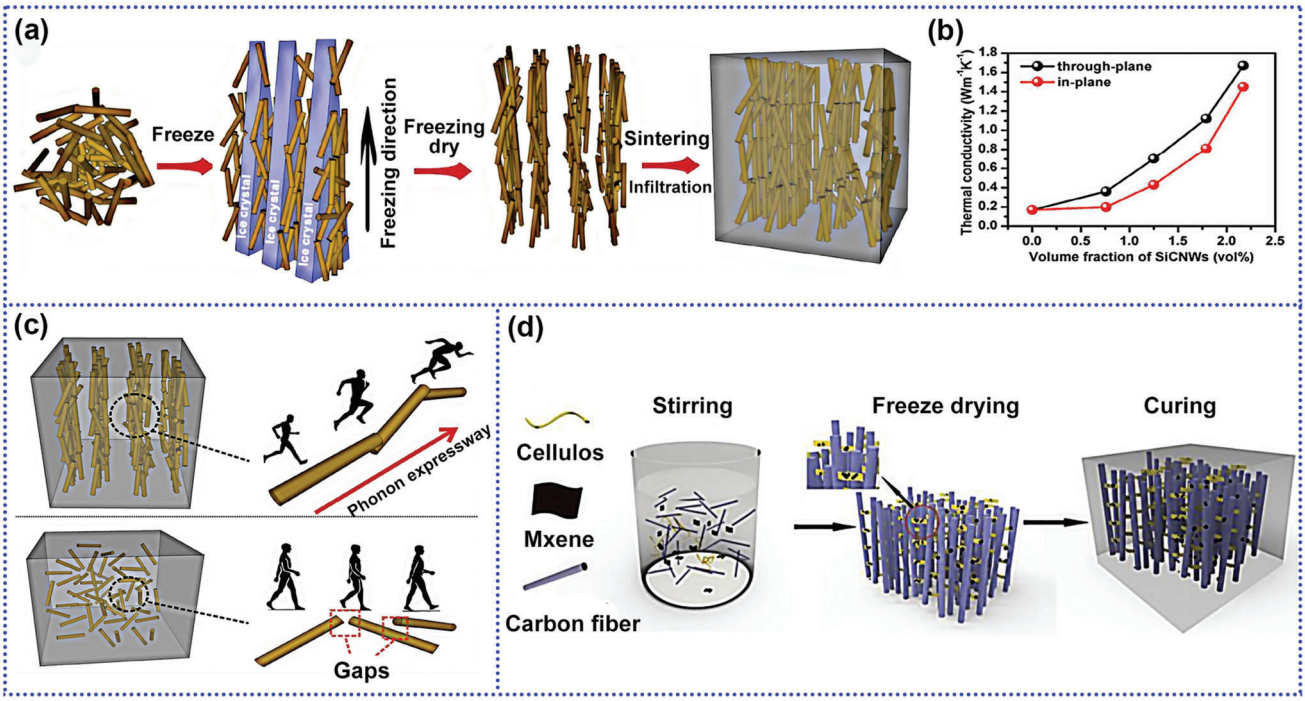

Figure 6. Carbide filled composites. a) Schematic illustration of forming SiC nanowire network. b) Through-plane and in-plane thermal conductivity of 3D SiCNW/epoxy composites with different filler loadings. c) Illustration of thermally conductive paths for composites filled with oriented SiCNW network and randomly dispersed SiCNWs. Reproduced with permission.[142] Copyright 2018, American Chemical Socity. d) The preparation process of CF-M/epoxy composites. Reproduced with permission.[149] Copyright 2020, Elsevier.

(CF)-MXenes foams by freeze-drying method, followed by the injection of epoxy resin to obtain CF-M/epoxy composites with a thermal conductivity of 9.68 W m^{-1} K^{-1} at 30.2 wt% filler content, while achieving higher glass transition temperature and lower thermal expansion coefficient (Figure 6d).[149]

Oxide ceramic materials are already in widespread use in electrical insulation packaging because of their low price. Among them, silicon oxide (SiO_2), zinc oxide (ZnO), aluminum oxide (Al_2O_3), and magnesium oxide (MgO) are mainly used as thermally conductive particles. SiO_2 has excellent electrical insulation and stable chemical properties.[150] However, due to its low intrinsic λ value (≈4 W m^{-1} K^{-1}), thermal conductivity of composite materials containing SiO_2 is lower than other filler systems at the same filling amount.

ZnO is a semiconductor material with excellent thermal stability and thermal conductivity (≈30 W m^{-1} K^{-1}).[52] Its wider band gap (3.3 eV) brings the advantages of strong ability to maintain the electric field, high breakdown voltage, and high endurable power. However, due to its relatively high dielectric constant, its application in the electrical and electronic fields is greatly restricted, and it is mainly used as a rubber additive.

Al_2O_3 has eight different crystal structures, among which α-alumina is noteworthy due to its high stability, compact structure, low activity, excellent electrical insulation performance, high λ value (30–36 W m^{-1} K^{-1}), and excellent dielectric properties.[151,152] Wang et al. fabricated flower-like Al_2O_3 (f-Al_2O_3) from nano spherical aluminum powder and water, then coated Al_2O_3 on the surface of boron nitride nanosheets (BNNSs@f-Al_2O_3). The planar BNNs were aligned in the polymer along the in-plane direction when the material by hot pressing the material. With the Al_2O_3 connecting adjacent BNNs, a thermal conductive network was constructed along the in-plane direction of the polymer. This strategy achieves COC/BNNSs @f-Al_2O_3 composites that simultaneously have high thermal conductivity, high $T_{decomp.}$, low CTE, and low dielectric constant (**Figure 7**a–c).[153]

MgO is a colorless and transparent crystal with strong resistance to high and low temperatures (as high as 2500 °C and as low as -270 °C), high corrosion resistance, excellent electrical insulation properties, and high λ value (≈40 W m^{-1} K^{-1}). It is also a valuable filler for multiple applications.

Nitrides have recently been under the research spot light recently in thermally conductive fillers. They have high thermal conductivity, excellent electrical insulation performance, and low linear expansion coefficient compared with oxides. It is a thermally conductive filler with great application potential.[31] At present, the nitrides mainly used as thermally conductive fillers include silicon nitride (Si_3N_4), aluminum nitride (AlN), and boron nitride (BN).

The thermal conductivity of Si_3N_4 mainly depends on the composition and microstructure of Si_3N_4. For example, Si_3N_4 with β crystal structure has a high λ value (≈180 W m^{-1} K^{-1}), low dielectric constant, high corrosion resistance, and temperature oxidation resistance, which is the potential to be used in designing thermally conductive composites.[154] In the experiments of Yuan et al., Si_3N_4 powders were modified by F8261,

© 2023 Wiley-VCH GmbH

16163028, 0, Downloaded from https://onlinelibrary.wiley.com/doi/10.1002/adfm.202301549 by University of California - Los Ange, Wiley Online Library on [16/06/2023]. See the Terms and Conditions (https://onlinelibrary.wiley.com/terms-and-conditions) on Wiley Online Library for rules of use; OA articles are governed by the applicable Creative Commons License

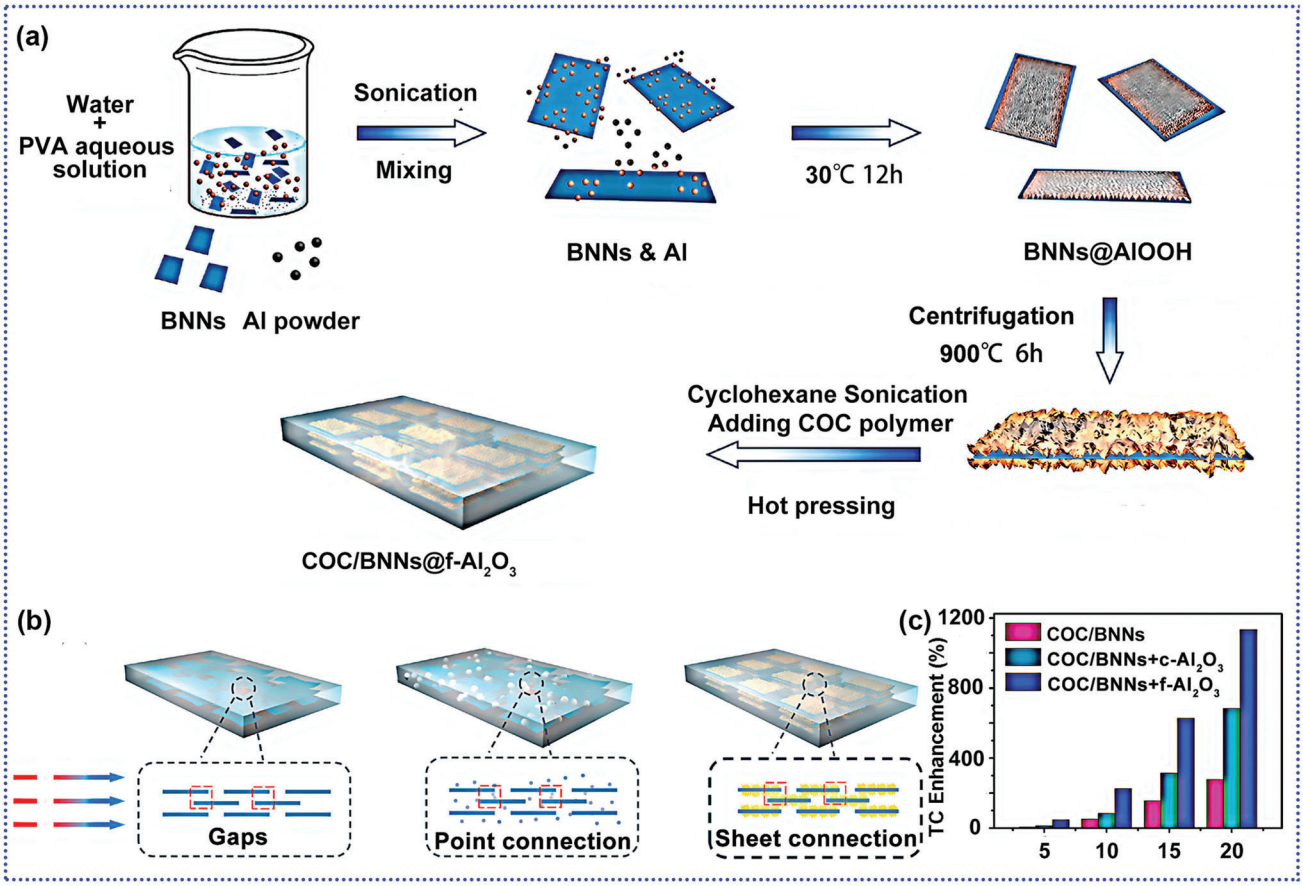

Figure 7. Oxide filled composites. a) The fabrication process of COC/BNNSs@f-Al_2O_3 composite. b) The illustration of thermal conductivity enhancement mechanism. c) Thermal conductivity enhancement of various composites compared with COC. Reproduced with permission.[153] Copyright 2021, Elsevier.

a silane containing several fluorine atoms, and used to make a Si_3N_4/PTFE composite, where characterizations showed that the modified Si_3N_4 powders had better compatibility with PTFE compared with unmodified Si_3N_4. The Si_3N_4/PTFE composites exhibited low dielectric loss, low dielectric constant, high thermal conductivity ($\lambda = 1.3$ W m^{-1} K^{-1}), and low water absorption at a filler content of 62 vol%.[155]

AlN, a material with hexagonal crystal structure, has a high λ value (≈320 W m^{-1} K^{-1}), high dielectric constant, high resistivity, and low thermal expansion coefficient, and has received extensive attention in electronic packaging and insulation.[156,157] However, its industrial production is severely bottlenecked since AlN powder can easily absorb moisture and hydrolyze, which degrades its electrical insulation, thermal conductivity, and other physical properties.[158] A conventional mitigation strategy is to treat the surface with a coupling agent/surfactant to improve its hydrolysis resistance.[159] Lule and Kim modified AlN with different treating agents (3-aminopropyl) triethoxysilane (APTES), vinyltriethoxysilane (VTES), and polysilazane (PSZ), and used these modified AlN fillers to fabricate poly(butylene succinate) (PBS) composites. The most notable enhancement in thermal conductivity was seen in VTES-AlN, where the λ value of the composites was enhanced by 67.3% compared to the neat PBS at 5% filler content.[160]

BN is an electrical insulator with a band gap width of 5–6 eV.[161,162] It has four different crystalline forms, including cubic boron nitride (c-BN), hexagonal boron nitride (h-BN), rhombohedral boron nitride (r-BN), and wurtzite boron nitride (w-BN). Among them, h-BN, an analog hexagonal structure to graphite, is one of the inorganic materials with the best thermal conductivity of the ceramics, with an in-plane thermal conductivity of 180 W m^{-1} K^{-1}, low density, high breakdown voltage, excellent mechanical strength, low dielectric loss, and outstanding insulating properties, which has led to its extensive application in the electronic packaging sector.[163–166] In addition, with the introduction of BN fillers, polymeric composites also exhibit a very low coefficient of thermal expansion and excellent dielectric stability in a wide range of temperatures and frequencies.[167] Gu et al. first prepared micrometer BN/polyamide acid (mBN/PAA) compound by in situ polymerization, and then obtained mBN/PAA electrospun fibers via electrospinning. The mBN/polyimide (mBN/PI) composites were also fabricated with a high λ value, excellent dielectric properties and thermal stability at the same time as low filler loading (**Figure 8**a).[168]

As a 1D tubular material, boron nitride nanotubes (BNNTs) have similar thermal conductivity to CNTs and superb oxidation resistance and insulating properties, which can realize high ther-

 © 2023 Wiley-VCH GmbH

16163028, 0, Downloaded from https://onlinelibrary.wiley.com/doi/10.1002/adfm.202301549 by University of California - Los Ange, Wiley Online Library on [16/06/2023]. See the Terms and Conditions (https://onlinelibrary.wiley.com/terms-and-conditions) on Wiley Online Library for rules of use; OA articles are governed by the applicable Creative Commons License

16163028, 0, Downloaded from https://onlinelibrary.wiley.com/doi/10.1002/adfm.202301549 by University of California - Los Ange, Wiley Online Library on [16/06/2023]. See the Terms and Conditions (https://onlinelibrary.wiley.com/terms-and-conditions) on Wiley Online Library for rules of use; OA articles are governed by the applicable Creative Commons License

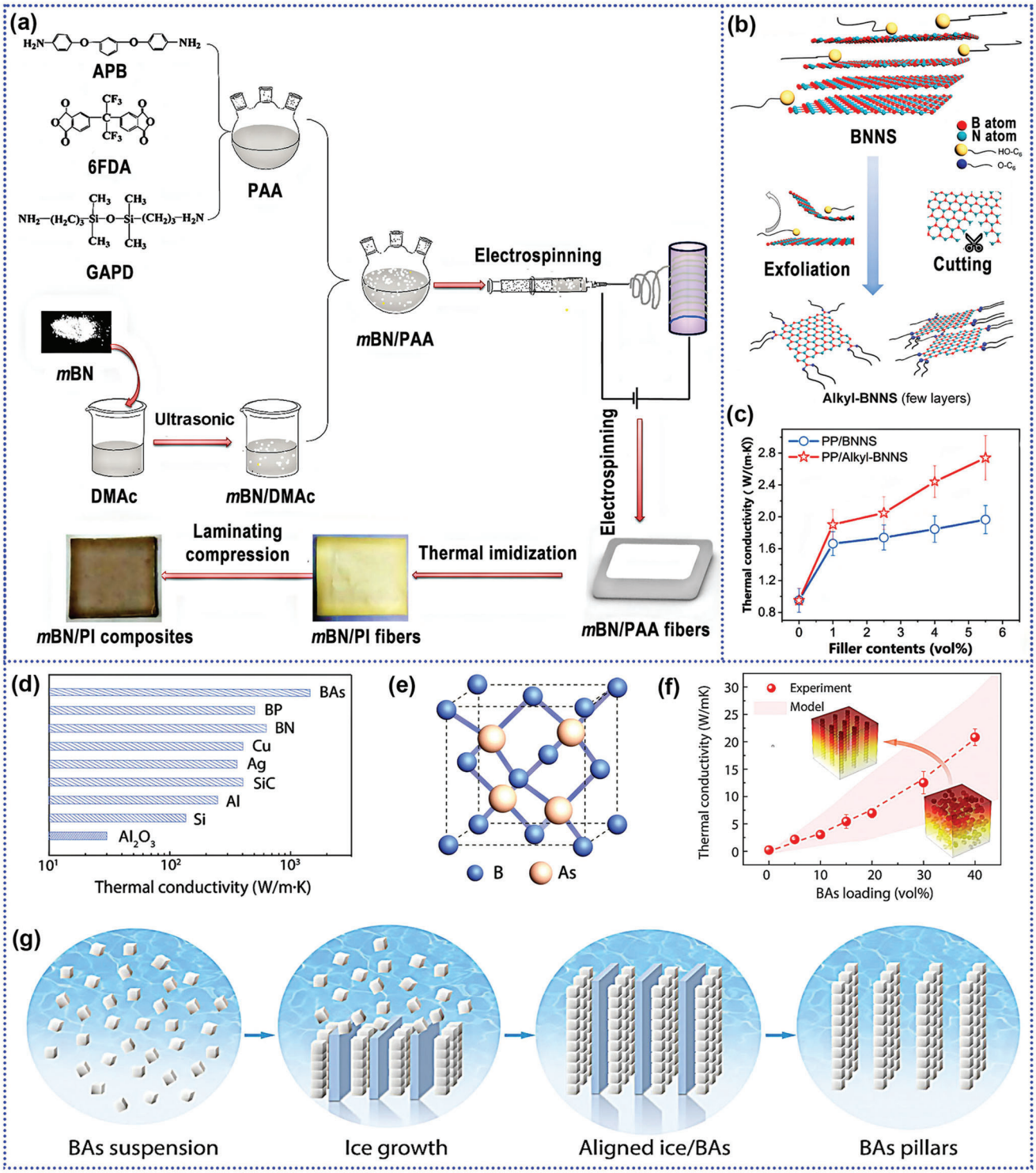

Figure 8. Nitride filled composites. a) Schematic diagram of the fabrication for the mBN/PI composites. Reproduced with permission.[168] Copyright 2017, Elsevier. b) Schematic for preparing Alkyl-BNNS in hexanol by sonification. c) In-plane thermal conductivity of PP/BNNS(PP/Alkyl-BNNS) as a function of filler contents. Reproduced with permission.[182] Copyright 2021, Elsevier. d) Thermal conductivity distribution of materials. e) Schematic of the zinc-blende crystal structure of cubic BAs. f) Thermal conductivity of s-BAs with different loadings. g) Schematic illustrating the self-assembly process through freeze-drying of BAs suspensions to form aligned BAs pillars. Reproduced with permission.[185] Copyright 2021, Nature Communications.

 © 2023 Wiley-VCH GmbH

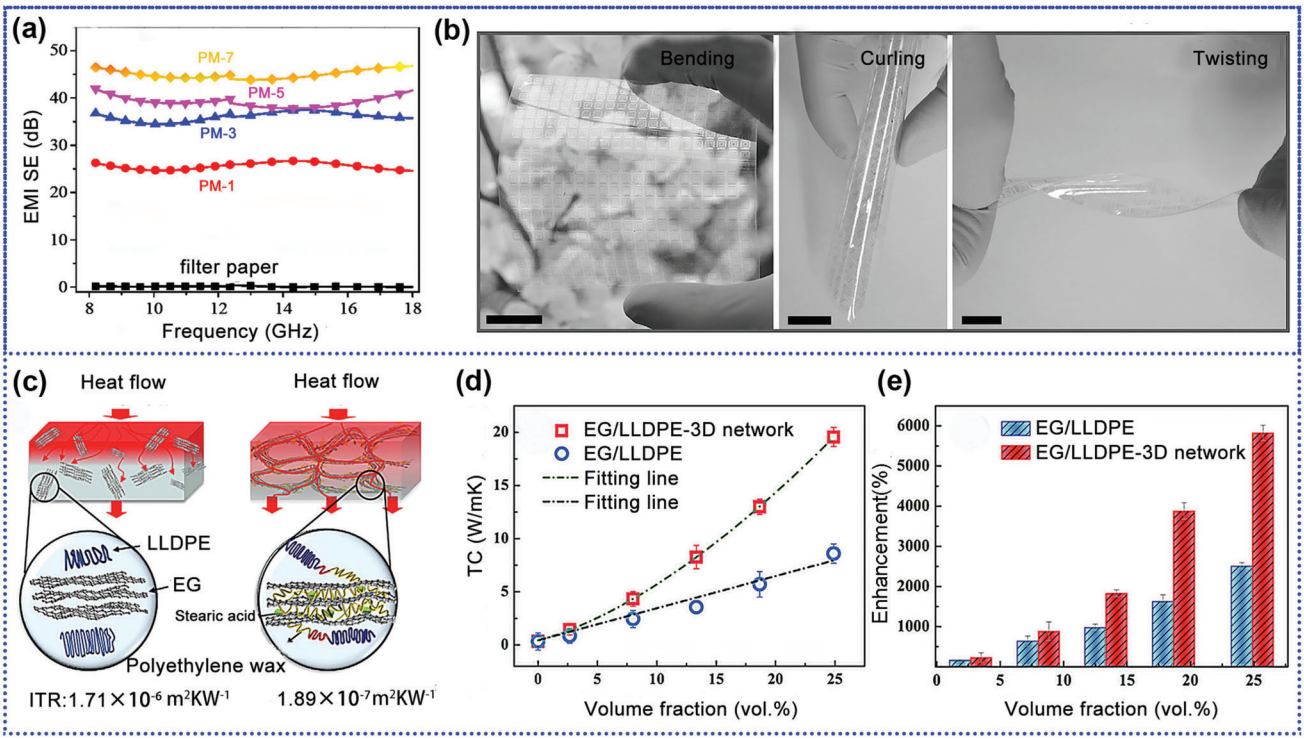

Figure 9. Carbon based filler filled composites. a) EMI SE of the filter paper and the PDMS-coated MXene-filter in the X and Ku band. Reproduced with permission.[189] Copyright 2020, Elsevier. b) Optical images of the transparent and flexible graphene nanomesh field-effect transistors device arrays under bending, curling, and twisting conditions, respectively. Reproduced with permission.[210] Copyright 2017, Wiley–VCH GmbH. c) The scheme of heat transfer path in composites. d) Thermal conductivity and e) enhancement of composites. Reproduced with permission.[220] Copyright 2021, Elsevier.

mal conductivity of composite materials at low additions.[169,170] Kim et al. incorporated BNNTs into PVP solution and enhanced the dispersion of BNNTs in PVP by electrospinning. Meanwhile, the ketone groups in PVP interacted with BNNTs through intermolecular forces, which effectively reduced the interfacial thermal resistance between the filler and the polymer matrix. Composites with a filler content of 30 wt% exhibited a λ value that was about two times compared with that of bulk PVP.[171]

Boron nitride nanosheets (BNNSs) are 2D sheet-like materials with a structure similar to graphene.[172–174] It has a lot of excellent properties, such as good mechanical properties, electrical insulation properties, thermal stability, high thermal conductivity (λ of 600 W m^{-1} K^{-1} in the in-plane direction, and 30 W m^{-1} K^{-1} in the vertical direction), and low dielectric loss.[175–180] Compared with BNNTs, the huge heat transfer area of BNNSs can effectively reduce the interfacial thermal resistance between it and the polymer, and a higher λ value can be achieved with a smaller filling amount.[5,181] Xie et al. prepared alkyl-modified BNNSs by sonicating BNNSs in hexanol, imbuing some of its surface with alkyl groups, which helped incorporate it into polypropylene via melt mixing. Since this one-step modified BNNSs yielded a well-maintained hexagonal crystalline lattice, coupled with the absence of interfacial thermal resistance due to the grafted alkyl groups, the λ value was enhanced to 2.74 W m^{-1} K^{-1} at a very low filler dosage (only 5.5 vol%) (Figure 8b,c).[182]

Boron arsenide (BAs) is a new class of boron compound semiconductor with high thermal conductivity (2200 W m^{-1} K^{-1}), excellent elastic compliance, and high flexibility.[183,184] The application of BAs in thermal management only started a few years ago, therefore, the exploration of its use as a filler is considerably limited, but there is significant potential in it being utilized for the thermal management of flexible electronic products. Cui et al. prepared self-assembled BAs crystals by chemical vapor transport, then organized the filler into a 3D skeleton by the ice template method and finally injected a polymer matrix into this skeleton. The λ value of the composite was enhanced to 21 W m^{-1} K^{-1} at a BAs content of 40 vol% (Figure 8d–g).[185]

3.1.2. Carbon

Carbon-based fillers have potential application value in thermal management. The continuous development of carbon-based materials has played a critical role in promoting the application and high-quality development of polymer-based thermal conductive materials.[186] Since carbon can take the form of various structures, it has been widely used in multiple diverse fields such as electronics, information, energy, computing, and lasers.[106,187,188] It has excellent characteristics in terms of thermal conductivity, electrical conductivity, temperature resistance, corrosion resistance, electromagnetic shielding, low density, mechanical properties, and interfacial properties (**Figure 9**a).[181,186,189,190]

Compared with metal and ceramic materials, carbon-based materials are more suitable as thermally conductive fillers for polymer matrix composites due to various reasons. First, carbon-based materials have higher thermal conductivity, which means

© 2023 Wiley-VCH GmbH

16163028, 0, Downloaded from https://onlinelibrary.wiley.com/doi/10.1002/adfm.202301549 by University of California - Los Ange, Wiley Online Library on [16/06/2023]. See the Terms and Conditions (https://onlinelibrary.wiley.com/terms-and-conditions) on Wiley Online Library for rules of use; OA articles are governed by the applicable Creative Commons License

that under the same filler loading, carbon-based fillers can increase the λ value of composite materials to a greater extent.[4,191] Secondly, the surface modification of carbon-based materials is easier to achieve, which is beneficial in reducing the interfacial thermal resistance by promoting better interactions with polymers.[192] Moreover, the low thermal expansion coefficient and electromagnetic shielding properties of carbon-based fillers can comprehensively optimize the overall performance of composite materials.[13,189,193] The most important aspect is that the weight of carbon-based materials is very light, which conforms to the trend of modern electronic products toward lightweight development.[106,194] Despite the ultrahigh λ value and outstanding mechanical flexibility of carbon-based materials, their high electrical conductivity restricts their applications in a number of electronic fields where components have electrical insulation requirements.[137,166,195,196] This problem can be solved by the surface modification of the filler and the distribution control of the spatial structure.[4,197]

Diamond is the material with the highest λ value typically found in nature (≈2000 W m^{-1} K^{-1}) and can be employed to improve composite materials' thermal conductivity.[198,199] In recent years, nanodiamonds (ND) have received significant interest in being used as fillers for polymer matrices, which inherit to some extent the superior properties of bulk diamond, with excellent electrical properties, optical properties, mechanical properties, and high thermal conductivity.[188,200] Song et al. prepared cellulose/nanodiamond (CND) composites and the λ value of the composites was increased to 5.37 W m^{-1} K^{-1} at an ND content of 5 wt%. The CND composite was converted from a composite hydrogel to a thermally conductive plastic with an in-plane oriented structure by inducing gelation transition through the use of a hot press. The hydrogen bonds between cellulose and ND facilitate the effective dispersion of ND, which, together with the oriented structure of cellulose molecular chains, effectively enhances the heat transfer efficiency.[201]

Carbon black (CB) is an amorphous carbon additive, and its electrical and thermal properties are closely tied to its structure, surface properties, and particle size. After being embedded within a polymer, the electrical and thermal conductivity of the matrix can be improved.[202] Zhao et al. obtained CB/graphene foam (GF)/polydimethylsiloxane (PDMS) composites, and found that including 8 wt% CB improved the thermal conductivity and storage modulus of the resulting composites were improved by 72% and 10%, respectively, compared to virgin GF/PDMS composites. The addition of CB formed a double network in the composites, which substantially improved the λ value and other properties of the composites.[203]

Graphite has excellent thermal conductivity (≈400 W m^{-1} K^{-1}), affordability, good dispersibility in the polymer matrix, and is recognized as an ideal conductive filler for preparing thermally conductive composite materials.[9,204,205] Feng et al. prepared graphite/PP composites with an efficiently established segregated network structure by compression molding PP resin particles coated with graphite flakes, where the λ value of the composites reached 5.4 W m^{-1} K^{-1} at 21.2 vol% graphite flake content.[206]

Graphene is a 2D nanomaterial composed of six-membered carbon rings.[164,207–209] It can be warped into 0D fullerenes, rolled into 1D CNTs, and stacked into 3D graphite, which is the basic unit of other graphite materials. It also has extraordinary mechanical, electrical, and thermal properties (Figure 9b).[3,106,210–213] Each carbon atom in graphene is sp^2 hybridized, and the free movement of π electrons endows graphene with ultrahigh in-plane thermal (≈5300 W m^{-1} K^{-1}) and electrical conductivity, which makes it possible to realize polymer composites with high λ values under a relatively low graphene loading.[214–217] Qin et al. reported that graphene was coated in a commercial melamine-formaldehyde foam to form a backbone. PDMS was then poured into this backbone to prepare RGO@MF/PDMS composites with a hyperelastic double continuous network, and the thermal conductivity was enhanced to 1.68 W m^{-1} K^{-1}.[218]

Expanded graphite (EG) is an exfoliated form of graphite with a thickness of 20–100 nm. The λ value of the expanded graphite-filled composites depends on the degree of EG exfoliation, its dispersion in the matrix, and its aspect ratio (Figure 9c–e).[219,220] A treatment method for inducing and controlling the degree of EG expansion, namely inductively coupled plasma (ICP), was designed and developed by Kim et al. The relationship between the volume expansion of EG and the λ value of the composites was further investigated. It was found that EG with higher volume expansion had higher thermal conductivity enhancement at the same filler loading. The maximum thermal conductivity of the resulting composites with a 3D thermal conductivity network reached 10.77 W m^{-1} K^{-1}.[221]

Carbon nanotubes (CNTs) are anisotropic nanomaterials with high modulus and strength, showing excellent elasticity.[222–225] The sp^2 hybridized carbon atoms enable the efficient transmission of phonons along the tube axis, resulting in high in-plane thermal conductivity. However, phonons are severely scattered perpendicular to the tube axis. Therefore, $\lambda_{\perp}$ is one or two orders of magnitude lower than $\lambda_{\parallel}$.[186] CNTs can be divided into single-walled carbon nanotubes (SWCNTs) and multi-walled carbon nanotubes (MWCNTs). MWCNTs have the highest thermal conductivity because they have the smallest specific surface area, and the heat transfer through their inner walls is not negatively influenced by defects on their outer walls.[226] Morishita et al. fabricated MWCNT/PA6/PPS/(3-glycidyloxypropyl)trimethoxysilane (GOPTS) composites by using GOPTS as a highly reactive shell-forming agent. Then nanosized PPS domains were covered on the end of MWCNT to prevent the formation of conductive paths. The λ value of composite was greatly improved, and the insulation properties were maintained, while the elastic modulus and heat resistance were greatly enhanced.[227]

Carbon fiber is also a vital carbon-based filler. Since CF is composed of an annular geometry parallel to the fiber axis, the λ value (estimated up to 2000 W m^{-1} K^{-1}) along the fiber axis is much higher than the transverse thermal conductivity (10–110 W m^{-1} K^{-1}).[228–230] Using a small amount of CF instead of inorganic thermally conductive fillers can simultaneously improve the polymer's thermal conductivity and mechanical properties.[231] However, its surface is smooth, and the interface adhesion with the polymer matrix is very weak, so it needs to be surface treated to gain appreciable interactions between the CF and polymer.[228,232] Feng et al. oxidized the surface of carbon fibers (OCF) by treating them with a HNO_3/H_2SO_4 mixed acid, and various characterizations showed that the oxygen-containing groups were successfully grafted onto the carbon fiber surface. When included into

© 2023 Wiley-VCH GmbH

16163028, 0, Downloaded from https://onlinelibrary.wiley.com/doi/10.1002/adfm.202301549 by University of California - Los Ange, Wiley Online Library on [16/06/2023]. See the Terms and Conditions (https://onlinelibrary.wiley.com/terms-and-conditions) on Wiley Online Library for rules of use; OA articles are governed by the applicable Creative Commons License

phenolic resin (PR), it was found that the λ value of OCF/PR composites increased 4.16 times compared with that of pure phenolic resin at a filling content of 0.7 wt%, while the λ value of CF/PR composites improved only 3.71 times. Meanwhile, the mechanical properties of OCF/PR composites were also meaningfully improved compared with CF/PR composites.[233] A phase change composite (PCC) with anisotropic thermal conductivity was prepared by Sheng et al. by vacuum-impregnating paraffin into vertically aligned porous carbon scaffolds. At a carbon ratio of 8.8 wt%, the thermal conductivity along the fiber axis was 0.77 W m^{-1} K^{-1} (greater than three times that of pure paraffin), while the thermal conductivity perpendicular to the fiber axis was 0.58 W m^{-1} K^{-1}. The aligned and hollow carbon fiber supports inside the composite were obtained by direct carbonization of rolled cotton sheets with aligned and hollow cellulose fibers, due to the hollow carbon fibers and porous scaffolds on capillary adsorption of liquid paraffin, the composites show good shape stability against leakage when they are heated to temperatures above the melting point of paraffin. In addition, the composite exhibits a high thermal storage capacity and good recyclability.[234]

The continuous emergence of new thermally conductive fillers offers a broader range of ideas for the preparation of highly thermally conductive composites. The use of crystalline or continuous oriented polymers with a high thermal conductivity as alternative fillers to conventional thermally conductive fillers allows the formation of a continuous thermal conductivity path within the polymer matrix. This strategy avoids the introduction of additional interfacial thermal resistance and thus enhances the thermal conductivity of the material more substantially.[235,236] Zhang et al. oriented the polyethylene microfibers (PEMF) through a scalable mold-fixation process and injected polydimethylsiloxane (PDMS) liquid precursor into the structure by vacuum infiltration. Subsequently, the above sample was cured at 80 °C to obtain a composite of vertically aligned PEMF encapsulated by PDMS. This sample could be cut into the desired shapes by a room-temperature water-cutting technique, avoiding any damage to the phonon-delivery structure due to local heating. The final sample obtained achieved an out-of-plane thermal conductivity of 38.27 W m^{-1} K^{-1} at a PEMF content of 55% and increased with increasing PEMF content, while its in-plane thermal conductivity was in the range of 0.24–0.53 W m^{-1} K^{-1}. In addition to the excellent thermal conductivity, the composite has excellent electrical insulation properties as well as high dielectric stability properties. The scalable mold used in this experiment allows the polymer fibers to be arranged into a continuous structure of various complex shapes and multidirectional arrangements, enabling fine control of the polymer fiber content and packing density within the composite. Compared to conventional composites filled with thermally conductive fillers, this method effectively uses ultra-long, highly stretched PEMF to ensure the continuity of the thermal conductivity path and avoid additional interfacial phonon scattering.[236]

Further, inspired by the structure of tropocollagen, Chen et al. processed hierarchically arranged polybenzoxazole (PBO) fibers into a spiral structure and vacuum-impregnated epoxy into this PBO textile to obtain a fully organic epoxy/PBO bulk material. Due to the utilization of the fully organic PBO as an alternative thermal-transport unit to the inorganic filler, the interfacial thermal resistance between the PBO crystals is suppressed to the order of 10^{-10} m^2 K W^{-1}, both in the in-plane and out-of-plane directions. The method constructs a 3D continuous thermal conductivity pathway within the composite with out-of-plane thermal conductivity of 10.85 W m^{-1} K^{-1} and in-plane thermal conductivity of 7.15 W m^{-1} K^{-1} at a PBO content of 33 vol%. Using theoretical molecular simulations with classical nonlinear modeling, the high thermal conductivity of the material is attributed to the hierarchical molecular, spiral, and weaving structure of the PBO, as well as to the noncrystalline chains carrying overlapping phonon densities of states, thus thermally bridging adjacent highly thermally conductive crystals in the PBO fibers. In addition to the high thermal conductivity, the composite has excellent properties such as high mechanical strength, flexibility, lightweight and non-combustibility. This research provides important ideas for the application of organic polymers in thermal management.[235]

The addition of rigid fillers such as metals, ceramics, and carbon materials can substantially improve the thermal conductivity of composites, but at the same time, high filler loading can lead to degradation of their soft mechanical response (e.g. increased modulus and decreased stretchability). Low-modulus polymer composites typically exhibit poor heat transfer properties due to limitations in phonon transport in soft and deformable materials.[237,238] Liquid metal (LM) (including gallium and Bi-InSn) has excellent properties such as high thermal/electrical conductivity, chemical stability, non-toxicity, low viscosity, and deformability, and can be used as thermally conductive fillers to improve the thermal performance of composites. Due to its fluidity, it can improve the thermal conductivity of polymer composites without altering the mechanical properties of the material, exhibiting a unique coupling of electrical, thermal, and mechanical properties.[239,240] The deformability of LM builds thermal conductivity pathways in situ within the composite, possessing strain and thermal-mechanical coupling as the thermal conductivity of the filler is electronically dominated and the filler can deform with the surrounding matrix. Multifunctional LM composites are currently used in thermal interface layers, soft robotics, and soft electronics.[241,242] The balance between high thermal conductivity and high flexibility was achieved for the first time in a new polymer composite prepared by Wang et al. by embedding BNNSs-LM binary fillers into poly(urea-urethane) elastomer (PUUE). The composite has a unique thermal-mechanical-healing combination with low modulus, self-restoration, high loading of rigid fillers, and high thermal conductivity (In-plane thermal conductivity up to 26.6 ±1.63 W m^{-1} K^{-1}). Due to the orientation of the BNNSs and the bridging effect of the LM on the rigid fillers, the thermal conductivity of the composite is maintained and even increased in the deformed state. In addition, the BNNSs effectively disconnect the electrical percolation from the LM and therefore ensure the electrical insulation properties of the composite. This work provides an extremely valuable and innovative idea for efficient heat dissipation in flexible electronics.[44]

3.2. Shapes, Size Distribution, and Aspect Ratio of Fillers

Thermally conductive fillers are diverse in geometry and size, where differences in the filler sizes influence the λ value of the final polymer composite in different ways. For instance, the shape

© 2023 Wiley-VCH GmbH

16163028, 0, Downloaded from https://onlinelibrary.wiley.com/doi/10.1002/adfm.202301549 by University of California - Los Ange, Wiley Online Library on [16/06/2023]. See the Terms and Conditions (https://onlinelibrary.wiley.com/terms-and-conditions) on Wiley Online Library for rules of use; OA articles are governed by the applicable Creative Commons License

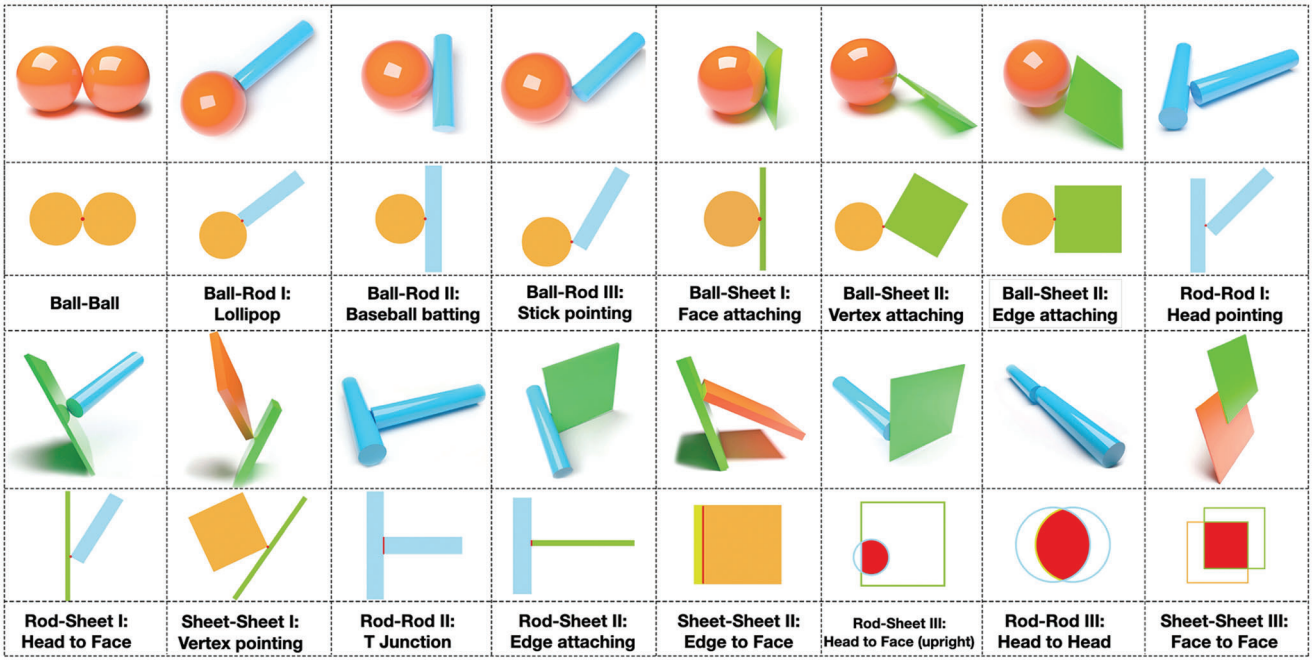

Figure 10. Schematic drawing of different types of contact between fillers and polymers.

of the filler affects the type of contact between the fillers (**Figure 10**). The contact areas are determined by the contact type, which in turn affects its contact thermal resistance, ultimately affecting the λ values of the final polymer composites.[156,243,244] Compared with spherical fillers, fibrous and lamellar fillers can form a larger contact area between the fillers and the matrix, provide a wider path for phonon transmission, and improve the λ value of composite materials by decreasing the interface contact thermal resistance.[245,246] However, the excessively high aspect ratio of the filler means that the size of the filler is quite large in a certain dimension, thereby increasing the possibility of defects in the composite material and thus adversely affecting the overall performance of the composite material.

The geometric size of the filler influences its dispersion and accumulation in the polymer matrix, which in turn affects the λ value of composite material. Large-size fillers reduce the total interfacial thermal resistance by reducing the contact area between the fillers and the polymers, thereby improving the λ value of the composite.[158] Moradi et al. investigated the relationship between particle size and thermal conductivity of particle-filled composites. In order to exclude the interference from other factors, no surface treatments were applied to BN particles. It was found that the λ value of epoxy-BN composites with the same volume fraction of filler increased with the increase of BN particle size.[247]

However, some studies have shown that smaller-sized fillers are more effective in improving thermal conductivity. It is believed that at the same filling amount, the number of small-sized fillers is much higher than that of large-sized fillers, which is more effective for the formation of heat conduction paths. When the particle size is too large, close packing cannot be formed between the fillers, which is unfavorable for forming heat conduction paths. Ren et al. prepared spherical BNs of different sizes using spray drying granulation and vacuum sintering methods. The obtained spherical BNs were then filled into polydimethylsiloxane (PDMS) to prepare BN/DMS composites. After comparison, it was found that the composite filled with spherical BN with a particle size of 89.0 µm had a higher λ value than the composite filled with spherical BN with a particle size of 160.0 µm. Moreover, the thermal conductivity of the spherical BN/PDMS composites was four times higher than that of the platelet-like BN/PDMS composites at a filler content of 50 wt% (**Figure 11**).[248]

What cannot be ignored is that the small-sized fillers tend to accumulate and aggregate in the polymer matrix with increasing filler loading, which increases the number of interface defects.[249] Moreover, when the spacing between fillers is further reduced, various minor defects are likely to form large cracks, which destroy the continuity of the polymer matrix and makes the composite material prone to fracture under stress concentration.[250] Considering that the number of interfaces formed by larger-sized fillers in the polymer is much lower than in smaller ones, it is more likely that larger-size fillers can lead to the improvement of λ values in composite materials.

3.3. Filler Loading

From the point of view of the thermal conduction path theory, it is difficult for the thermally conductive particles to contact each other to form an effective thermal conductivity network at low filler content.[132] Therefore, a certain amount of filler is needed to obtain a high thermal conductivity.[19,229,251] However, high loading of fillers will result in other problems, such as a decrease in mechanical properties, increase in cost, change in the insulation

© 2023 Wiley-VCH GmbH

16163028, 0, Downloaded from https://onlinelibrary.wiley.com/doi/10.1002/adfm.202301549 by University of California - Los Ange, Wiley Online Library on [16/06/2023]. See the Terms and Conditions (https://onlinelibrary.wiley.com/terms-and-conditions) on Wiley Online Library for rules of use; OA articles are governed by the applicable Creative Commons License

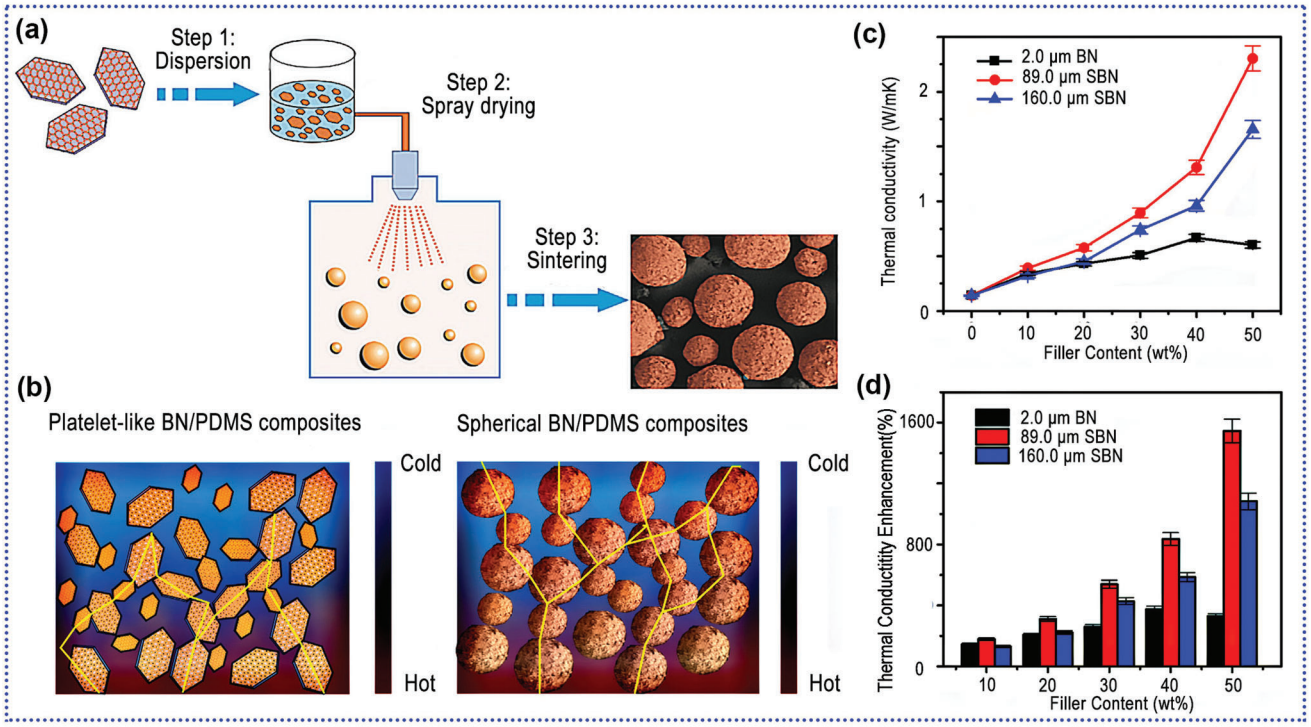

Figure 11. Systems filled with fillers of different shapes, sizes and aspect ratios. a) Schematic illustration of the spherical BN fabrication procedure. b) Schematic diagram of the comparison of thermal-conduction path between the platelet-like BN/PDMS composites and spherical BN/PDMS composites. c) Thermal conductivity of the BN/PDMS composites as a function of filler contents. d) Thermal conductivity enhancement with the increase of the filler content. Reproduced with permission.[248] Copyright 2019, Elsevier.

properties of the material when using conductive fillers, and so on.[39,48,252–254]

Many studies in recent years have continued to achieve effective thermal conductivity networks at low filler contents, where not only were the λ values of the materials substantially improved but also a variety of excellent properties of the polymer were maintained.[255–258] For example, Han et al. prepared aerogels with boron nitride nanosheets aligned by a bidirectional freezing technique and then prepared BNNS/epoxy composites by infiltrating epoxy resin into the BNNS structure. The λ value of the composite was enhanced to 6.07 W m^{-1} K^{-1} at a filler content of only 15 vol% (**Figure 12**a,b).[259] Furthermore, Li et al. prepared epoxy composites with a 3-D graphene network structure using a liquid nitrogen-driven assembly approach combined with an ice template method. The resulting composites exhibited excellent mechanical properties and a heat transfer enhancement efficiency of 431% for 1 wt% loading. This method significantly reduces the amount of thermally conductive fillers in the composite by creating an effective thermal conductivity network (Figure 12c,d).[32]

3.4. Orientation of Filler

The thermal conductivity of the filled thermally conductive composite is also related to the spacial orientation of the filler in the polymer matrix.[260–262] In 1D and 2D materials with a high aspect ratio, the magnitude of λ in the direction of longer dimensions is higher than that along other transverse directions.[263,264] By aligning these fillers in the length direction, a high λ value can be achieved with low filler content.[265,266] At present, there are many methods to achieve the directional arrangement of fillers, such as the use of electric fields,[267] magnetic fields,[268,269] filtration methods,[270] hot-pressing, and electrostatic spinning.[271]

Electric field-controlled alignment is a method to achieve directional alignment of electrically responsive materials under an external electric field. Usually, particles with conductive properties or non-conductive particles coated with materials with excellent dielectric properties are placed between two electrodes, and an electric potential is applied by parallel electrodes to cause the electrically responsive particles to achieve directional alignment along the electric field direction via electrophoresis and dielectrophoresis.[204,272–274] Using an electric field, Guo et al. achieved the directional alignment of graphene in a PVDF matrix. The thermal conductivity of obtained graphene/PVDF composite membranes was 226% larger than pure PVDF at 20 wt% graphene content. The crystallinity and thermal stability of composite have also been improved (**Figure 13**a).[275]

Magnetic field-controlled alignment is an operation that applies on the thermally conductive fillers with superparamagnetic properties, which is usually facilitated by surface coating nanoparticles to make the fillers magnetically responsive.[156,276] An external magnetic field remotely controls the orientation of the filler in a low-viscosity suspension. After solidification, the filler in the liquid maintains the magnetically imposed orientation.[16] Kim et al. reported a method to enhance the λ

© 2023 Wiley-VCH GmbH

16163028, 0, Downloaded from https://onlinelibrary.wiley.com/doi/10.1002/adfm.202301549 by University of California - Los Ange, Wiley Online Library on [16/06/2023]. See the Terms and Conditions (https://onlinelibrary.wiley.com/terms-and-conditions) on Wiley Online Library for rules of use; OA articles are governed by the applicable Creative Commons License

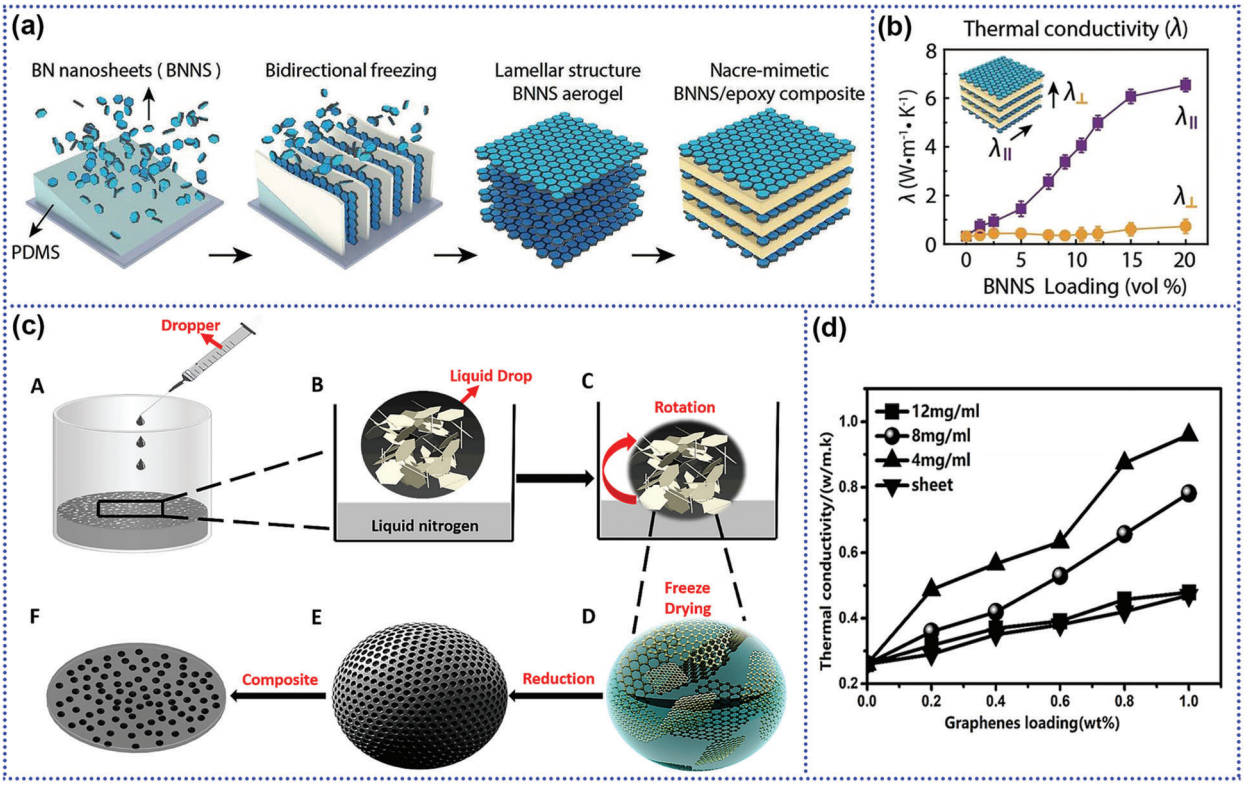

Figure 12. The effect of filler content on the thermal conductivity of composites. a) Fabrication route of BNNS/epoxy composites. b) Thermal conductivity in the parallel ($\lambda_{||}$) and perpendicular ($\lambda_{\perp}$) directions of the composites. Reproduced with permission.[259] Copyright 2019, Wiley–VCH GmbH. c) Fabrication route of the graphene oxide microspheres/epoxy resin composites. d) Thermal conductivity of the composites. Reproduced with permission.[32] Copyright 2019, Elsevier.

value of composites by orienting the filler with the magnetic field. First, BNNPs were prepared through liquid-phase exfoliation, during which the BNNPs and Fe_3O_4 particles were bonded via van der Waals attraction. Due to the superparamagnetic properties of Fe_3O_4, the BNNPs achieved an oriented arrangement in the polymer matrix when exposed to a magnetic field. The final composite gained a thermal conductivity of 1.07 W m^{-1} K^{-1} at a filler loading of 20 wt%, which is 72.6% higher than that of the untreated BN composite at the same filler ratio. Apart from this, the thermal and mechanical properties of the composites were also improved due to the effective stress transfer (Figure 13b).[277]

Vacuum-assisted filtration is also a preparation method to achieve a directional arrangement of fillers in the polymer. Especially for 2D fillers, the effect of gravity could be leveraged to achieve parallel alignment in the polymer.[278,279] When the filler content reaches a certain level, the parallel-aligned fillers will form thermal conductivity paths, thus significantly improving the in-plane thermal conductivity of the composite.[280,281] Wang et al. used vacuum-assisted filtration to arrange BNNSs in poly(ethylene-co-vinyl acetate) in preparing composites whose in-plane thermal conductivity reached 13.2 W m^{-1} K^{-1} at a BNNSs content of 50 wt%. The significant increase in λ value of the system was mainly ascribed to the highly oriented BNNSs, which allowed the establishment of an effective thermal conductivity network for heat transfer (Figure 13c,d).[282]

Hot-pressing is a process where an orderly arrangement of fillers along the in-plane direction can be realized using compression at high temperatures, which can be implemented at an industrial scale. It is a promising method as it can yield a layer-by-layer assembling filler structure during the fabrication process with minimal defects.[249,263] Hu et al. reported that epoxy resin/oriented BN composites were prepared via hot-pressing, where the vertically applied pressure resulted in a well-ordered BN microstructure in the composites. This method takes full advantage of the difference in thermal conductivity of h-BN in the in-plane and out-of-plane directions. Remarkably, the reported in-plane thermal conductivity of the composite was 6.09 W m^{-1} K^{-1} at 50 wt% content, while it is merely 2.44 W m^{-1} K^{-1} for epoxy resin/random BN composites (Figure 13e–h).[263]

3.5. Hybrid Filler Strategy

It is challenging to appreciably raise the λ value of a composite through the use of a single type of filler.[51,254,283] Hybrid systems, where different types,[129,284] morphologies,[37,260] and sizes[285] of high thermal conductivity fillers can increase the system's filling rate to form thermal paths, thereby reducing the viscosity of system, to trigger a synergistic effect between fillers to obtain better thermal conductivity (**Figure 14**a–f).[15,286,287] The synergistic ef-

© 2023 Wiley-VCH GmbH

16163028, 0, Downloaded from https://onlinelibrary.wiley.com/doi/10.1002/adfm.202301549 by University of California - Los Ange, Wiley Online Library on [16/06/2023]. See the Terms and Conditions (https://onlinelibrary.wiley.com/terms-and-conditions) on Wiley Online Library for rules of use; OA articles are governed by the applicable Creative Commons License

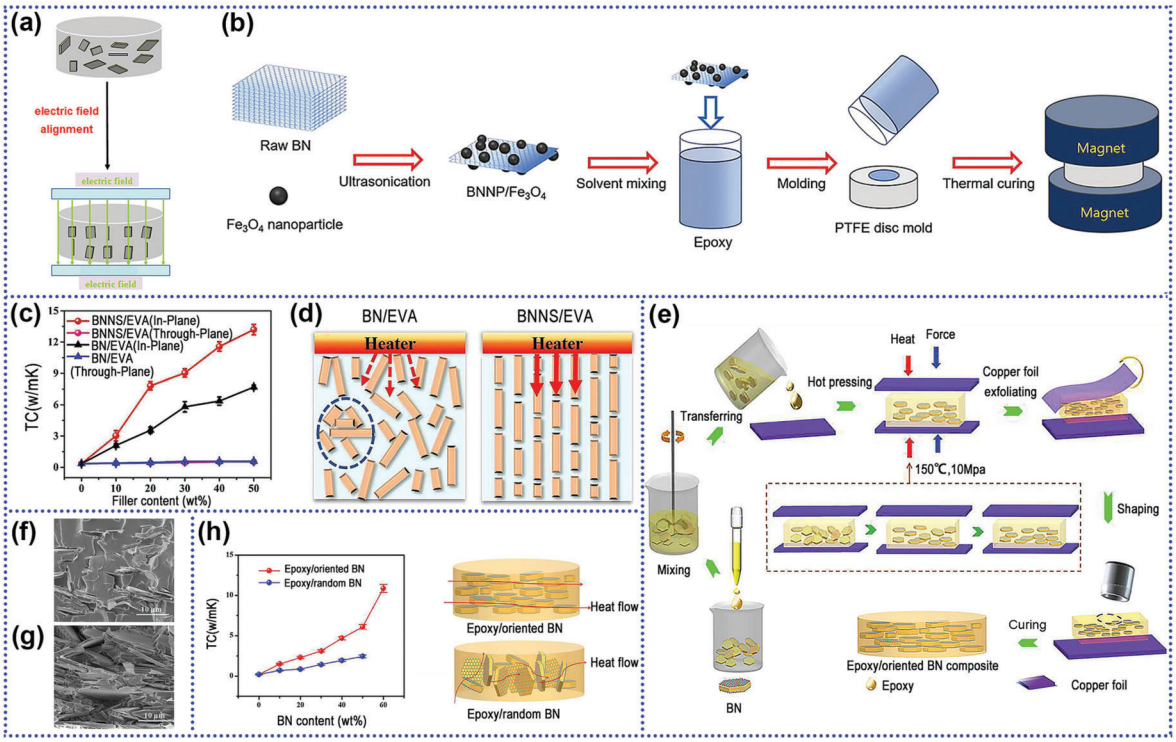

Figure 13. Oriented arrangement of fillers within the composite. a) The electric field was employed during membrane casting. Reproduced with permission.[275] Copyright 2016, Elsevier. b) Fabrication procedure of vertically aligned BNNP/Fe_3O_4 composite. Reproduced with permission.[277] Copyright 2019, Elsevier. c) In-plane and through-plane λ value of BNNS/EVA and BN/EVA composite films. d) Diagram of thermal conductive pathways in composites. Reproduced with permission.[282] Copyright 2019, Elsevier. e) Illustration of the fabricated process of the composites. f, g) Fracture microstructures of epoxy resin/oriented BN composites at 10 wt% loading (f) and 50 wt% loading (g). h) Thermal conductivity and Schematic heat flowing paths of composites. Reproduced with permission.[263] Copyright 2018, Elsevier.

fect in the binary thermally conductive filler system is calculated as:

$$f = \frac{\lambda_{AB/P} - \lambda_P}{(\lambda_{A/P} - \lambda_P) + (\lambda_{B/P} - \lambda_P)} \quad (1)$$

where $\lambda_{AB/P}$, λ_P, $\lambda_{A/P}$, and $\lambda_{B/P}$ represent the thermal conductivity of the binary hybrid system, the thermal conductivity of the pure polymer, the thermal conductivity of the composite filled with filler A, and the thermal conductivity of the composite filled with filler B, respectively.[41,288] Owais et al. prepared epoxy nanocomposites using a ternary hybrid filler system to obtain a composite with a high λ value and high electrical insulation characteristics (Figure 14g).[289] Zhang et al. constructed a membrane of interpenetrating fibers of carbon nanotube (CNT)@carbonized polyvinyl alcohol (αPVA) and polyimide (PI)/boron nitride nanosheets (BNNS). After electrospinning precursor solutions for both fibers, the membrane was subjected to high temperatures, leading to the carbonization of PVA, which exposed the CNT in the PVA and connected isolated BNNS on the PI/BNNS fibers to form an interpenetrating thermally conductive network chain. The resulting PI/BNNS/CNT@αPVA membranes achieved high in-plane thermal conductivity of 8.4 W m^{-1} K^{-1} at a low filling amount (with 30 wt% BNNS and 0.3 wt% CNT).[290]

3.6. Functionalization

Large interfacial thermal resistance is one of the critical factors hindering the improvement of the λ of composites.[130,170,291,292] The introduction of highly thermally conductive fillers to the polymer matrix creates many interfaces between the polymer and the fillers, resulting in interfacial thermal resistance.[98,198] Meanwhile, because of the difference in polarity between the polymer matrix and the filler, the corresponding interfacial compatibility is poor, making it hard for the powder to be uniformly dispersed in the polymer, resulting in aggregation.[226,293] Coupled with gaps and defects in the interface, all these factors will affect the thermal conductivity and other mechanical properties of the composite material.[294] Moreover, due to the difference in density and atomic arrangement between the two phases of the polymer matrix and the fillers, the vibrations of the phonons in two phases are inconsistent, resulting in phonon scattering at the interface, which leads to a decrease in λ values.[291,295–297]

Surface modification of the filler will improve interfacial interactions between the polymer and the filler, thereby improving the λ value of the composite material.[298,299] There are two main strategies to improve the interfacial compatibility and reduce the interfacial thermal resistance between the polymer matrix and the fillers: covalent functionalization and noncovalent functionalization.

© 2023 Wiley-VCH GmbH

16163028, 0, Downloaded from https://onlinelibrary.wiley.com/doi/10.1002/adfm.202301549 by University of California - Los Ange, Wiley Online Library on [16/06/2023]. See the Terms and Conditions (https://onlinelibrary.wiley.com/terms-and-conditions) on Wiley Online Library for rules of use; OA articles are governed by the applicable Creative Commons License

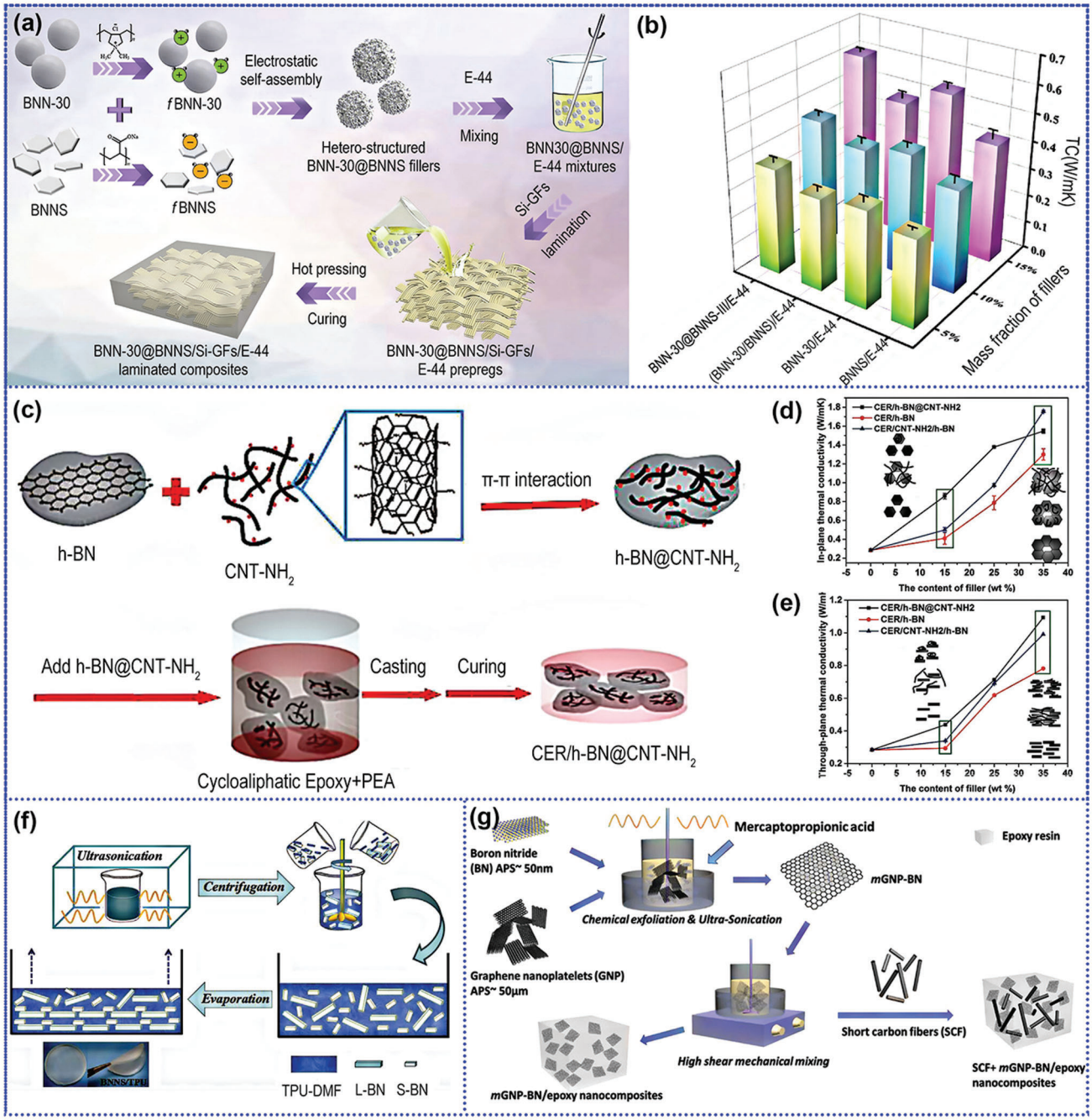

Figure 14. Hybridization between different fillers. a) Schematic diagram of preparation for BNN-30@BNNS/Si-GFs/E-44 laminated composites. b) λ values of the epoxy composites with 15 wt% fillers. Reproduced with permission.[283] Copyright 2021, Elsevier. c) Illustration of the procedures for preparation the composite film. d) In-plane and e) through-plane thermal conductivity of the composite film as the function of filler content. Reproduced with permission.[284] Copyright 2018, Elsevier. f) Schematic illustration for the synthesis processes of BNNS/TPU nanocomposite films. Reproduced with permission.[286] Copyright 2019, Elsevier. g) Schematic presentation of the preparation of *m*GNP-BN and 3 wt% SCF + *m*GNP-BN/epoxy nanocomposites. Reproduced with permission.[289] Copyright 2019, Elsevier.

3.6.1. Covalent Functionalization

To significantly improve the λ value of materials, most studies have focused on increasing the interaction between the polymer and the fillers, and the formation of covalent bonds has undoubtedly become one of the tactics.[49,296,300] Covalent functionalization is done by introducing chemical groups on the surface of the fillers in the form of covalent bonds to promote interfacial interactions between the filler and the polymer.[301,302] Commonly used covalent modifiers in-

 © 2023 Wiley-VCH GmbH

16163028, 0, Downloaded from https://onlinelibrary.wiley.com/doi/10.1002/adfm.202301549 by University of California - Los Ange, Wiley Online Library on [16/06/2023]. See the Terms and Conditions (https://onlinelibrary.wiley.com/terms-and-conditions) on Wiley Online Library for rules of use; OA articles are governed by the applicable Creative Commons License

clude silane coupling agents, fluorine, Lewis acids and bases, dopamine, etc.

Silane-based surface treatment have been widely used to increase compatibility between the filler and the polymer.[293,303] Guo et al. synthesized fluorine-containing PI via a sequential in-situ polymerization, then γ-aminopropyl triethoxy silane (KH-560) and aminopropyllsobutyl polyhedral oligomeric silsesquioxane (NH_2-POSS) were employed to functionalize the BN fillers. The reported λ value (0.71 W m^{-1} K^{-1}) of f-BN/PI composites was higher than that of unfunctionalized BN/PI composites (0.19 W m^{-1} K^{-1}) under the same loading (**Figure 15**a,b).[127] Jiang et al. grafted APTES on the surface of hydroxylated BN through covalent interaction. Composites with a 3D segregated structure were fabricated by forming core–shell BN@PPS composite particles and subsequently hot pressing them to achieve a high λ value of 4.15 W m^{-1} K^{-1} (Figure 15c).[304] In addition, Yang et al. combined KH-560 and NH_2-POSS to modify BN, significantly improving the thermal conductivity of the composite material after functionalization.[305]

Fluorination modification can be used to control the electrical insulation of the carbon-based filler by tuning the degree of fluorination.[306–308] This is possible because the degree of fluorination of carbon-based materials corresponds to the molar ratio of F/C atoms, and the bandgap of a material generally increases with the increase of the F/C molar ratio.[309,310] Wang et al. introduced fluorinated CNT (FCNT) into a polymer and reported an in-plane thermal conductivity of 14.1 W m^{-1} K^{-1} at a filler dosage of 35 wt%, along with excellent electrical insulation (Figure 15d,e).[1] At present, the research on fluorination of fillers in the field of insulation and heat conduction is still in its infancy, and there is enormous room for exploration.

Lewis acid-base interactions (δ+-δ-) are noncovalent and occur between electron pair acceptors and the electron pair donors through a ligand covalent bonding. Noncovalent modification of fillers can significantly enhance the interaction between the filler and polymer.[178,311] Su et al. prepared flexible fiber-reinforced laminated composites combined with functionalized graphene (f-G) and hexagonal boron nitride (h-BN) by colloid-blending and self-assembly technology. Weak base diethylenetriamine (DETA) reduces GO to graphene and introduces pentagon-heptagon rings to the graphene sheet surface. The process utilizes Lewis acid-base interactions between DETA and GO to improve the compatibility between the filler and the polymer. The in-plane thermal conductivity of the resulting composite was enhanced to approximately 4.20 W m^{-1} K^{-1}.[312]

As a convenient and environmentally friendly strategy, dopamine chemistry is mainly used to modify thermally conductive fillers.[313] Dopamine (DA) is a biomolecule which can be easily oxidized under weak alkaline conditions to form an adhesive polydopamine (PDA) coating on the substrate material.[314,315] Based on this unique property, DA can modify conductive fillers to form an insulating PDA coating on their surface to suppress electrical conduction. PDA can also improve the interface compatibility between the filler and the polymer matrix, thereby enhancing the dispersion effect of the fillers.[269,316] Ding et al. made a polydopamine-modified h-BN (h-BN@PDA)/polyimide composites via vacuum filtration and hot pressing. A large number of hydrogen bonds were formed between the hydroxyl- and amino-rich PDA and PI matrix, which greatly enhanced the compatibility between the filler and the polymer, resulting in not only a considerable increase in the thermal conductivity of the composites (the in-plane thermal conductivity reached 3.01 W m^{-1} K^{-1} when the filler loading was 20 vol%) but also a corresponding improvement in the mechanical properties and thermal stability (Figure 15f–j).[317]

The formation of covalent bonds can promote phonon coupling and thermal transmission, improve the wettability between fillers and polymers, and improve the dispersion of fillers in the polymer. But formation of covalent bond often affects the interfacial properties of the fillers.[41,165,318–320] For example, research has shown that when chemical groups are grafted onto the surface of graphene through covalent bonds, the λ value of the composite is not always significantly enhanced.[321,322] This is because the chemical modification of graphene undermines the conjugated structure of its surface, reduces the mean free path of phonons, and increases the scattering of phonons. Jiang et al. explored the enhancement effect of GO and GR on the λ value of the composites separately. By comparison, it was found that the λ value of GO(BN-OH)/PS composites was significantly lower than that of GR(BN)/PS composites with the same filler dosage. The reason for this result is that the introduction of oxygen-containing groups destroys the integrity of the crystal structure and causes phonon scattering, which is not conducive to the enhancement of the λ value of the composites (**Figure 16**a,b).[294] Therefore, the λ value of modified graphene has not been markedly improved as expected.

A recent report on dopamine-modified CNT perfectly avoids the drawbacks associated with covalent modification, which dramatically improves the compatibility between filler and polymer by covalent modification without destroying the CNT crystal structure. Xie et al. combined mussel-inspired chemistry and surface-initiated reversible addition-fragmentation chain transfer (RAFT) polymerization to enhance the interaction between CNT and epoxy resin. Firstly, PDA was coated on the CNT surfaces, followed by nondestructive grafting of polymethyl methacrylate (PMMA) or polyglycidyl methacrylate (PGMA) macromolecular chains onto PDA encapsulated CNTs by noncovalent or covalent forces, respectively. It was finally concluded that the polymer@CNT composites with covalent interfaces exhibit more significant advantages in improving the composites' thermal conductivity as well as other properties (Figure 16c–e).[300]

3.6.2. Noncovalent Interactions

Noncovalent interactions can improve the compatibility between polymer and filler without damaging the crystal structure,[226,319,323] including π–π stacking,[17] hydrogen bonds,[255,324] etc. The electron of one molecule interacts with the empty orbital of another molecule to form a noncovalent force close to the strength of the covalent bond.

π–π stacking originates from the attraction between charged clouds of different signs between aromatic systems. It is a weak interaction exhibited by a π-electron conjugated system in conformity with a special spatial arrangement.[325,326] Wang et al. modified CNTs with dopamine to improve the interfacial interaction

© 2023 Wiley-VCH GmbH

16163028, 0, Downloaded from https://onlinelibrary.wiley.com/doi/10.1002/adfm.202301549 by University of California - Los Ange, Wiley Online Library on [16/06/2023]. See the Terms and Conditions (https://onlinelibrary.wiley.com/terms-and-conditions) on Wiley Online Library for rules of use; OA articles are governed by the applicable Creative Commons License

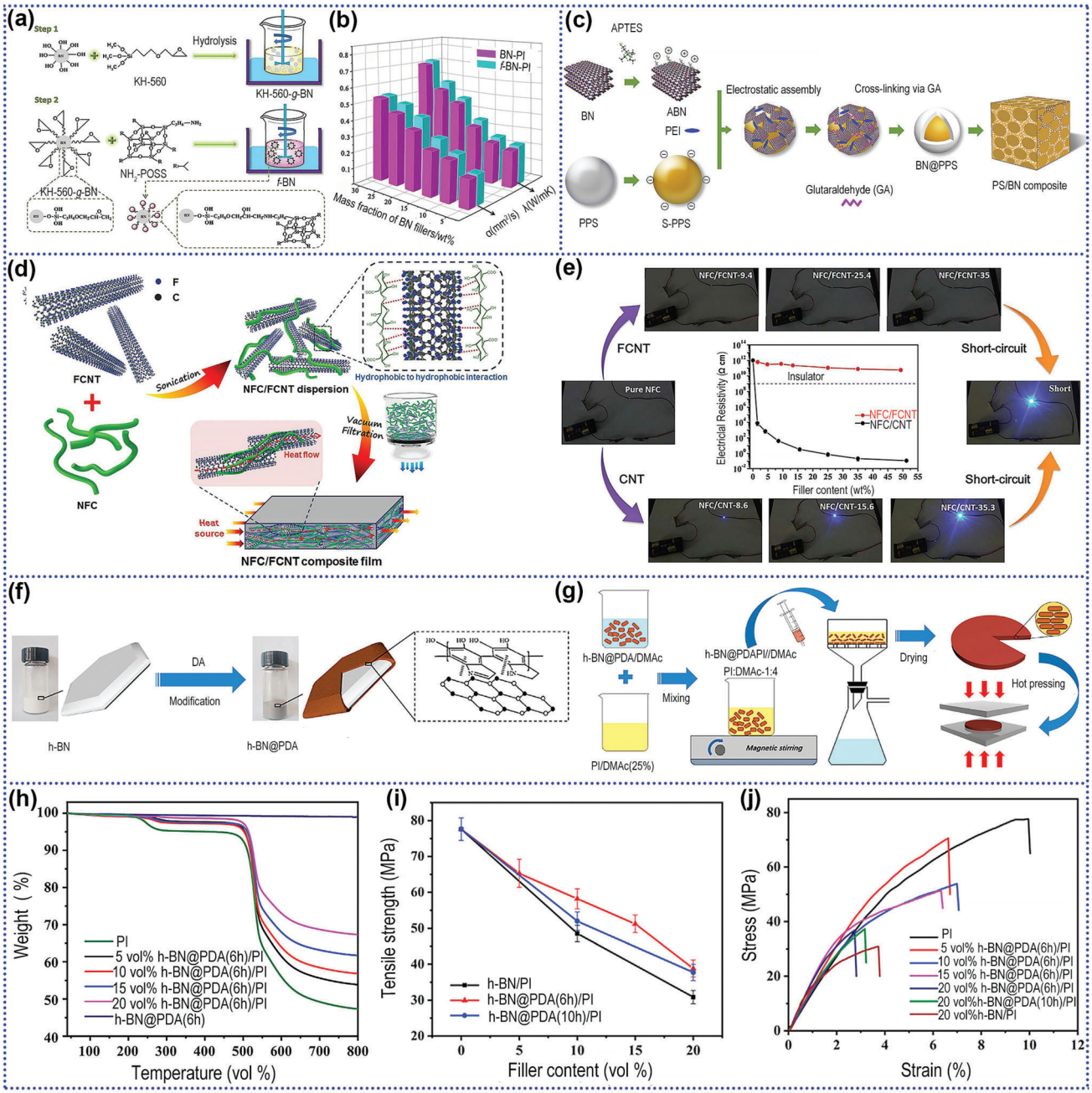

Figure 15. Covalent functionalization of fillers (1). a) Diagram of the general preparation process of the *f*-BN. b) Thermal conductivities of the PI-based thermally conductive composites. Reproduced with permission.[127] Copyright 2019, Elsevier. c) Illustration of the synthesis process of BN@PPS and PPS/BN composite. Reproduced with permission.[304] Copyright 2017, Elsevier. d) Illustration of the preparation of the NFC/FCNT composite films. e) Volume electrical resistance of composite films with various filler dosage, and the photos of the NFC-based films as the conductor (4 mm×12 mm) to obtain a LED. Reproduced with permission.[1] Copyright 2018, American Chemical Society. f) Illustration of PDA modification. g) The preparation process of h-BN@PDA/PI composites. h) TGA curves for h-BN@PDA(6h)/PI composites. i) The corresponding tensile fracture strength of PI and PI composites. j) The stress–strain curves of pure PI and PI composites. Reproduced with permission.[317] Copyright 2020, Elsevier.

between CNTs and the ethylene-vinyl acetate copolymer (EVA) matrix. The affinity between CNTs and PDA was derived from π–π stacking interactions between the aromatic rings in PDA chains and others on the CNTs. After noncovalent modification, the lattice integrity of CNTs was not destroyed, which ensured its inherent thermal and electrical conductivity. The thermal conductivity and EMI shielding effectiveness (EMI SE) of the final prepared CNT@PDA/EVA composites were significantly enhanced (**Figure 17**a,b).[327]

As a classic noncovalent bond, the hydrogen bond is 10–100 times stronger than the van der Waals force, which can efficiently enhance the thermal conductivity of composite materials.[118]

 © 2023 Wiley-VCH GmbH

16163028, 0, Downloaded from https://onlinelibrary.wiley.com/doi/10.1002/adfm.202301549 by University of California - Los Ange, Wiley Online Library on [16/06/2023]. See the Terms and Conditions (https://onlinelibrary.wiley.com/terms-and-conditions) on Wiley Online Library for rules of use; OA articles are governed by the applicable Creative Commons License

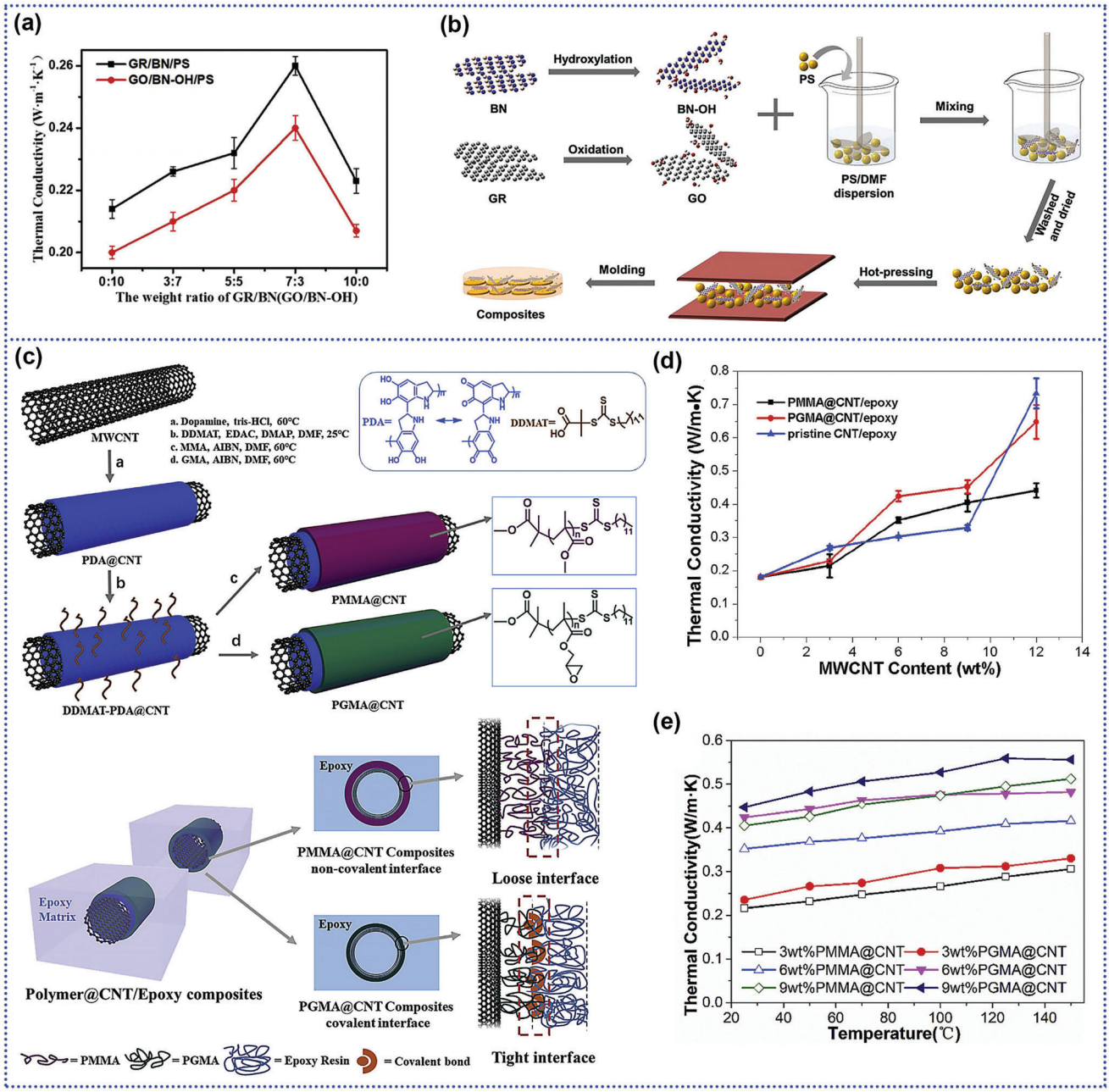

Figure 16. Covalent functionalization of fillers (2). a) The λ value of the composites varied with the weight ratio of GR/BN (GO/BN-OH). b) Illustration of the formation of PS composites. Reproduced with permission.[294] Copyright 2020, Elsevier. c) Illustration of the preparation process of polymer@CNTs by RAFT Polymerization. d) Thermal conductivity of the CNT and polymer@CNT composites at 25 °C. e) Thermal conductivity of the polymer@CNT composites at various temperatures. Reproduced with permission.[300] Copyright 2017, Elsevier.

Jiang et al. leveraged the hydrogen bonding between hydroxylated BN and polyvinyl alcohol to control the formation of a 3-D interconnected BN network and then used vacuum-assisted impregnation to infiltrate PAI into the skeleton. The resulting PAI/3D-BN composites reached a high λ value of 1.17 W m^{-1} K^{-1} at a low BN dosage of 4 wt%. This report also provides a guided hydrogen bond strategy for many applications (Figure 17c–f).[255]

A question of interest regarding 2D fillers is whether it is more beneficial to perform in-plane or edge modification. Many studies have shown that in-plane grafting of modifiers on 2D materials can disrupt the conjugate structure of material, generating defects on the 2D material and causing phonon scattering, affecting the intrinsic λ value of filler and the overall composite.[328]

On the contrary, edge modification can improve the interfacial compatibility between filler and polymer without destroying

© 2023 Wiley-VCH GmbH

16163028, 0, Downloaded from https://onlinelibrary.wiley.com/doi/10.1002/adfm.202301549 by University of California - Los Ange, Wiley Online Library on [16/06/2023]. See the Terms and Conditions (https://onlinelibrary.wiley.com/terms-and-conditions) on Wiley Online Library for rules of use; OA articles are governed by the applicable Creative Commons License

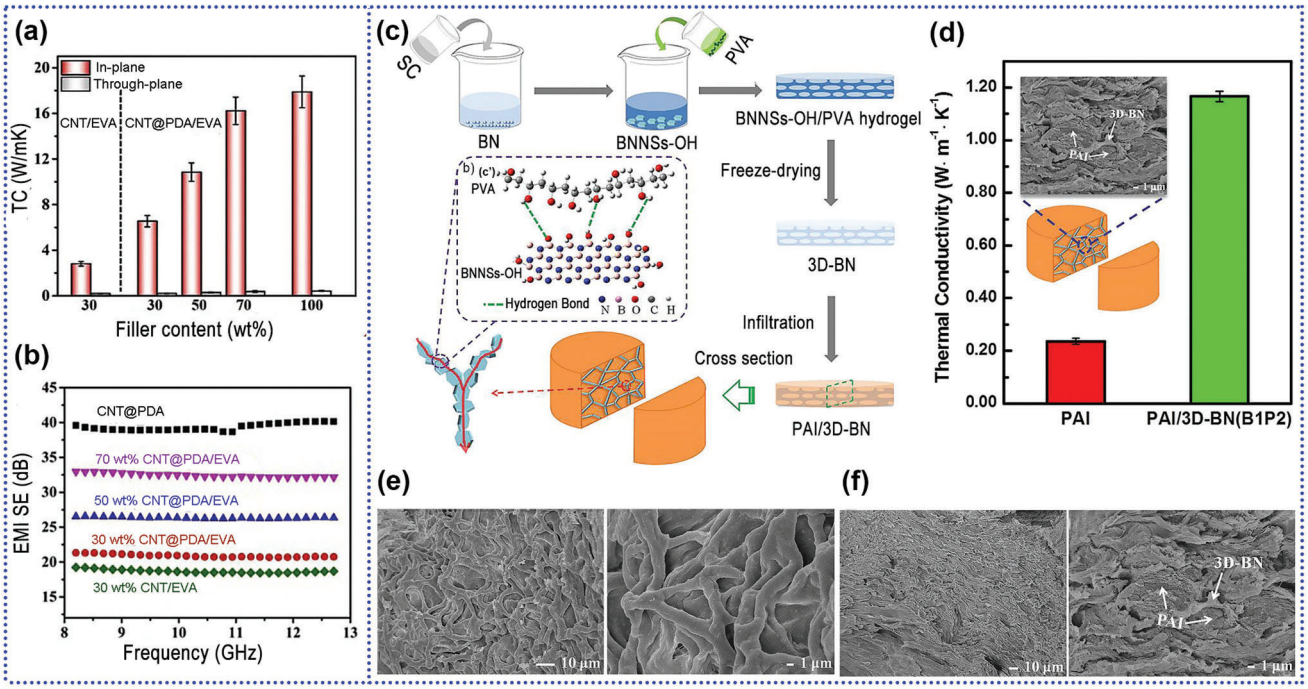

Figure 17. Noncovalent functionalization of fillers. a) TCs of CNT@PDA/EVA films. b) EMI SE of CNT/EVA and CNT@PDA/EVA films. Reproduced with permission.[327] Copyright 2020, Elsevier. c) Illustrates of the preparation progress of PAI/3D-BN composites, diagram of the structure of the composites and the hydrogen bond between PVA and BNNSs-OH (c'). d) The TC of the composites. e) The SEM image of 3D BN network. f) The SEM image of composite. Reproduced with permission.[255] Copyright 2018, American Chemical Society.

the crystal structure and preventing phonon scattering within the 2D material.[329] The influence that edge defects impart on fillers has a negligible effect on their intrinsic λ values, so it has a tremendous impact on improving the overall thermal conductivity of composites.[328] Wu et al. explored the in-plane modification and edge modification of BNNS on the λ value of a composite. Among them, nitric acid oxidation was used to cause in-plane hydroxylation of BNNS (POH-BNNS), while aqueous ball milling was employed to hydroxylate the edge of BNNS (EOH-BNNS). It was found that the λ value of POH-BNNS filled nanocomposites increased by only 10.2% at low OH content. With an increase in the OH content, the surface defects also increased, and the thermal conductivity decreased even further. In contrast, the thermal conductivity of EOH-BNNS nanocomposites increased by almost 100%. This study demonstrates that edge hydroxylation reduces the interfacial thermal resistance while preserving lattice integrity in the filler, thus promoting phonon transport.[328]

3.7. Building a 3D Network

As mentioned above, controlling interfacial thermal resistance is essential for improving the λ value of composites and is positively correlated with the magnitude of the interfacial area.[251,330] Moreover, the total interfacial area of the composite reduces with the increase of the filler dimension.[284,331] Therefore, by constructing a 3D interconnected skeleton structure to serve as a thermally conductive network chain, part of the heat is transferred along the direction of the skeleton, and the λ value of the composite material can be significantly improved.[292,295,332] **Figure 18** simulates the efficiency of heat transfer in pure polymers, blended complexes, and composites with 3D thermally conductive network structures. There have been many methods for constructing 3D network structures, such as ice-template,[330,333,334] segregated structure, and chemical vapor deposition.

The ice-templating method, which utilizes self-assembly induced by ice crystal growth followed by the vacuum filtration of polymer matrix, is a widely used method for building 3D networks.[149,335,336] This method utilizes the volume repulsion of ice crystals to orient the fillers along the ice growth direction, forming an effective vertically interconnected thermally conductive network at the micron and nanometer scales.[94,133,337] Li et al. built a thermally conductive graphene aerogel (GA) network with a 3D skeleton using ice templating. The λ value of GA- epoxy composites reached 2.69 W m^{-1} K^{-1} at an ultralow GA dosage of 1.11 vol%, and the λ value of composites was highly dependent on the surface properties of GO, which showed an increasing trend with the increase of GA reduction degree.[338] Inspired by the annual ring structure of trees, Lin et al. obtained PDMS/G-MWCNT composite aerogels with "multi-concentric cylinders" by air drying in combination with the freeze-drying method. At a low filler content of 6.0 vol.%, the through-plane thermal conductivity enhancement can reach 744%.[260]

© 2023 Wiley-VCH GmbH

16163028, 0, Downloaded from https://onlinelibrary.wiley.com/doi/10.1002/adfm.202301549 by University of California - Los Ange, Wiley Online Library on [16/06/2023]. See the Terms and Conditions (https://onlinelibrary.wiley.com/terms-and-conditions) on Wiley Online Library for rules of use; OA articles are governed by the applicable Creative Commons License

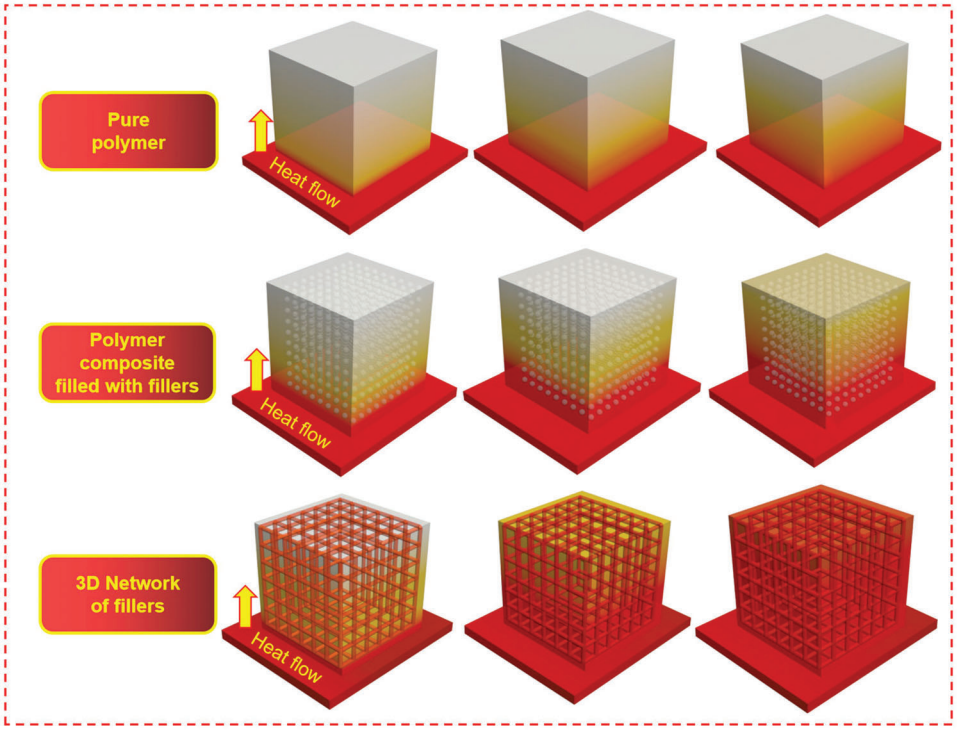

Figure 18. Illustration of 3D thermally conductive network structures for improved efficiency of heat transfer in pure polymers, blended complexes, and composites.

The fabrication of composites with segregated structures has been regarded as a promising strategy in raising the thermal conductivity of a material the by forming a cocontinuous phase of fillers in the polymer matrix at a low filler amount.[266,297,339] There are currently two approaches to a segregated structure of the composites.

The first one is to mix the fillers with the polymer and distribute the fillers in a polymer phases or at the interface of two mutually immiscible polymer phases by physical or chemical interaction to achieve a continuous distribution of the fillers.[340] Wang et al. employed the in situ polymerization and emulsion template method to obtain PS@BN composite with λ value of 0.94 W m^{-1} K^{-1} at 33.3 wt% filler content while effectively enhancing the mechanical strength and thermal stability of the composites. The method is based on oil-water interface assembly, using BN to stabilize Styrene oil droplets in the aqueous phase to form a stable Pickering emulsion and using in-situ polymerization to synthesize PS microspheres with very thin BN layer covered surface. The 3D thermally conductive BN network is formed by hot-compressing PS@BN microspheres based on the initial microsphere template (**Figure 19**a–d).[341] Xu et al. constructed a thermally conductive skeleton with a 3D structure using NH_4HCO_3 as a sacrificial material and then infusing epoxy into this skeleton to obtain the 3D-BN/epoxy that achieves a high thermal conductivity of 6.11 W m^{-1} K^{-1} while achieving low dielectric constant and excellent electrical insulation properties (Figure 19e–f).[196]

The second one is to use polymer spheres or other solid material as templates, distribute the filler on the surface of polymer spheres, and then hot-pressing composites in a mold to form a continuous filler network, or remove the template material and immerse another polymer material in that thermally conductive skeleton.[342,343] Leng et al. proposed a method to enhance the thermal conductivity of composites by a 3-D foam structure. The resulting BN/epoxy composites achieved a λ value of 1.98 W m^{-1} K^{-1} and showed improved dielectric and mechanical properties.[344] Also,Xiao et al. manufactured an epoxy/SiC_w composite. The PS/SiC_w compound was first prepared using PS microspheres as templates, which were then removed by sintering to obtain a porous SiC_w skeleton. Finally, the epoxy is injected into the frame. The resulting epoxy/SiC_w composite has an λ value of 0.43 W m^{-1} K^{-1} with only 3.91 vol% of SiC_w, nearly two times higher than that of pure epoxy (Figure 19g).[252]

By chemical vapor deposition (CVD), a vapor of gaseous reactant or liquid reactant is introduced into the chamber to react with a substrate.[136] The desired reactants can be obtained by controlled conditions.[345] However, CVD has drawbacks, such as high preparation cost, harsh reaction conditions, and low efficiency. Shen et al. fabricated multilayer graphene networks (MGW) with a 3D graphene structure by first compressing multiple stacked layers of Ni foam together. CVD was used to deposit a web of graphene which was then etched to produce a thermally conductive 3D skeleton, where liquid epoxy resin was infiltrated into the porous scaffold to produce the final structure. The exhibited λ value was equal to 8.8 W m^{-1} K^{-1} with a graphene content of 8.3 wt%.[346] Ji et al. constructed 3D networks using the CVD method and electrostatic flocking method to improve

© 2023 Wiley-VCH GmbH

16163028, 0, Downloaded from https://onlinelibrary.wiley.com/doi/10.1002/adfm.202301549 by University of California - Los Ange, Wiley Online Library on [16/06/2023]. See the Terms and Conditions (https://onlinelibrary.wiley.com/terms-and-conditions) on Wiley Online Library for rules of use; OA articles are governed by the applicable Creative Commons License

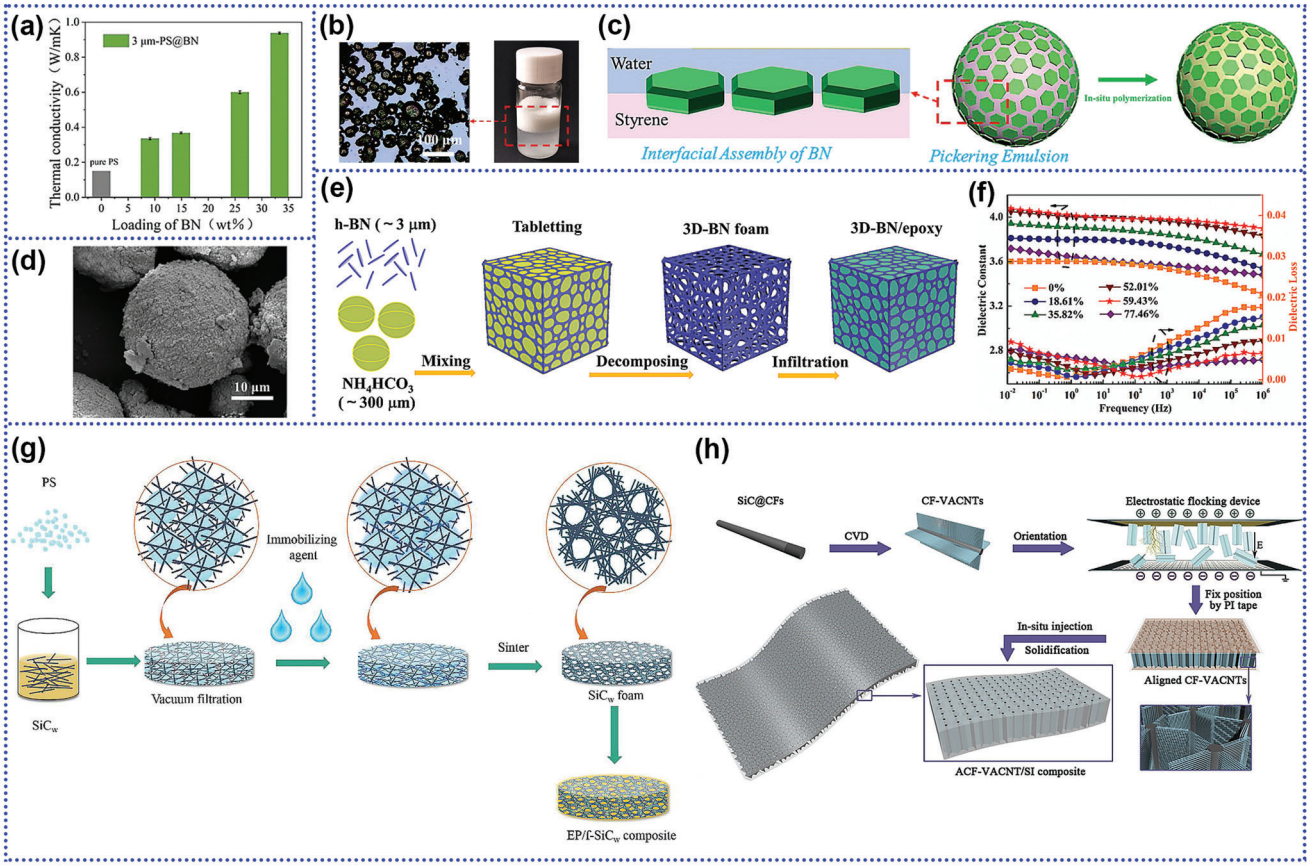

Figure 19. Construction of a 3D thermal conductivity network. a) The λ of composite versus different BN dosage. b) The image and photos of pickering emulsion. c) Schematic of pickering emulsion and the formation of PS@BN microspheres. d) SEM image of a PS@BN microsphere. Reproduced with permission.[341] Copyright 2019, American Chemical Society. e) Diagrammatic illustration of formation of the 3D-BN/epoxy composites. f) Dielectric properties as a function of frequency. Reproduced with permission.[196] Copyright 2020, Elsevier. Illustrations of g) Preparation of EP/f-SiCw composites. Reproduced with permission.[252] Copyright 2019, Elsevier. h) Preparation procedure for ACF-VACNT/SI composite. Reproduced with permission.[347] Copyright 2018, Elsevier.

the λ value in an aligned carbon fiber-carbon nanotube/Silastic (ACF-VACNT/SI) composite. The composite obtained possessed high λ value in both the axial and the radial directions of the CFs (Figure 19h).[347]

While constructing a 3D network structure can obtain a high λ value at lower filling amounts,[6,7] the methods (such as the ice template method, chemical vapor deposition method, etc.) are often time consuming, complicated, and challenging to adopt to industrial production.[210,344,348]

3.8. Polymer Matrix

Among the factors that influence the λ values of composites, the importance of the polymer matrix itself is often neglected, since it plays a crucial role as the hosting phase in determining the overall performance of composite.[349,350] Some studies have shown matrices with higher λ have a higher thermal conductivity.[197] A facile and effective method to prepare graphene/thermoplastic composites was reported by Alam et al. The efficiency of enhancing the λ value was studied for composites made of PE, PP, PVA (polyvinyl alcohol), and PVDF (polyvinylidene fluoride), respectively. It was found that the thermal conductivity of PE, PP, PVA, and PVDF composites' was 1.84, 1.53, 1.43, and 1.47 W m^{-1} K^{-1}, respectively, when the graphene content was 10 wt%.[351]

When a large amount of rigid filler is added, the modulus of the composite material rises sharply, making it impossible for the TIM to adequately fill the gap between the heater and the heat sink, resulting in a high contact thermal resistance. The problem can be solved by applying high pressure to make the TIM more closely in contact with the two interfaces, thus reducing the contact thermal resistance. However, for electronics vulnerable to external forces, this method is not feasible and increases complications in the practical application process.[352,353] Furthermore, during cyclic heating and cooling, the bonding between the TIM and the interface is highly susceptible, seriously affecting the long-term serviceability of the TIM. On the other hand, TIMs can be designed as soft, self-adhesive, or flowable composites with low modulus, which can easily fill the gap at low applied pressure (<650 kPa) and more effectively reduce the contact thermal resistance.[354]

The main strategies for the preparation of such composites are: 1) Using a small amount of filler to create an effective thermal conductivity path and implanting the thermal conductivity

© 2023 Wiley-VCH GmbH

16163028, 0, Downloaded from https://onlinelibrary.wiley.com/doi/10.1002/adfm.202301549 by University of California - Los Ange, Wiley Online Library on [16/06/2023]. See the Terms and Conditions (https://onlinelibrary.wiley.com/terms-and-conditions) on Wiley Online Library for rules of use; OA articles are governed by the applicable Creative Commons License

Table 2. λ values of common polymers.

Polymers	λ (Wm^{-1} K^{-1})	Ref	Polymers	λ (Wm^{-1} K^{-1})	Ref
High density polyethylene (HDPE)	0.44	[202]	Polyetheretherketone (PEEK)	0.25	[63]
Low density polyethylene (LDPE)	0.30	[202]	Poly (dimethylsiloxane) (PDMS)	0.25	[202]
Polyurethane (PU)	0.21	[350]	Epoxy resin (EP)	0.23	[350]
Polyphenylene sulfide (PPS)	0.29	[350]	Polypropylene(PP)	0.21	[63]
Nylon-6 (PA6)	0.25	[202]	Polyvinylidene difluoride (PVDF)	0.2	[63]
Polyimide (PI)	0.27	[63]	Polymethylmethacrylate (PMMA)	0.21	[202]
Polytetrafluoroethylene (PTFE)	0.27	[202]	Polyvinyl chloride (PVC)	0.21	[350]
Silicone rubber (SR)	0.21	[63]	Polystyrene (PS)	0.19	[63]

path into a low modulus polymer, minimizing the effect of rigid filler on polymer properties. 2) Replacing the rigid filler with liquid metal, so that the softness of the polymer is maintained to a great extent without changing the filler content, resulting in a composite material with high thermal conductivity while maintaining good wettability and compliance.[352,355] Inspired by the molecular-level mechanism analysis of macroscopic mechanical properties, Cai et al. developed a soft polydimethylsiloxane/aluminum composite gel with high toughness and low thermal resistance by extending the polymer strands and controlling the filler content in the composite gel. Lengthening of the polymer strands facilitates their unfolding to prevent crack propagation and increases softness and intrinsic toughness, thereby counteracting the negative effects of filler addition on flexibility and elastic modulus. The addition of appropriate fillers complicates the force propagation path, increases stress dissipation and intrinsic toughness, and reduces thermal resistance. The resulting composite gel exhibits excellent flexibility (high stretchability of 6.91 and low elastic modulus of 340 kPa), high toughness (4741.48 J m^{-2}), and low thermal resistance (0.14 cm^2 K W^{-1} at 10 pressure). In addition, the composite was found to still have efficient heat dissipation properties after several cycles when operating at high power conditions (**Table 2**).[356]

3.9. Processing Technology

The processing technique can also affect the λ value of composite materials.[297] Various methods have been used to improve the dispersion of fillers in the polymer and help build effective heat conduction paths to increase the thermal conductivity of polymer composites. The methods used to increase their thermal conductivity mainly include the blending method,[337,357] in situ polymerization, 3D printing, and electrospinning.[192,358]

The blending method includes four main categories: mechanical blending, solution blending, melt blending, and suspension/emulsion blending. Among them, solution blending is a traditional method for preparing thermally conductive composites.[359] The fillers are randomly distributed in a composite, and it requires a high loading of filler to form thermally conductive paths.[294,355] For example, Cao et al. modified CNTs with (3-aminopropyl) trimethoxysilane (APTMS) and then prepared A-CNTs/PVDF composites using a solution blending method. The obtained composite showcased a λ value of 2.15 W m^{-1} K^{-1} when the dosage of A-CNTs was 40 vol%.[360]

In comparison, melt mixing is a classical method for preparing thermoplastic composites, which is relatively economical, environmentally friendly, and can be easily implemented on an industrial scale compared to other methods.[220,361,362] However, when the filler loading increases, the viscosity of the composite also increases, which leads to a requirement for high shear forces and temperatures to disperse the filler in polymer.[212,363] Chi et al. formed iron oxide nanoparticles (Fe_3O_4) on the surface of low-density polyethylene (LDPE) particles by solvothermal reaction and then modified the surface with polydopamine (PDA). Then the Fe_3O_4/LDPE composites were treated under a constant magnetic field at 130 °C for 30 min to form Fe_3O_4 conductive chains in the polymer. The composites exhibited higher λ value and dielectric constants than the Fe_3O_4/LDPE composites with random dispersion of fillers at the same dosage. The surface treatment of PDA did not improve the conductivity of the composite, but simultaneously improved the compatibility of Fe_3O_4 nanoparticles and LDPE matrix, which combined to enhance various properties of the composites.[364]

In-situ polymerization can occur in the presence of the filler, which can be well dispersed in the polymer matrix.[101] Oh and Kim fabricated BN/PMMA composites via in situ polymerization and hot-pressing. The thermal conductivity of the composites was 3.73 W m^{-1} K^{-1} at a BN loading of 70 wt%. In order to establish good interfacial bonding between the PMMA and BN, BN was first silanized by VTES. After that, the BN/PMMA composites were successfully fabricated by covalently linking the modified BN and PMMA. The composites showed significant enhancements in thermal conductivity compared to the conventional melt-blended BN/PMMA composites.[365]

3D printing is a relatively new manufacturing method. When the polymer composite material is extruded in a melt, the thermally conductive fillers are oriented and overlap with each other, markedly enhancing the λ value of the polymer composite material in a certain direction.[366–368] Jia et al. utilized fused deposition modeling (FDM) to prepare polymer/graphite-based composites, where graphite flakes were aligned in the in-plane direction, showing a high through-plane thermally conductive of 5.5 W m^{-1} K^{-1}.[369]

Among these processing methods, electrospinning technology has attracted growing attention.[370,371] The λ value of

© 2023 Wiley-VCH GmbH

16163028, 0, Downloaded from https://onlinelibrary.wiley.com/doi/10.1002/adfm.202301549 by University of California - Los Ange, Wiley Online Library on [16/06/2023]. See the Terms and Conditions (https://onlinelibrary.wiley.com/terms-and-conditions) on Wiley Online Library for rules of use; OA articles are governed by the applicable Creative Commons License

a material can be adjusted by changing the diameter of the electrospun fiber.[372] This fabrication method can also lead to the uniform dispersion of fillers.[373,374] In addition to the possible alignment of thermally conductive fillers and oriented polymeric nanofibers, electrospun composites have shorter contact distances between the thermally conductive fillers and ultimately further improve the λ value of composites, compared with materials made from methods that produce worse filler dispersion uniformity.[48,358] Also, the adsorption of fillers on electrospun fibers can be used to improve the performance of electrospun films.[22,178] Guo et al. used a combination of electrospinning, cold pressing, and hot pressing to prepare an oriented GNPs/PS composite with an in-plane λ value of 4.72 W m^{-1} K^{-1}, higher than that of random GNPs/PS composite with the same GNPs content.[375] Chen et al. prepared a PVA/BNNS membrane with electrospun materials, then rolled them up to generate cylinders, followed by infiltrating polydimethylsiloxane (PDMS) into the porous cylinders using vacuum-assisted impregnation. The through-plane λ value of the composite was increased by 10 times at a filler content of 15.6 vol%.[370]

3.10. Other Factors

3.10.1. Dispersion of Fillers

To improve the dispersibility of fillers in the polymer matrix, researchers have developed enormous strategies to improve the surface properties of fillers. When a filler is uniformly dispersed in a polymer, polymer chains with low thermal conductivity surround the fillers, which is not conducive to effective heat transfer.[376] On the contrary, when the thermally conductive filler is segregated in the polymer, heat conduction paths can be formed in the segregated sites, thereby increasing the final λ value of the composite material.[377] Most of the current preparation techniques enable the fillers to be distributed in a thermally conductive network chain to achieve high λ value of the composite at low filler dosage.[376,378,379]

3.10.2. Interfaces in Polymer Composites

The interface is the dominating barrier to heat transfer. It is generally assumed that the interface is a sub-nanometer scale in thickness. The interfacial structure changes when the dispersed phase (thermally conductive fillers) is distinct from the polymer.[380] The interface in composite materials usually includes the following parts: the original contact area between the polymer and the fillers, the solid-liquid layer formed by diffusion between the polymer and the fillers, and the surface coating introduced by the surface modification of the fillers.[103,381] Hence, the chemical composition and structure of the interfaces in polymer composites are often intricate. There are three main properties observed in interfaces, which are: transmission, blocking, scattering, and absorption. First, the transmission effect means that the interface plays a role as a bridge between the polymer and the fillers, ensuring the continuity of the polymer and the fillers and realizing the effective transfer of properties between the different components.[382] Second, the blocking effect manifests in interfaces that can mechanically block crack propagation and reduce stress concentration. Third, scattering and absorption effects refer to the ability of the interface to scatter and absorb light waves, acoustic waves, and thermoelastic waves, etc.[115,116]

4. Applications of Thermal Conductive Polymer Composites in Electronic Devices

In this section, some emerging applications of thermal conductivity polymer composites in advanced electronic devices are reviewed, such as advanced electronic packaging, LED devices, energy storage devices, electrocaloric cooling devices, solar cells, etc.

4.1. Electronic Packaging

The integrated circuits industry manufactures microelectronic elements with increasing insulative packaging and power density, increasing demands for dissipative heat transfer. The integrated circuits industry is basically concerned with the design, manufacturing, and electronic packaging of the chip. The electronic packaging materials play a crucial role in the performance and reliability of the electronic devices. In designing packaging materials, it is expected that they are heat conductive, can bear/transfer stresses, and are well isolated to keep the entire system from external disturbance. Electronic packaging technology is classified into ceramic packaging, metal packaging, and polymer packaging, where most of the encapsulant materials are polymeric materials, specifically epoxies, by virtue of their low price and easy processability.

In 3D packaging systems, thermally conductive composites are used as underfill materials to fill the gaps between solder bumps and promote the transfer of heat in electronics devices. Epoxy underfills are typical polymer packaging materials in flip-chip packaging tech (**Figure 20**a–e). Nevertheless, the poor reliability and CTE mismatch between IC chips and substrate, are ever present challenges that remain to be addressed.[383]

In the packaging process of electronics, TIMs are usually employed at all interfaces between two solid materials. Generally, at interfaces between heat-generating dies and integrated heat spreaders as well as between the integrated heat spreader and a heat sink, which are termed TIM1 and TIM2, respectively (Figure 20d). Usually, the MOSFET is the principal heating device in switching power supplies. Thus, Chen et al. used oriented BNNS nanocomposite films as TIMs to transfer heat between a MOSFET and heat sink. These nanocomposite films can be easily prepared by electrospinning a polymer and BNNSs nanofibers, and it exhibited both high thermal conductivity and excellent electrical insulation (Figure 20f,g).[22]

Copper clad laminates (CCLs) have a sandwich structure, which is composed of insulation layers covered with copper foils on both sides, where polymers are most commonly used insulating layer materials. As a base material for printed circuit boards (PCBs), CCLs provide mechanical support and effective linkage for electronic components, ensuring good insulation for signal transmission. As electronic information technology is developing

© 2023 Wiley-VCH GmbH

16163028, 0, Downloaded from https://onlinelibrary.wiley.com/doi/10.1002/adfm.202301549 by University of California - Los Ange, Wiley Online Library on [16/06/2023]. See the Terms and Conditions (https://onlinelibrary.wiley.com/terms-and-conditions) on Wiley Online Library for rules of use; OA articles are governed by the applicable Creative Commons License

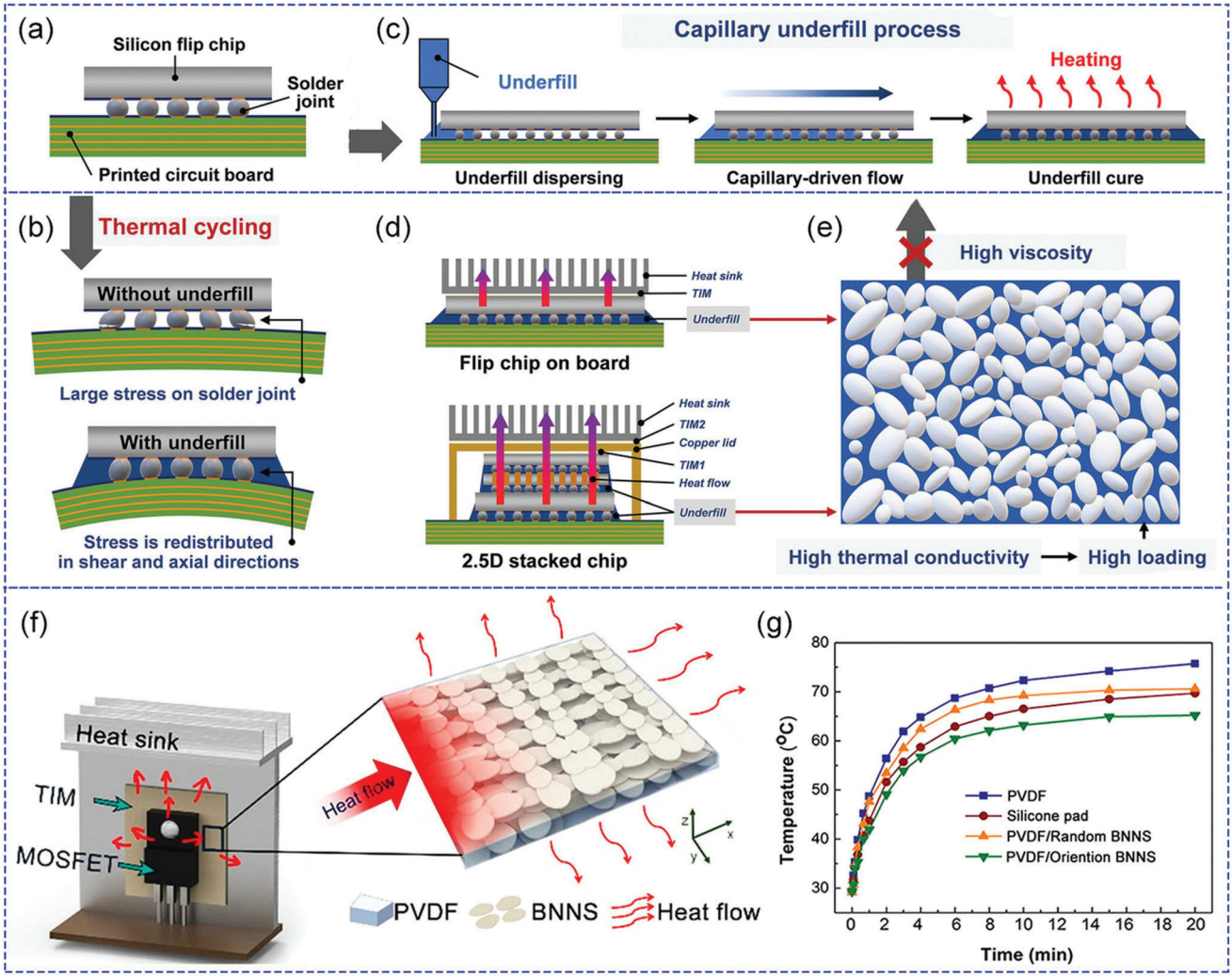

Figure 20. Application of composite materials in electronic packaging. a) Schematic of flip chip packaging. b) Effects of thermal stress on solder joints with and without underfill polymers. c) Routine capillary underfill process. d) Thermal transfer in flip-chip on board and 2.5D stacked chip package. e) Underfill composites with high particle loading. Reproduced with permission.[383] Copyright 2022, Wiley–VCH GmbH. f) Schematic of the structures of the TIM materials. g) Device surface temperature VS Time. Reproduced with permission.[22] Copyright 2018, American Chemical Society.

towards high frequency and high integration, the performance requirements for CCLs have become increasingly strict, especially high thermal conductivity, as well as low dielectric constant and dielectric loss to avoid potential signal delays or losses. Dispersing ceramic fillers in polymer matrices can prepare electronic substrates with good thermal conductivity. However, thermally conducting polymer composites used in electronic equipment need some level of mechanical strength. To solve this problem of mechanical strength, fiber materials with ceramic fillers are used to prepare PCBs for 5G communication technology.[384]

4.2. LEDs Devices

Owing to their lower photoelectric conversion efficiency, LED lights inevitably generate plenty of heat, which may severely limit their performance. For instance, miniature LED displays integrate a huge number of mini LEDs in a small panel area. The heat generated by these LEDs can cause chromatic aberrations in the display and reduce the light output and lifetime of the LEDs. Therefore, thermally conductive polymer materials can be placed between the LED chip and CU heat sink as a thermal interface material to manage the heat transfer and guarantee the stable operation of the LED (**Figure 21**a–c).[52,220,348,357,385]

4.3. Solar Cells

Photovoltaic (PV) technology is a revolutionary device that produces green energy to help humanity overcome challenges related to energy production and emissions. However, due to the low photoelectric conversion efficiency of solar cells, most of the absorbed solar radiation is dissipated in the form of heat, which further suppresses the photoelectric conversion efficiency of solar cells. Dissipating the heat that builds up inside the cells has become a paramount issue to tackle in order to guarantee

© 2023 Wiley-VCH GmbH

16163028, 0, Downloaded from https://onlinelibrary.wiley.com/doi/10.1002/adfm.202301549 by University of California - Los Ange, Wiley Online Library on [16/06/2023]. See the Terms and Conditions (https://onlinelibrary.wiley.com/terms-and-conditions) on Wiley Online Library for rules of use; OA articles are governed by the applicable Creative Commons License

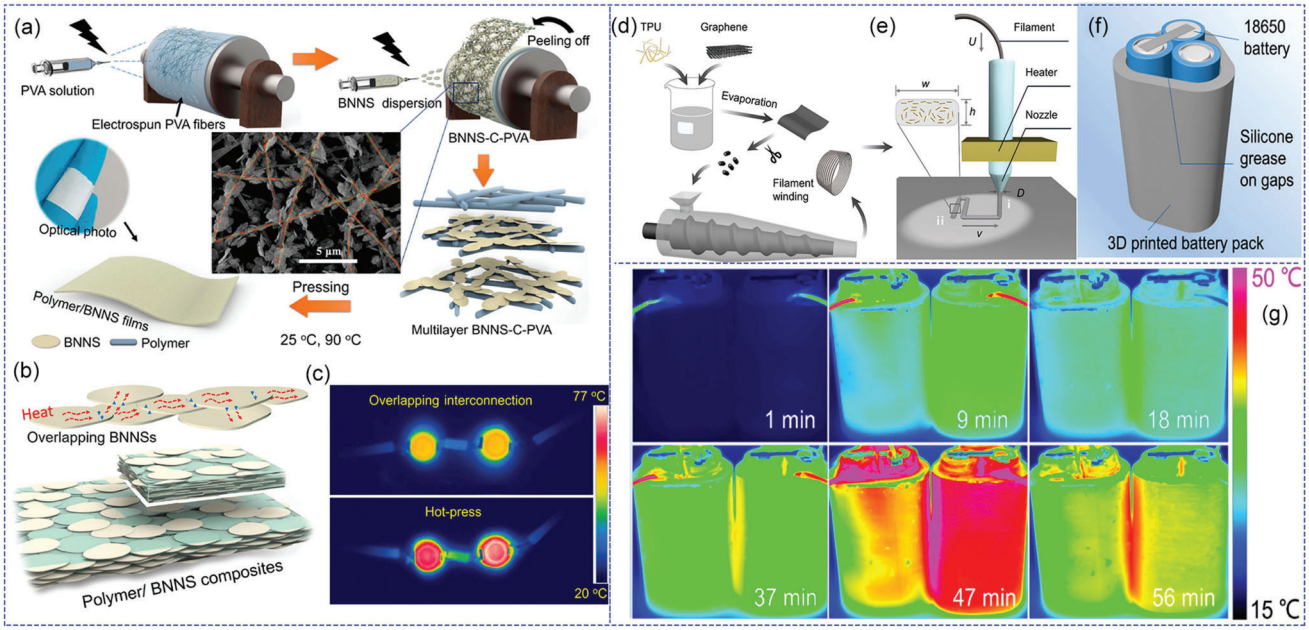

Figure 21. Application of composite materials in LEDs devices. a) Schematic of the preparation of PVA/BNNS composites. b) Diagram of nanocomposites with overlapping BNNSs. c) Thermal imaging of two LEDs integrated with nanocomposites with different BNNS structures. Reproduced with permission.[348] Copyright 2019, American Chemical Society. d) Schematic of the preparation of graphene/TPU filaments. e) Typical FDM printing process of composites which contains an extrusion (i) and a deposition (ii) process. f) Schematics of the battery testing setup for thermal imaging detection. g) Thermal imaging detection of 3D printed pure TPU battery pack (left) and graphene/TPU battery pack (right). Reproduced with permission.[367] Copyright 2021, American Chemical Society.

extended cell lifespan and increased photovoltaic conversion efficiencies.[386–388]

EVA is a typical PV module encapsulation polymer material, where more than 80% of PV modules are encapsulated by EVA. In addition, polyvinyl fluoride film is often used as the back material for batteries. However, both of EVA and polyvinyl fluoride have low thermal conductivity (all less than 0.4 W m^{-1} K^{-1}), which can lead to significant heat build-up. Therefore, the introduction of fillers that combine high thermal conductivity and electrical insulation in polymer materials is an effective means to improve the thermal conductivity of solar cell encapsulation materials and back materials.[389]

4.4. Energy Storage Devices

Electrochemical energy storage devices generate excessive heat during the charging/discharging process, leading to the rapid degradation of capacity and thermal runaway. Prolonged operation at a high temperature can soften the polymer separator of lithium-ion batteries and supercapacitors, resulting in their short circuiting. Thermally conductive composites with high ionic conductivity can be used as separators or all-solid polymer electrolytes for lithium-ion batteries and capacitors, effectively dissipating the heat generated during operation (Figure 21d–g).[367]

In the field of electric vehicles, numerous accidents have been caused by failures related to thermal build-up in car batteries. Specifically, the rapid accumulation of heat during battery charging/discharging is the main cause of battery fires. In addition, uneven temperature distribution can seriously threaten the performance and lifetime of battery. With this, there is a considerable venue for thermally conductive polymer composites to create more economical and societal impacts.[390,391]

4.5. Electrocaloric Cooling Devices

Due to the giant electrocaloric effect found in dielectrics, electrocaloric cooling devices are emerging as an environmentally friendly cooling alternative to more energy intensive methods. However, the low thermal conductivity of ferroelectric polymer materials (such as P(VDF-TrFE) limits their electrocaloric cooling performance. Introduction of thermally conductive ceramics into ferroelectric polymers can effectively increase the in-plane thermal conductivity of pyroelectric films, which facilitates heat transfer in a particular direction.[392,393]

4.6. Other Applications

As previously mentioned, heat accumulation in electronic devices is generally detrimental to their stability and service life. Therefore, the usage of efficient thermally conductive composites is not only a requirement for current electronics but also for the development of next-generation electronic devices. The applications of thermally conductive composites in some new areas are also emerging, such as heat dissipation films in thermoelectric generators,[394] personal thermal management,[395–397] and thermal switches.[398]

© 2023 Wiley-VCH GmbH

16163028, 0, Downloaded from https://onlinelibrary.wiley.com/doi/10.1002/adfm.202301549 by University of California - Los Ange, Wiley Online Library on [16/06/2023]. See the Terms and Conditions (https://onlinelibrary.wiley.com/terms-and-conditions) on Wiley Online Library for rules of use; OA articles are governed by the applicable Creative Commons License

5. Conclusions and Outlook

In conclusion, we holistically review the advancement of thermally conductive polymer composites and outline a technical roadmap. The key factors that influence its thermally conductive performance can be summarized as: i) thermally conductive filler types (Ceramics and carbons were emphatically introduced), ii) the shape, size, aspect ratio, loading, and oriented arrangement of thermally conductive fillers, iii) hybrid fillers strategy, iv) filler functionalization, v) 3D thermal conductive networks, vi) polymer matrices, vii) processing technologies, viii) external conditions and ix) other factors (dispersion and interface).

In order to improve the intrinsic thermal conductivity of polymer matrices, the macromolecule system with high intrinsic thermal conductivities can be achieved by designing and changing the molecules and chain structures to obtain specific physical structures (such as orientated structure, liquid crystal structures, and crystalline structures, etc.). For filled thermally conductive polymers, the thermal conductivity of the fillers, the structure of thermally conductive network, and the interface between polymer and fillers strongly influence the thermal conductivity of composites.

Despite the progresses that have been made so far, certain challenges remain that need to be addressed for the further development thermally conductive polymer composite technology:

(i) To achieve a significant increase in thermal conductivity of composites prepared in the traditional way, a large amount of thermally conductive fillers must be added, and the addition of too many thermally conductive fillers not only harms the mechanical properties of the material, but also increases the interfacial thermal resistance. This is due to the introduction of more interfaces that lead to more scattering sites for phonons, hampering heat flow in the material. Thus, achieving high thermal conductivity with low filler content is still a hot topic in current research.

(ii) The intrinsic λ value of polymers is extremely low, but the polymer matrix clearly occupies the largest proportion with the greatest influence on composite properties. Therefore, an in-depth study of the mechanism of thermal conductivity in intrinsic polymers would be beneficial to improve the λ value of final products.

(iii) Most of the research on thermally conductive polymer composites is limited to theoretical and experimental levels. How to gain an understanding of this on the level of industrialized mass production is also an urgent problem to be solved in the future.

(iv) Present mechanisms and models of heat conduction are not perfect: an in-depth study of heat conduction mechanisms is required and this needs to be approached from a multidisciplinary standpoint. Computer simulation and machine learning are powerful tools to build new heat conduction models and design the next generation of thermally conductive products.

(v) The λ values of polymer composites obtained with different testing equipment show obvious differences. Characterization methods for thermal conductivity need to be normalized and standardized to make the λ values comparable.

(vi) Smart materials are developing rapidly, designing and preparing functional thermally conductive materials is becoming increasingly important, such as thermal conducting material with efficient EMI shielding, thermal conducting material with rapid self-healing capability,[103,399,400] and thermal conducting material with sensing capabilities, etc.

Acknowledgements

Z.W. and Z.W. contributed equally to this work. This work was supported by the Open Project Fund of the Key Laboratory of Engineering Dielectrics and Its Application (2018EDAQY05), Heilongjiang Province Postdoctoral Funded Project (LBH-Q21019), National Natural Science Foundation of China (52237006), Heilongjiang Province Natural Science Foundation (LH2020E087) and National Natural Science Foundation of China (32201491). X.H.Z .acknowledges the support from NSERC-Alberta Innovated Advanced Program. B.B.X. is grateful for the support from the Engineering and Physical Sciences Research Council (EPSRC, UK) grant-EP/N007921.

Conflict of Interest

The authors declare no conflict of interest.

Keywords

functional materials, polymer composites, thermal conductivity

Received: February 9, 2023
Revised: April 24, 2023
Published online:

[1] X. Wang, P. Wu, *ACS Appl. Mater. Interfaces* **2018**, *10*, 34311.
[2] Y. Guo, K. Ruan, J. Gu, *Mater. Today Phys.* **2021**, *20*, 100456.
[3] Y. Wang, X. Zhang, X. Ding, Y. Li, P. Zhang, M. Shu, Q. Zhang, Y. Gong, K. Zheng, B. Wu, X. Tian, *Compos. Sci. Technol.* **2021**, *205*, 108693.
[4] K. Kim, J. Kim, *Polymer* **2016**, *101*, 168.
[5] C. Tan, H. Zhu, T. Ma, W. Guo, X. Liu, X. Huang, H. Zhao, Y. Z. Long, P. Jiang, B. Sun, *Nanoscale* **2019**, *11*, 20648.
[6] X. Wang, P. Wu, *Chem. Eng. J.* **2018**, *348*, 723.
[7] Y. Lin, Q. Kang, H. Wei, H. Bao, P. Jiang, Y. W. Mai, X. Huang, *Nanomicro Lett.* **2021**, *13*, 180.
[8] C. Xiao, Y. Tang, L. Chen, X. Zhang, K. Zheng, X. Tian, *Composites, Part A* **2019**, *121*, 330.
[9] S. Zhang, Y. Tian, X. Gu, W. Tang, J. Sun, *Polym. Compos.* **2018**, *39*, E891.
[10] Y. Guo, K. Ruan, X. Yang, T. Ma, J. Kong, N. Wu, J. Zhang, J. Gu, Z. Guo, *J. Mater. Chem. C* **2019**, *7*, 7035.
[11] K. Kim, H. Ju, J. Kim, *Compos. Sci. Technol.* **2016**, *123*, 99.
[12] J. Ying, X. Tan, L. Lv, X. Wang, J. Gao, Q. Yan, H. Ma, K. Nishimura, H. Li, J. Yu, T. H. Liu, R. Xiang, R. Sun, N. Jiang, C. Wong, S. Maruyama, C. T. Lin, W. Dai, *ACS Nano* **2021**, *15*, 12922.
[13] Y. Zhang, B. Tang, Y. Liu, R. Feng, S. Song, C. Xiong, L. Dong, *Polym. Compos.* **2020**, *41*, 1673.
[14] H. Jiang, Z. Wang, H. Geng, X. Song, H. Zeng, C. Zhi, *ACS Appl. Mater. Interfaces* **2017**, *9*, 10078.
[15] D. Wang, H. Wei, Y. Lin, P. Jiang, H. Bao, X. Huang, *Compos. Sci. Technol.* **2021**, *213*,108953.

 © 2023 Wiley-VCH GmbH

16163028, 0, Downloaded from https://onlinelibrary.wiley.com/doi/10.1002/adfm.202301549 by University of California - Los Ange, Wiley Online Library on [16/06/2023]. See the Terms and Conditions (https://onlinelibrary.wiley.com/terms-and-conditions) on Wiley Online Library for rules of use; OA articles are governed by the applicable Creative Commons License

[16] C. Yu, J. Zhang, Z. Li, W. Tian, L. Wang, J. Luo, Q. Li, X. Fan, Y. Yao, *Composites, Part A* **2017**, *98*, 25.
[17] S. Ryu, H. Oh, J. Kim, *Mater. Chem. Phys.* **2019**, *223*, 607.
[18] Y. Zhou, S. Wu, Y. Long, P. Zhu, F. Wu, F. Liu, V. Murugadoss, W. Winchester, A. Nautiyal, Z. Wang, Z. Guo, *ES Mater. Manuf.* **2020**, *7*, 4.
[19] B. Sun, X. Huang, *npj Flexible Electron.* **2021**, *5*, 12.
[20] Z. Shen, J. Feng, *Compos. Sci. Technol.* **2019**, *170*, 135.
[21] J. Liu, W. Li, Y. Guo, H. Zhang, Z. Zhang, *Composites, Part A* **2019**, *120*, 140.
[22] J. Chen, X. Huang, B. Sun, P. Jiang, *ACS Nano* **2019**, *13*, 337.
[23] C.-P. Feng, L.-Y. Yang, J. Yang, L. Bai, R.-Y. Bao, Z.-Y. Liu, M.-B. Yang, H.-B. Lan, W. Yang, *Compos. Commun.* **2020**, *22*, 100528.
[24] W. Yu, C. Liu, L. Qiu, P. Zhang, W. Ma, Y. Yue, H. Xie, L. S. Larkin, *Eng. Sci.* **2018**, *2*, 1.
[25] H. Zhang, Q. He, H. Yu, M. Qin, Y. Feng, W. Feng, *Adv. Funct. Mater.* **2023**, *33*, 2211985.
[26] H. Yu, P. Guo, M. Qin, G. Han, L. Chen, Y. Feng, W. Feng, *Compos. Sci. Technol.* **2022**, *222*, 109406.
[27] Z. Zhang, J. Qu, Y. Feng, W. Feng, *Compos. Commun.* **2018**, *9*, 33.
[28] Y. Cai, H. Yu, C. Chen, Y. Feng, M. Qin, W. Feng, *Carbon* **2022**, *196*, 902.
[29] H. Yu, Y. Feng, C. Chen, H. Zhang, L. Peng, M. Qin, W. Feng, *Adv. Sci.* **2022**, *9*, 2201331.
[30] L. Peng, H. Yu, C. Chen, Q. He, H. Zhang, F. Zhao, M. Qin, Y. Feng, W. Feng, *Adv. Sci.* **2023**, *10*, 2205962.
[31] K. Zhang, P. Tao, Y. Zhang, X. Liao, S. Nie, *Carbohydr. Polym.* **2019**, *213*, 228.
[32] C. Li, X.-L. Zeng, L.-Y. Tan, Y.-M. Yao, D.-L. Zhu, R. Sun, J.-B. Xu, C.-P. Wong, *Chem. Eng. J.* **2019**, *368*, 79.
[33] D. Wang, Y. Lin, D. Hu, P. Jiang, X. Huang, *Composites, Part A* **2020**, *130*, 105754.
[34] N. Song, H. Pan, X. Liang, D. Cao, L. Shi, P. Ding, *J. Mater. Chem. C* **2018**, *6*, 7085.
[35] Y. Zhou, F. Liu, C.-Y. Chen, *Adv. Compos. Hybrid Mater.* **2019**, *2*, 46.
[36] D. Pan, S. Luo, Y. Feng, X. Zhang, F. Su, H. Liu, C. Liu, X. Mai, N. Naik, Z. Guo, *Composites, Part B* **2021**, *222*, 109039.
[37] X. Zhuang, Y. Zhou, F. Liu, *Mater. Res. Express* **2017**, *4*, 015018.
[38] E.-C. Cho, C.-W. Chang-Jian, Y.-S. Hsiao, K.-C. Lee, J.-H. Huang, *Composites, Part A* **2016**, *90*, 678.
[39] Y. Zhou, F. Liu, H. Wang, *Polym. Compos.* **2017**, *38*, 803.
[40] Y.-F. Zhang, Y.-J. Ren, H.-C. Guo, S.-l. Bai, *Appl. Therm. Eng.* **2019**, *150*, 840.
[41] Z.-G. Wang, F. Gong, W.-C. Yu, Y.-F. Huang, L. Zhu, J. Lei, J.-Z. Xu, Z.-M. Li, *Compos. Sci. Technol.* **2018**, *162*, 7.
[42] Y. Guo, X. Yang, K. Ruan, J. Kong, M. Dong, J. Zhang, J. Gu, Z. Guo, *ACS Appl. Mater. Interfaces* **2019**, *11*, 25465.
[43] Y. Lin, X. Huang, J. Chen, P. Jiang, *High Voltage* **2017**, *2*, 139.
[44] D. Wang, D. Liu, J. Xu, J. Fu, K. Wu, *Mater. Horiz.* **2022**, *9*, 640.
[45] H. Ma, Z. Tian, *J. Mater. Res.* **2018**, *34*, 126.
[46] Z. Weng, K. Wu, F. Luo, F. Xiao, Q. Zhang, S. Wang, M. Lu, *Composites, Part A* **2018**, *110*, 106.
[47] M. Cao, C. Du, H. Guo, X. Li, S. Song, F. Handan Tezel, B. Li, *Composites, Part A* **2018**, *115*, 331.
[48] Y. Guo, G. Xu, X. Yang, K. Ruan, T. Ma, Q. Zhang, J. Gu, Y. Wu, H. Liu, Z. Guo, *J. Mater. Chem. C* **2018**, *6*, 3004.
[49] X. Li, Y. Feng, C. Chen, Y. Ye, H. Zeng, H. Qu, J. Liu, X. Zhou, S. Long, X. Xie, *J. Mater. Chem. A* **2018**, *6*, 20500.
[50] J. Cui, S. Zhou, *J. Mater. Chem. C* **2018**, *6*, 550.
[51] D. Zou, X. Huang, Y. Zhu, J. Chen, P. Jiang, *Compos. Sci. Technol.* **2019**, *177*, 88.
[52] X. Yang, C. Liang, T. Ma, Y. Guo, J. Kong, J. Gu, M. Chen, J. Zhu, *Adv. Compos. Hybrid Mater.* **2018**, *1*, 207.
[53] K. Ren, X. Liu, S. Chen, Y. Cheng, W. Tang, G. Zhang, *Adv. Funct. Mater.* **2020**, *30*, 2004003.
[54] J. Gu, K. Ruan, *Nano-Micro Lett* **2021**, *13*, 110.
[55] Y.-J. Wu, L. Fang, Y. Xu, *npj Comput. Mater.* **2019**, *5*, 56.
[56] K. Ruan, X. Shi, Y. Guo, J. Gu, *Compos. Commun.* **2020**, *22*, 100518.
[57] X. Xu, J. Chen, J. Zhou, B. Li, *Adv. Mater.* **2018**, *30*, 1705544.
[58] X. Xu, J. Zhou, J. Chen, *Adv. Funct. Mater.* **2020**, *30*, 1904704.
[59] J. Chen, X. Xu, J. Zhou, B. Li, *Rev. Mod. Phys.* **2022**, *94*, 025002.
[60] K. Yuan, J. Shi, W. Aftab, M. Qin, A. Usman, F. Zhou, Y. Lv, S. Gao, R. Zou, *Adv. Funct. Mater.* **2020**, *30*, 1904228.
[61] Z. Tong, S. Li, X. Ruan, H. Bao, *Phys. Rev. B* **2019**, *100*, 144306.
[62] L. Zhang, H. Deng, Q. Fu, *Compos. Commun.* **2018**, *8*, 74.
[63] H. Zhang, X. Zhang, Z. Fang, Y. Huang, H. Xu, Y. Liu, D. Wu, J. Zhuang, J. Sun, *J. Compos. Sci.* **2020**, *4*, 180.
[64] Z. Han, X. Yang, W. Li, T. Feng, X. Ruan, *Comput. Phys. Commun.* **2022**, *270*, 108179.
[65] A. J. H. McGaughey, A. Jain, H.-Y. Kim, *J. Appl. Phys.* **2019**, *125*, 011101.
[66] K. Ghosh, A. Kusiak, J.-L. Battaglia, *Phys. Rev. Mater.* **2021**, *5*, 073605.
[67] Y. Zhao, S. Zeng, G. Li, C. Lian, Z. Dai, S. Meng, J. Ni, *Phys. Rev. B* **2021**, *104*, 224304.
[68] R. Yang, S. Yue, Y. Quan, B. Liao, *Phys. Rev. B* **2021**, *103*, 184302.
[69] X. Yan, B. Wang, Y. Hai, D. R. Kripalani, Q. Ke, Y. Cai, *Sci. China: Phys., Mech. Astron.* **2022**, *65*, 117004.
[70] X. Li, S. Lee, *Phys. Rev. B* **2019**, *99*, 085202.
[71] C. Zhang, Z. Zeng, Q. Sun, Y. Chen, *J. Appl. Phys.* **2021**, *130*, 205101.
[72] G. Chen, *Nat. Rev. Phys.* **2021**, *3*, 555.
[73] Z. Zhang, Y. Ouyang, Y. Guo, T. Nakayama, M. Nomura, S. Volz, J. Chen, *Phys. Rev. B* **2020**, *102*, 195302.
[74] K. Ghosh, A. Kusiak, J.-L. Battaglia, *Phys. Rev. B* **2020**, *102*, 094311.
[75] C. Zhang, Z. Guo, *Int. J. Heat Mass Transfer* **2021**, *181*, 121847.
[76] Y. Xia, K. Pal, J. He, V. Ozolins, C. Wolverton, *Phys. Rev. Lett.* **2020**, *124*, 065901.
[77] X. Gu, Z. Fan, H. Bao, C. Y. Zhao, *Phys. Rev. B* **2019**, *100*, 064306.
[78] Y. Guo, M. Bescond, Z. Zhang, M. Luisier, M. Nomura, S. Volz, *Phys. Rev. B* **2020**, *102*, 196412.
[79] S.-N. Li, B.-Y. Cao, *Int. J. Heat Mass Transfer* **2021**, *173*, 121225.
[80] G. Mascali, V. Romano, *Phys. A* **2020**, *548*, 124489.
[81] D. Jou, V. A. Cimmelli, *Commun. Appl. Ind. Math.* **2016**, *7*, 196.
[82] P. Desmarchelier, A. Beardo, F. X. Alvarez, A. Tanguy, K. Termentzidis, *Int. J. Heat Mass Transfer* **2022**, *194*, 123003.
[83] X. Ran, Y. Huang, M. Wang, *Int. J. Heat Mass Transfer* **2023**, *201*, 123624.
[84] O. Zobiri, A. Atia, M. Arıcı, *Micro Nanostruct.* **2022**, *163*, 107123.
[85] A. I. Zhmakin, *Tech. Phys.* **2021**, *66*, 1.
[86] O. E. Raichev, G. M. Gusev, F. G. G. Hernandez, A. D. Levin, A. K. Bakarov, *Phys. Rev. B* **2020**, *102*, 195301.
[87] M. P. Medlar, E. C. Hensel, *J. Heat Transfer* **2023**, *145*, 022501.
[88] W. Miao, M. Wang, *Phys. Rev. B* **2021**, *103*, 125412.
[89] A. Singh, B. P. Majee, J. D. Gupta, A. K. Mishra, *J. Phys. Chem. C* **2023**, *127*, 3787.
[90] E. A. A. Pogna, X. Jia, A. Principi, A. Block, L. Banszerus, J. Zhang, X. Liu, T. Sohier, S. Forti, K. Soundarapandian, B. Terres, J. D. Mehew, C. Trovatello, C. Coletti, F. H. L. Koppens, M. Bonn, H. I. Wang, N. van Hulst, M. J. Verstraete, H. Peng, Z. Liu, C. Stampfer, G. Cerullo, K. J. Tielrooij, *ACS Nano* **2021**, *15*, 11285.
[91] I. I. Al-Qasir, A. A. Campbell, G. Sala, J. Y. Y. Lin, Y. Cheng, F. F. Islam, D. L. Abernathy, M. B. Stone, *Carbon* **2020**, *168*, 42.
[92] Z. Chen, N. Andrejevic, T. Smidt, Z. Ding, Q. Xu, Y. T. Chi, Q. T. Nguyen, A. Alatas, J. Kong, M. Li, *Adv. Sci.* **2021**, *8*, 2004214.
[93] Z. Yu, Y. Feng, D. Feng, X. Zhang, *Phys. Chem. Chem. Phys.* **2019**, *22*, 337.
[94] T. Huang, Y. Li, M. Chen, L. Wu, *Compos. Sci. Technol.* **2020**, *198*, 108322.

© 2023 Wiley-VCH GmbH

16163028, 0, Downloaded from https://onlinelibrary.wiley.com/doi/10.1002/adfm.202301549 by University of California - Los Ange, Wiley Online Library on [16/06/2023]. See the Terms and Conditions (https://onlinelibrary.wiley.com/terms-and-conditions) on Wiley Online Library for rules of use; OA articles are governed by the applicable Creative Commons License

[95] Y. Zhang, Y.-J. Heo, Y.-R. Son, I. In, K.-H. An, B.-J. Kim, S.-J. Park, *Carbon* **2019**, *142*, 445.
[96] A. Li, C. Zhang, Y. F. Zhang, *Polymers* **2017**, *9*, 437.
[97] N. Burger, A. Laachachi, M. Ferriol, M. Lutz, V. Toniazzo, D. Ruch, *Prog. Polym. Sci.* **2016**, *61*, 1.
[98] C. Chen, Y. Xue, Z. Li, Y. Wen, X. Li, F. Wu, X. Li, D. Shi, Z. Xue, X. Xie, *Chem. Eng. J.* **2019**, *369*, 1150.
[99] L. Tang, M. He, X. Na, X. Guan, R. Zhang, J. Zhang, J. Gu, *Compos. Commun.* **2019**, *16*, 5.
[100] Y. Li, G. Xu, Y. Guo, T. Ma, X. Zhong, Q. Zhang, J. Gu, *Composites, Part A* **2018**, *107*, 570.
[101] X. Yang, Y. Guo, X. Luo, N. Zheng, T. Ma, J. Tan, C. Li, Q. Zhang, J. Gu, *Compos. Sci. Technol.* **2018**, *164*, 59.
[102] J. Gu, X. Meng, Y. Tang, Y. Li, Q. Zhuang, J. Kong, *Composites, Part A* **2017**, *92*, 27.
[103] F. Zhang, Y. Feng, W. Feng, *Mater. Sci. Eng., R* **2020**, *142*, 100580.
[104] C.-P. Feng, L. Bai, Y. Shao, R.-Y. Bao, Z.-Y. Liu, M.-B. Yang, J. Chen, H.-Y. Ni, W. Yang, *Adv. Mater. Interfaces* **2018**, *5*, 1700946.
[105] F. Kargar, Z. Barani, R. Salgado, B. Debnath, J. S. Lewis, E. Aytan, R. K. Lake, A. A. Balandin, *ACS Appl. Mater. Interfaces* **2018**, *10*, 37555.
[106] Y. Fu, J. Hansson, Y. Liu, S. Chen, A. Zehri, M. K. Samani, N. Wang, Y. Ni, Y. Zhang, Z.-B. Zhang, Q. Wang, M. Li, H. Lu, M. Sledzinska, C. M. S. Torres, S. Volz, A. A. Balandin, X. Xu, J. Liu, *2D Mater.* **2020**, *7*, 012001.
[107] B. Shi, L. Dong, M. Li, B. Liu, K. Kim, X. Xu, J. Zhou, J. Liu, *Appl. Phys. Lett.* **2018**, *113*, 041902.
[108] J. U. Jang, H. E. Nam, S. O. So, H. Lee, G. S. Kim, S. Y. Kim, S. H. Kim, *Polymers* **2022**, *14*, 323.
[109] F. Kargar, Z. Barani, M. Balinskiy, A. S. Magana, J. S. Lewis, A. A. Balandin, *Adv. Electron. Mater.* **2018**, *5*, 1800558.
[110] R. Li, X. Yang, J. Li, Y. Shen, L. Zhang, R. Lu, C. Wang, X. Zheng, H. Chen, T. Zhang, *Mater. Today Phys.* **2022**, *22*, 100594.
[111] H. Ma, Z. Tian, *Appl. Phys. Lett.* **2017**, *110*, 091903.
[112] L. Bai, X. Zhao, R.-Y. Bao, Z.-Y. Liu, M.-B. Yang, W. Yang, *J. Mater. Sci.* **2018**, *53*, 10543.
[113] C. Lu, S. W. Chiang, H. Du, J. Li, L. Gan, X. Zhang, X. Chu, Y. Yao, B. Li, F. Kang, *Polymer* **2017**, *115*, 52.
[114] B. Zhu, J. Liu, T. Wang, M. Han, S. Valloppilly, S. Xu, X. Wang, *ACS Omega* **2017**, *2*, 3931.
[115] N. Mehra, L. Mu, T. Ji, X. Yang, J. Kong, J. Gu, J. Zhu, *Appl. Mater. Today* **2018**, *12*, 92.
[116] N. Mehra, L. Mu, T. Ji, Y. Li, J. Zhu, *Compos. Sci. Technol.* **2017**, *151*, 115.
[117] C. Huang, X. Qian, R. Yang, *Mater. Sci. Eng., R* **2018**, *132*, 1.
[118] N. Mehra, L. Mu, J. Zhu, *Compos. Sci. Technol.* **2017**, *148*, 97.
[119] Y. Liu, G. J. Vancso, *Prog. Polym. Sci.* **2020**, *104*, 101233.
[120] X. Jiang, G. Reiter, W. Hu, *J. Phys. Chem. B* **2016**, *120*, 566.
[121] Y. Ouyang, Z. Zhang, Q. Xi, P. Jiang, W. Ren, N. Li, J. Zhou, J. Chen, *RSC Adv.* **2019**, *9*, 33549.
[122] M. Markov, J. Sjakste, G. Barbarino, G. Fugallo, L. Paulatto, M. Lazzeri, F. Mauri, N. Vast, *Phys. Rev. Lett.* **2018**, *120*, 075901.
[123] V. Martelli, J. L. Jiménez, M. Continentino, E. Baggio-Saitovitch, K. Behnia, *Phys. Rev. Lett.* **2018**, *120*, 125901.
[124] S. Ronca, T. Igarashi, G. Forte, S. Rastogi, *Polymer* **2017**, *123*, 203.
[125] C. Chen, H. Wang, Y. Xue, Z. Xue, H. Liu, X. Xie, Y.-W. Mai, *Compos. Sci. Technol.* **2016**, *128*, 207.
[126] Y. Zhou, X. Zhuang, F. Wu, F. Liu, *Crystals* **2018**, *8*, 398.
[127] Y. Guo, Z. Lyu, X. Yang, Y. Lu, K. Ruan, Y. Wu, J. Kong, J. Gu, *Composites, Part B* **2019**, *164*, 732.
[128] Y. Wang, W. Wu, D. Drummer, C. Liu, W. Shen, F. Tomiak, K. Schneider, X. Liu, Q. Chen, *Mater. Des.* **2020**, *191*, 108698.
[129] Q. Rong, H. Wei, X. Huang, H. Bao, *Compos. Sci. Technol.* **2019**, *184*, 107861.
[130] Y. Zhou, S. Yu, H. Niu, F. Liu, *Polymers* **2018**, *10*, 1412.
[131] H. Guo, J. Liu, Q. Wang, M. Liu, C. Du, B. Li, L. Feng, *Compos. Sci. Technol.* **2019**, *181*, 107713.
[132] G. He, X. Li, Y. Dai, Z. Yang, C. Zeng, C. Lin, S. He, *Composites, Part B* **2019**, *162*, 678.
[133] Y. Yao, Z. Ye, F. Huang, X. Zeng, T. Zhang, T. Shang, M. Han, W. Zhang, L. Ren, R. Sun, J. B. Xu, C. P. Wong, *ACS Appl. Mater. Interfaces* **2020**, *12*, 2892.
[134] Y. Bai, Y. Shi, S. Zhou, H. Zou, M. Liang, *Macromol. Mater. Eng.* **2021**, *306*, 2100267.
[135] J. Sun, X. Zhang, Q. Du, V. Murugadoss, D. Wu, Z. Guo, *ES Mater. Manuf.* **2021**, *13*, 1.
[136] X. Yao, B. G. Falzon, S. C. Hawkins, S. Tsantzalis, *Carbon* **2018**, *129*, 486.
[137] L. Ren, Q. Li, J. Lu, X. Zeng, R. Sun, J. Wu, J.-B. Xu, C.-P. Wong, *Composites, Part A* **2018**, *107*, 561.
[138] C. Ferraro, E. Garcia-Tuñon, V. G. Rocha, S. Barg, M. D. Fariñas, T. E. G. Alvarez-Arenas, G. Sernicola, F. Giuliani, E. Saiz, *Adv. Funct. Mater.* **2016**, *26*, 1636.
[139] D. He, Y. Wang, S. Song, S. Liu, Y. Deng, *ACS Appl. Mater. Interfaces* **2017**, *9*, 44839.
[140] Y. Yao, X. Zeng, G. Pan, J. Sun, J. Hu, Y. Huang, R. Sun, J. B. Xu, C. P. Wong, *ACS Appl. Mater. Interfaces* **2016**, *8*, 31248.
[141] T. Gao, H. Rong, K. H. Mahmoud, J. Ruan, S. M. El-Bahy, A. A. Faheim, Y. Li, M. Huang, M. A. Nassan, R. Zhao, *Adv. Compos. Hybrid Mater.* **2022**, *5*, 1158.
[142] Y. Yao, X. Zhu, X. Zeng, R. Sun, J. B. Xu, C. P. Wong, *ACS Appl. Mater. Interfaces* **2018**, *10*, 9669.
[143] H. Gholivand, S. Fuladi, Z. Hemmat, A. Salehi-Khojin, F. Khalili-Araghi, *J. Appl. Phys.* **2019**, *126*, 065101.
[144] C. Peng, P. Wei, X. Chen, Y. Zhang, F. Zhu, Y. Cao, H. Wang, H. Yu, F. Peng, *Ceram. Int.* **2018**, *44*, 18886.
[145] G. Song, R. Kang, L. Guo, Z. Ali, X. Chen, Z. Zhang, C. Yan, C.-T. Lin, N. Jiang, J. Yu, *New J. Chem.* **2020**, *44*, 7186.
[146] L. X. Liu, W. Chen, H. B. Zhang, Q. W. Wang, F. Guan, Z. Z. Yu, *Adv. Funct. Mater.* **2019**, *29*, 1905197.
[147] H. Cheng, L. Xing, Y. Zuo, Y. Pan, M. Huang, A. Alhadhrami, M. M. Ibrahim, Z. M. El-Bahy, C. Liu, C. Shen, X. Liu, *Adv. Compos. Hybrid Mater.* **2022**, *5*, 755.
[148] Y. Cao, M. Weng, M. H. H. Mahmoud, A. Y. Elnaggar, L. Zhang, I. H. El Azab, Y. Chen, M. Huang, J. Huang, X. Sheng, *Adv. Compos. Hybrid Mater.* **2022**, *5*, 1253.
[149] L. Guo, Z. Zhang, M. Li, R. Kang, Y. Chen, G. Song, S.-T. Han, C.-T. Lin, N. Jiang, J. Yu, *Compos. Commun.* **2020**, *19*, 134.
[150] L. Liu, F. Lv, Y. Zhang, P. Li, W. Tong, L. Ding, G. Zhang, *Composites, Part A* **2017**, *99*, 41.
[151] L. Ren, X. Zeng, X. Zhang, R. Sun, X. Tian, Y. Zeng, J.-B. Xu, C.-P. Wong, *Composites, Part A* **2019**, *119*, 299.
[152] Y. Ouyang, G. Hou, L. Bai, B. Li, F. Yuan, *Compos. Sci. Technol.* **2018**, *165*, 307.
[153] H. Wang, Q. Wang, Q. Zhang, H. Yang, J. Dong, J. Cheng, J. Tong, J. Wen, *Compos. Sci. Technol.* **2021**, *216*, 109048.
[154] L. Yin, X. Zhou, J. Yu, H. Wang, C. Ran, *Composites, Part A* **2016**, *90*, 626.
[155] Y. Yuan, Z. Li, L. Cao, B. Tang, S. Zhang, *Ceram. Int.* **2019**, *45*, 16569.
[156] C. Pan, K. Kou, Y. Zhang, Z. Li, G. Wu, *Composites, Part B* **2018**, *153*, 1.
[157] L. Liu, C. Cao, X. Ma, X. Zhang, T. Lv, *J. Macromol. Sci., Part A: Pure Appl.Chem.* **2020**, *57*, 398.
[158] S. L. Chung, J. S. Lin, *Molecules* **2016**, *21*, 670.
[159] Y. Yuan, Z. Chi, B. Tang, E. Li, S. Zhang, *J. Mater. Sci.: Mater. Electron.* **2018**, *29*, 14890.
[160] Z. Lule, J. Kim, *Polymers* **2019**, *11*, 148.
[161] D. G Ortiz, C. Pochat-Bohatier, J. Cambedouzou, S. Balme, M. Bechelany, P. Miele, *Langmuir* **2017**, *33*, 13394.

© 2023 Wiley-VCH GmbH

16163028, 0, Downloaded from https://onlinelibrary.wiley.com/doi/10.1002/adfm.202301549 by University of California - Los Ange, Wiley Online Library on [16/06/2023]. See the Terms and Conditions (https://onlinelibrary.wiley.com/terms-and-conditions) on Wiley Online Library for rules of use; OA articles are governed by the applicable Creative Commons License

[162] H. Fang, S.-L. Bai, C. P. Wong, *Compos. Commun.* **2016**, *2*, 19.
[163] S. Mateti, K. Yang, X. Liu, S. Huang, J. Wang, L. H. Li, P. Hodgson, M. Zhou, J. He, Y. Chen, *Adv. Funct. Mater.* **2018**, *28*, 1707556.
[164] K. Wu, C. Lei, W. Yang, S. Chai, F. Chen, Q. Fu, *Compos. Sci. Technol.* **2016**, *134*, 191.
[165] P. Li, H. Shen, Z. Qian, X. Yang, N. Zhao, C. Zhu, J. Xu, *J. Mater. Sci.* **2017**, *53*, 4189.
[166] C. Yu, W. Gong, W. Tian, Q. Zhang, Y. Xu, Z. Lin, M. Hu, X. Fan, Y. Yao, *Compos. Sci. Technol.* **2018**, *160*, 199.
[167] J. Gu, S. Xu, Q. Zhuang, Y. Tang, J. Kong, *IEEE Trans. Dielectr. Electr. Insul.* **2017**, *24*, 784.
[168] J. Gu, Z. Lv, Y. Wu, Y. Guo, L. Tian, H. Qiu, W. Li, Q. Zhang, *Composites, Part A* **2017**, *94*, 209.
[169] T. Li, Z. Tang, Z. Huang, J. Yu, *Phys. E* **2017**, *85*, 137.
[170] C. Fu, Q. Li, J. Lu, S. Mateti, Q. Cai, X. Zeng, G. Du, R. Sun, Y. Chen, J. Xu, C.-P. Wong, *Compos. Sci. Technol.* **2018**, *165*, 322.
[171] D. Kim, M. You, J. H. Seol, S. Ha, Y. A. Kim, *J. Phys. Chem. C* **2017**, *121*, 7025.
[172] S. Chen, R. Xu, J. Liu, X. Zou, L. Qiu, F. Kang, B. Liu, H. M. Cheng, *Adv. Mater.* **2019**, *31*, 1804810.
[173] K. Wu, J. Fang, J. Ma, R. Huang, S. Chai, F. Chen, Q. Fu, *ACS Appl. Mater. Interfaces* **2017**, *9*, 30035.
[174] W. Luo, Y. Wang, E. Hitz, Y. Lin, B. Yang, L. Hu, *Adv. Funct. Mater.* **2017**, *27*, 1701450.
[175] D. Gonzalez-Ortiz, C. Pochat-Bohatier, S. Gassara, J. Cambedouzou, M. Bechelany, P. Miele, *Green Chem.* **2018**, *20*, 4319.
[176] Y. Chen, Q. Kang, P. Jiang, X. Huang, *Nano Res.* **2020**, *14*, 2424.
[177] C. Lei, Y. Zhang, D. Liu, X. Xu, K. Wu, Q. Fu, *Compos. Sci. Technol.* **2021**, *214*, 108995.
[178] C.-G. Yin, Y. Ma, Z.-J. Liu, J.-C. Fan, P.-H. Shi, Q.-J. Xu, Y.-L. Min, *Polymer* **2019**, *162*, 100.
[179] W. Zhu, X. Gao, Q. Li, H. Li, Y. Chao, M. Li, S. M. Mahurin, H. Li, H. Zhu, S. Dai, *Angew. Chem., Int. Ed. Engl.* **2016**, *55*, 10766.
[180] J. Wang, D. Zhang, Y. Zhang, W. Cai, C. Yao, Y. Hu, W. Hu, *J. Hazard. Mater.* **2019**, *362*, 482.
[181] C. Tan, Z. Dong, Y. Li, H. Zhao, X. Huang, Z. Zhou, J. W. Jiang, Y. Z. Long, P. Jiang, T. Y. Zhang, B. Sun, *Nat. Commun.* **2020**, *11*, 3530.
[182] Z. Xie, K. Wu, D. Liu, Q. Zhang, Q. Fu, *Compos. Sci. Technol.* **2021**, *208*, 1805053.
[183] T. Feng, L. Lindsay, X. Ruan, *Phys. Rev. B* **2017**, *96*, 61201(R).
[184] J. S. Kang, M. Li, H. Wu, H. Nguyen, Y. Hu, *Appl. Phys. Lett.* **2019**, *115*, 122103.
[185] Y. Cui, Z. Qin, H. Wu, M. Li, Y. Hu, *Nat. Commun.* **2021**, *12*, 1284.
[186] F. Lv, M. Qin, F. Zhang, H. Yu, L. Gao, P. Lv, W. Wei, Y. Feng, W. Feng, *Carbon* **2019**, *149*, 281.
[187] Z. Liu, Z. Chen, F. Yu, *Sol. Energy Mater. Sol. Cells* **2019**, *192*, 72.
[188] Y. Zhang, K. Y. Rhee, D. Hui, S.-J. Park, *Composites, Part B* **2018**, *143*, 19.
[189] D. Hu, X. Huang, S. Li, P. Jiang, *Compos. Sci. Technol.* **2020**, *188*, 107995.
[190] Y.-H. Zhao, Z.-K. Wu, S.-L. Bai, *Int. J. Heat Mass Transfer* **2016**, *101*, 470.
[191] J. Yang, E. Zhang, X. Li, Y. Zhang, J. Qu, Z.-Z. Yu, *Carbon* **2016**, *98*, 50.
[192] X. Yuan, W. Li, H. Liu, N. Han, X. Zhang, *Compos. Commun.* **2016**, *2*, 5.
[193] D. Hu, S. Wang, C. Zhang, P. Yi, P. Jiang, X. Huang, *Nano Res.* **2021**, *14*, 2837.
[194] Y. Zhang, J. R. Choi, S.-J. Park, *Composites, Part A* **2018**, *109*, 498.
[195] J. Zhang, X. Wang, C. Yu, Q. Li, Z. Li, C. Li, H. Lu, Q. Zhang, J. Zhao, M. Hu, Y. Yao, *Compos. Sci. Technol.* **2017**, *149*, 41.
[196] X. Xu, R. Hu, M. Chen, J. Dong, B. Xiao, Q. Wang, H. Wang, *Chem. Eng. J.* **2020**, *397*, 125447.
[197] C.-P. Feng, S.-S. Wan, W.-C. Wu, L. Bai, R.-Y. Bao, Z.-Y. Liu, M.-B. Yang, J. Chen, W. Yang, *Compos. Sci. Technol.* **2018**, *167*, 456.
[198] K. Sato, Y. Tominaga, Y. Hotta, H. Shibuya, M. Sugie, T. Saruyama, *Adv. Powder Technol.* **2018**, *29*, 972.
[199] Y. Zhang, J. R. Choi, S.-J. Park, *Composites, Part A* **2017**, *101*, 227.
[200] Y. Tominaga, K. Sato, Y. Hotta, H. Shibuya, M. Sugie, T. Saruyama, *Cellulose* **2018**, *25*, 3973.
[201] N. Song, D. Cao, X. Luo, Y. Guo, J. Gu, P. Ding, *J. Mater. Chem. C* **2018**, *6*, 13108.
[202] C. I. Idumah, A. Hassan, *Rev. Chem. Eng.* **2016**, *32*, 413.
[203] Y.-H. Zhao, Y.-F. Zhang, Z.-K. Wu, S.-L. Bai, *Composites, Part B* **2016**, *84*, 52.
[204] Y. Guo, Y. Chen, E. Wang, M. Cakmak, *ACS Appl. Mater. Interfaces* **2017**, *9*, 919.
[205] F. Xu, D. Bao, Y. Cui, Y. Gao, D. Lin, X. Wang, J. Peng, H. Geng, H. Wang, *Adv. Compos. Hybrid Mater.* **2022**, *5*, 2235.
[206] C. Feng, H. Ni, J. Chen, W. Yang, *ACS Appl. Mater. Interfaces* **2016**, *8*, 19732.
[207] L. Peng, Z. Xu, Z. Liu, Y. Guo, P. Li, C. Gao, *Adv. Mater.* **2017**, *29*, 1700589.
[208] Z. Zhang, M. Liu, M. M. Ibrahim, H. Wu, Y. Wu, Y. Li, G. A. M. Mersal, I. H. El Azab, S. M. El-Bahy, M. Huang, Y. Jiang, G. Liang, P. Xie, C. Liu, *Adv. Compos. Hybrid Mater.* **2022**, *5*, 1054.
[209] Z. Zhao, R. Zhao, P. Bai, W. Du, R. Guan, D. Tie, N. Naik, M. Huang, Z. Guo, *J. Alloys Compd.* **2022**, *902*, 163484.
[210] C. Li, L. Qiu, B. Zhang, D. Li, C. Y. Liu, *Adv. Mater.* **2016**, *28*, 1510.
[211] Y. Yang, X. Yang, X. Zou, S. Wu, D. Wan, A. Cao, L. Liao, Q. Yuan, X. Duan, *Adv. Funct. Mater.* **2017**, *27*, 1604096.
[212] P. Zhang, J. Zeng, S. Zhai, Y. Xian, D. Yang, Q. Li, *Macromol. Mater. Eng.* **2017**, *302*, 1700068.
[213] I. Bustero, I. Gaztelumendi, I. Obieta, M. A. Mendizabal, A. Zurutuza, A. Ortega, B. Alonso, *Adv. Compos. Hybrid Mater.* **2020**, *3*, 31.
[214] D. Liu, Q.-Q. Kong, H. Jia, L.-J. Xie, J. Chen, Z. Tao, Z. Wang, D. Jiang, C.-M. Chen, *Carbon* **2021**, *183*, 216.
[215] A. Li, C. Zhang, Y.-F. Zhang, *Composites, Part A* **2017**, *103*, 161.
[216] J. Huang, Y. Zhu, L. Xu, J. Chen, W. Jiang, X. Nie, *Compos. Sci. Technol.* **2016**, *129*, 160.
[217] D. G Ortiz, C. Pochat-Bohatier, J. Cambedouzou, M. Bechelany, P. Miele, *Colloids Surf., A* **2019**, *563*, 183.
[218] M. Qin, Y. Xu, R. Cao, W. Feng, L. Chen, *Adv. Funct. Mater.* **2018**, *28*, 1805053.
[219] W. Feng, M. Qin, Y. Feng, *Carbon* **2016**, *109*, 575.
[220] B. Wei, L. zhang, S. Yang, *Chem. Eng. J.* **2021**, *404*, 1805053.
[221] H. S. Kim, J. H. Kim, W. Y. Kim, H. S. Lee, S. Y. Kim, M.-S. Khil, *Carbon* **2017**, *119*, 40.
[222] F. Zhang, Y. Feng, M. Qin, T. Ji, F. Lv, Z. Li, L. Gao, P. Long, F. Zhao, W. Feng, *Carbon* **2019**, *145*, 378.
[223] N. Komatsu, Y. Ichinose, O. S. Dewey, L. W. Taylor, M. A. Trafford, Y. Yomogida, G. Wehmeyer, M. Pasquali, K. Yanagi, J. Kono, *Nat. Commun.* **2021**, *12*, 4931.
[224] P. Wang, T. Song, H. M. Abo-Dief, J. Song, A. K. Alanazi, B. Fan, M. Huang, Z. Lin, A. A. Altalhi, S. Gao, L. Yang, J. Liu, S. Feng, T. Cao, *Adv. Compos. Hybrid Mater.* **2022**, *5*, 1100.
[225] S. Gao, X. Zhao, Q. Fu, T. Zhang, J. Zhu, F. Hou, J. Ni, C. Zhu, T. Li, Y. Wang, V. Murugadoss, G. A. M. Mersal, M. M. Ibrahim, Z. M. El-Bahy, M. Huang, Z. Guo, *J. Mater. Sci. Technol.* **2022**, *126*, 152.
[226] S. Yuan, J. Bai, C. K. Chua, J. Wei, K. Zhou, *Composites, Part A* **2016**, *90*, 699.
[227] T. Morishita, Y. Katagiri, T. Matsunaga, Y. Muraoka, K. Fukumori, *Compos. Sci. Technol.* **2017**, *142*, 41.
[228] F. Yan, L. Liu, M. Li, M. Zhang, L. Shang, L. Xiao, Y. Ao, *Composites, Part A* **2019**, *125*, 105530.

© 2023 Wiley-VCH GmbH

16163028, 0, Downloaded from https://onlinelibrary.wiley.com/doi/10.1002/adfm.202301549 by University of California - Los Ange, Wiley Online Library on [16/06/2023]. See the Terms and Conditions (https://onlinelibrary.wiley.com/terms-and-conditions) on Wiley Online Library for rules of use; OA articles are governed by the applicable Creative Commons License

[229] F. Yan, L. Liu, M. Li, M. Zhang, L. Xiao, Y. Ao, *J. Mater. Sci.* **2018**, *53*, 8108.
[230] J. Ma, T. Shang, L. Ren, Y. Yao, T. Zhang, J. Xie, B. Zhang, X. Zeng, R. Sun, J.-B. Xu, C.-P. Wong, *Chem. Eng. J.* **2020**, *380*, 122550.
[231] X.-w. Zhao, C.-g. Zang, Q.-k. Ma, Y.-q. Wen, Q.-j. Jiao, *J. Mater. Sci.* **2016**, *51*, 4088.
[232] S. Chen, Y. Feng, M. Qin, T. Ji, W. Feng, *Carbon* **2017**, *116*, 84.
[233] A. Feng, G. Wu, C. Pan, Y. Wang, *J. Nanosci. Nanotechnol.* **2017**, *17*, 3786.
[234] N. Sheng, R. Zhu, K. Dong, T. Nomura, C. Zhu, Y. Aoki, H. Habazaki, T. Akiyama, *J. Mater. Chem. A* **2019**, *7*, 4934.
[235] X. Chen, K. Wu, Y. Zhang, D. Liu, R. Li, Q. Fu, *Adv. Mater.* **2022**, *34*, 2206088.
[236] Y. Zhang, C. Lei, K. Wu, Q. Fu, *Adv. Sci.* **2021**, *8*, 2004821.
[237] M. D. Bartlett, N. Kazem, M. J. Powell-Palm, X. Huang, W. Sun, J. A. Malen, C. Majidi, *Proc. Natl. Acad. Sci. USA* **2017**, *114*, 2143.
[238] A. B. M. T. Haque, R. Tutika, R. L. Byrum, M. D. Bartlett, *Adv. Funct. Mater.* **2020**, *30*, 2000832.
[239] H. Bark, M. W. M. Tan, G. Thangavel, P. S. Lee, *Adv. Energy Mater.* **2021**, *11*, 2101387.
[240] L.-C. Jia, Y.-F. Jin, J.-W. Ren, L.-H. Zhao, D.-X. Yan, Z.-M. Li, *J. Mater. Chem. C* **2021**, *9*, 2904.
[241] D. Yu, Y. Liao, Y. Song, S. Wang, H. Wan, Y. Zeng, T. Yin, W. Yang, Z. He, *Adv. Sci.* **2020**, *7*, 2000177.
[242] C. Guo, L. He, Y. Yao, W. Lin, Y. Zhang, Q. Zhang, K. Wu, Q. Fu, *Nanomicro Lett.* **2022**, *14*, 202.
[243] Z. Su, H. Wang, J. He, Y. Guo, Q. Qu, X. Tian, *ACS Appl. Mater. Interfaces* **2018**, *10*, 36342.
[244] V. Varshney, J. Lee, J. S. Brown, B. L. Farmer, A. A. Voevodin, A. K. Roy, *Front. Mater.* **2018**, *5*, 17.
[245] J. Lao, H. Xie, Z. Shi, G. Li, B. Li, G.-H. Hu, Q. Yang, C. Xiong, *ACS Sustainable Chem. Eng.* **2018**, *6*, 7151.
[246] C. Liu, M. Chen, D. Zhou, D. Wu, W. Yu, *J. Nanomater.* **2017**, *2017*, 6375135.
[247] S. Moradi, Y. Calventus, F. Roman, J. M. Hutchinson, *Polymers* **2019**, *11*, 1156.
[248] L. Ren, X. Zeng, R. Sun, J.-B. Xu, C.-P. Wong, *Chem. Eng. J.* **2019**, *370*, 166.
[249] Y.-J. Wan, G. Li, Y.-M. Yao, X.-L. Zeng, P.-L. Zhu, R. Sun, *Compos. Commun.* **2020**, *19*, 154.
[250] Z. Xu, Y. Chen, X. Chen, J. Zhang, S. Huang, A. Chen, X. Fu, F. Wu, P. Zhang, *J. Mater. Sci.* **2020**, *56*, 4225.
[251] Y.-j. Xiao, W.-y. Wang, T. Lin, X.-j. Chen, Y.-t. Zhang, J.-h. Yang, Y. Wang, Z.-w. Zhou, *J. Phys. Chem. C* **2016**, *120*, 6344.
[252] C. Xiao, L. Chen, Y. Tang, X. Zhang, K. Zheng, X. Tian, *Composites, Part A* **2019**, *116*, 98.
[253] X. Luo, G. Yang, D. W. Schubert, *Adv. Compos. Hybrid Mater.* **2021**, *5*, 250.
[254] H. Yan, X. Dai, K. Ruan, S. Zhang, X. Shi, Y. Guo, H. Cai, J. Gu, *Adv. Compos. Hybrid Mater.* **2021**, *4*, 36.
[255] F. Jiang, S. Cui, N. Song, L. Shi, P. Ding, *ACS Appl. Mater. Interfaces* **2018**, *10*, 16812.
[256] C. Xiao, Y. Guo, Y. Tang, J. Ding, X. Zhang, K. Zheng, X. Tian, *Composites, Part B* **2020**, *187*, 107855.
[257] B. Wu, R. Chen, R. Fu, S. Agathopoulos, X. Su, H. Liu, *Composites, Part A* **2020**, *137*, 105993.
[258] X. Wang, P. Wu, *ACS Appl. Mater. Interfaces* **2017**, *9*, 19934.
[259] J. Han, G. Du, W. Gao, H. Bai, *Adv. Funct. Mater.* **2019**, *29*, 1900412.
[260] Y. Lin, J. Chen, P. Jiang, X. Huang, *Chem. Eng. J.* **2020**, *389*, 123467.
[261] Y. Lin, J. Chen, S. Dong, G. Wu, P. Jiang, X. Huang, *J. Mater. Sci. Technol.* **2021**, *83*, 219.
[262] F. An, X. Li, P. Min, H. Li, Z. Dai, Z.-Z. Yu, *Carbon* **2018**, *126*, 119.
[263] J. Hu, Y. Huang, X. Zeng, Q. Li, L. Ren, R. Sun, J.-B. Xu, C.-P. Wong, *Compos. Sci. Technol.* **2018**, *160*, 127.
[264] Y. Guo, S. Wang, K. Ruan, H. Zhang, J. Gu, *npj Flexible Electron.* **2021**, *5*, 16.
[265] J. Hu, Y. Huang, Y. Yao, G. Pan, J. Sun, X. Zeng, R. Sun, J. B. Xu, B. Song, C. P. Wong, *ACS Appl. Mater. Interfaces* **2017**, *9*, 13544.
[266] A. Li, C. Zhang, Y.-F. Zhang, *Composites, Part A* **2017**, *101*, 108.
[267] H.-B. Cho, T. Nakayama, H. Suematsu, T. Suzuki, W. Jiang, K. Niihara, E. Song, N. S. A. Eom, S. Kim, Y.-H. Choa, *Compos. Sci. Technol.* **2016**, *129*, 205.
[268] Y. Zhan, Z. Long, X. Wan, C. Zhan, J. Zhang, Y. He, *Ceram. Int.* **2017**, *43*, 12109.
[269] C. Du, M. Li, M. Cao, S. Song, S. Feng, X. Li, H. Guo, B. Li, *ACS Appl. Mater. Interfaces* **2018**, *10*, 34674.
[270] Y. Yao, X. Zeng, R. Sun, J. B. Xu, C. P. Wong, *ACS Appl. Mater. Interfaces* **2016**, *8*, 15645.
[271] L. Yang, L. Zhang, C. Li, *Compos. Sci. Technol.* **2020**, *200*, 108429.
[272] E. M. Remillard, Q. Zhang, S. Sosina, Z. Branson, T. Dasgupta, C. D. Vecitis, *Carbon* **2016**, *100*, 578.
[273] K. Kim, H. Ju, J. Kim, *Ceram. Int.* **2016**, *42*, 8657.
[274] P. Gupta, M. Rajput, N. Singla, V. Kumar, D. Lahiri, *Polymer* **2016**, *89*, 119.
[275] H. Guo, X. Li, B. Li, J. Wang, S. Wang, *Mater. Des.* **2017**, *114*, 355.
[276] W.-T. Ma, S. R. Kumar, C.-T. Hsu, C.-M. Shih, S.-W. Tsai, C.-C. Yang, Y.-L. Liu, S. J. Lue, *J. Membr. Sci.* **2018**, *563*, 259.
[277] Y. Kim, J. Kim, *Compos. Sci. Technol.* **2020**, *188*, 107961.
[278] Y. Guo, H. Qiu, K. Ruan, Y. Zhang, J. Gu, *Nanomicro Lett* **2021**, *14*, 26.
[279] H. Fang, S.-L. Bai, C. P. Wong, *Composites, Part A* **2018**, *112*, 216.
[280] T. Ma, Y. Zhao, K. Ruan, X. Liu, J. Zhang, Y. Guo, X. Yang, J. Kong, J. Gu, *ACS Appl. Mater. Interfaces* **2020**, *12*, 1677.
[281] Y. Yao, X. Zeng, F. Wang, R. Sun, J.-b. Xu, C.-P. Wong, *Chem. Mater.* **2016**, *28*, 1049.
[282] Z.-G. Wang, W. Liu, Y.-H. Liu, Y. Ren, Y.-P. Li, L. Zhou, J.-Z. Xu, J. Lei, Z.-M. Li, *Composites, Part B* **2020**, *180*, 107569.
[283] X. Shi, R. Zhang, K. Ruan, T. Ma, Y. Guo, J. Gu, *J. Mater. Sci. Technol.* **2021**, *82*, 239.
[284] Z. Su, H. Wang, X. Ye, K. Tian, W. Huang, J. He, Y. Guo, X. Tian, *Composites, Part A* **2018**, *109*, 402.
[285] K. Ruan, Y. Guo, Y. Tang, Y. Zhang, J. Zhang, M. He, J. Kong, J. Gu, *Compos. Commun.* **2018**, *10*, 68.
[286] Z. Zhu, C. Li, E. Songfeng, L. Xie, R. Geng, C.-T. Lin, L. Li, Y. Yao, *Compos. Sci. Technol.* **2019**, *170*, 93.
[287] Y. Li, X. Tian, W. Yang, Q. Li, L. Hou, Z. Zhu, Y. Tang, M. Wang, B. Zhang, T. Pan, Y. Li, *Chem. Eng. J.* **2019**, *358*, 718.
[288] X. Hu, C. Zhu, H. Wu, X. Li, X. Lu, J. Qu, *Composites, Part A* **2022**, *154*, 106770.
[289] M. Owais, J. Zhao, A. Imani, G. Wang, H. Zhang, Z. Zhang, *Composites, Part A* **2019**, *117*, 11.
[290] X. Zhang, J. Dong, D. Pan, G. Yang, F. Su, Y. Ji, C. Liu, C. Shen, *Adv. Compos. Hybrid Mater.* **2021**, *4*, 1102.
[291] M. Yang, X. Wang, R. Wang, S. Qi, *J. Mater. Sci.: Mater. Electron.* **2017**, *28*, 16141.
[292] J. Dong, L. Cao, Y. Li, Z. Wu, C. Teng, *Compos. Sci. Technol.* **2020**, *196*, 108242.
[293] N. Yang, C. Xu, J. Hou, Y. Yao, Q. Zhang, M. E. Grami, L. He, N. Wang, X. Qu, *RSC Adv.* **2016**, *6*, 18279.
[294] F. Jiang, X. Cui, N. Song, L. Shi, P. Ding, *Compos. Commun.* **2020**, *20*, 100350.
[295] Y. Yao, J. Sun, X. Zeng, R. Sun, J. B. Xu, C. P. Wong, *Small* **2018**, *14*, 1704044.
[296] W. Yu, J. Fu, L. Chen, P. Zong, J. Yin, D. Shang, Q. Lu, H. Chen, L. Shi, *Compos. Sci. Technol.* **2016**, *125*, 90.
[297] P.-G. Ren, S.-Y. Hou, F. Ren, Z.-P. Zhang, Z.-F. Sun, L. Xu, *Composites, Part A* **2016**, *90*, 13.
[298] Y. Kim, H. Oh, J. Kim, *Ceram. Int.* **2019**, *45*, 24121.

© 2023 Wiley-VCH GmbH

16163028, 0, Downloaded from https://onlinelibrary.wiley.com/doi/10.1002/adfm.202301549 by University of California - Los Ange, Wiley Online Library on [16/06/2023]. See the Terms and Conditions (https://onlinelibrary.wiley.com/terms-and-conditions) on Wiley Online Library for rules of use; OA articles are governed by the applicable Creative Commons License

[299] J. Gu, C. Liang, J. Dang, W. Dong, Q. Zhang, *RSC Adv.* **2016**, *6*, 35809.
[300] A. Xie, Y. Wang, P. Jiang, S. Li, X. Huang, *Compos. Sci. Technol.* **2018**, *154*, 154.
[301] Y. Liu, Y. Fang, X. Liu, X. Wang, B. Yang, *Compos. Sci. Technol.* **2017**, *151*, 164.
[302] J.-H. Ding, H.-R. Zhao, H.-B. Yu, *2D Mater.* **2018**, *5*, 045015.
[303] C. Pan, K. Kou, Q. Jia, Y. Zhang, G. Wu, T. Ji, *Composites, Part B* **2017**, *111*, 83.
[304] Y. Jiang, Y. Liu, P. Min, G. Sui, *Compos. Sci. Technol.* **2017**, *144*, 63.
[305] X. Yang, L. Tang, Y. Guo, C. Liang, Q. Zhang, K. Kou, J. Gu, *Composites, Part A* **2017**, *101*, 237.
[306] P. Zhang, J. Zhao, K. Zhang, R. Bai, Y. Wang, C. Hua, Y. Wu, X. Liu, H. Xu, Y. Li, *Composites, Part A* **2016**, *84*, 428.
[307] C. Struzzi, M. Scardamaglia, N. Reckinger, J.-F. Colomer, H. Sezen, M. Amati, L. Gregoratti, R. Snyders, C. Bittencourt, *Nano Res.* **2017**, *10*, 3151.
[308] H. Han, H. Sun, F. Lei, J. Huang, S. Lyu, B. Wu, M. Yang, C. Zhang, D. Li, Z. Zhang, D. Sun, *ES Mater. Manuf.* **2022**, *15*, 53.
[309] X. Wang, P. Wu, *ACS Appl. Mater. Interfaces* **2019**, *11*, 21946.
[310] W. Qiu, W. Lin, Y. Tuersun, M. Ou, S. Chu, *Adv. Mater. Interfaces* **2021**, *8*, 2002187.
[311] V. Guerra, C. Wan, T. McNally, *Prog. Mater. Sci.* **2019**, *100*, 170.
[312] Z. Su, H. Wang, X. Ye, K. Tian, W. Huang, C. Xiao, X. Tian, *Composites, Part A* **2017**, *99*, 166.
[313] Y. Xie, Y. Yu, Y. Feng, W. Jiang, Z. Zhang, *ACS Appl. Mater. Interfaces* **2017**, *9*, 2995.
[314] Z.-G. Wang, M.-Z. Chen, Y.-H. Liu, H.-J. Duan, L. Xu, L. Zhou, J.-Z. Xu, J. Lei, Z.-M. Li, *J. Mater. Chem. C* **2019**, *7*, 9018.
[315] D. Yang, Y. Ni, X. Kong, D. Gao, Y. Wang, T. Hu, L. Zhang, *Compos. Sci. Technol.* **2019**, *177*, 18.
[316] Y. Liu, K. Wu, F. Luo, M. Lu, F. Xiao, X. Du, S. Zhang, L. Liang, M. Lu, *Composites, Part A* **2019**, *117*, 134.
[317] D. Ding, Z. Shang, X. Zhang, X. Lei, Z. Liu, Q. Zhang, Y. Chen, *Ceram. Int.* **2020**, *46*, 28363.
[318] T. Morishita, H. Okamoto, *ACS Appl. Mater. Interfaces* **2016**, *8*, 27064.
[319] J. Luo, F. Zhao, X. Fei, X. Liu, J. Liu, *Chem. Eng. J.* **2016**, *293*, 171.
[320] R. C. Zhang, D. Sun, A. Lu, S. Askari, M. Macias-Montero, P. Joseph, D. Dixon, K. Ostrikov, P. Maguire, D. Mariotti, *ACS Appl. Mater. Interfaces* **2016**, *8*, 13567.
[321] X. Huang, C. Zhi, Y. Lin, H. Bao, G. Wu, P. Jiang, Y.-W. Mai, *Mater. Sci. Eng., R* **2020**, *142*, 100577.
[322] T.-Y. Wang, J.-L. Tsai, *Comput. Mater. Sci.* **2016**, *122*, 272.
[323] Y. Wang, C. Yang, Y.-W. Mai, Y. Zhang, *Carbon* **2016**, *102*, 311.
[324] L. Jing, H. Li, R. Y. Tay, B. Sun, S. H. Tsang, O. Cometto, J. Lin, E. H. T. Teo, A. I. Y. Tok, *ACS Nano* **2017**, *11*, 3742.
[325] E. A. M. Hassan, L. Yang, T. H. H. Elagib, D. Ge, X. Lv, J. Zhou, M. Yu, S. Zhu, *Composites, Part B* **2019**, *171*, 70.
[326] H. Fang, Y. Zhao, Y. Zhang, Y. Ren, S. L. Bai, *ACS Appl. Mater. Interfaces* **2017**, *9*, 26447.
[327] Z.-G. Wang, Y.-L. Yang, Z.-L. Zheng, R.-T. Lan, K. Dai, L. Xu, H.-D. Huang, J.-H. Tang, J.-Z. Xu, Z.-M. Li, *Compos. Sci. Technol.* **2020**, *194*, 108190.
[328] K. Wu, P. Liao, R. Du, Q. Zhang, F. Chen, Q. Fu, *J. Mater. Chem. A* **2018**, *6*, 11863.
[329] M. M. Bernal, A. Di Pierro, C. Novara, F. Giorgis, B. Mortazavi, G. Saracco, A. Fina, *Adv. Funct. Mater.* **2018**, *28*, 1706954.
[330] C. Fu, C. Yan, L. Ren, X. Zeng, G. Du, R. Sun, J. Xu, C.-P. Wong, *Compos. Sci. Technol.* **2019**, *177*, 118.
[331] J. Chen, X. Huang, Y. Zhu, P. Jiang, *Adv. Funct. Mater.* **2017**, *27*, 1604754.
[332] X. Jiang, P. Ma, F. You, C. Yao, J. Yao, F. Liu, *RSC Adv.* **2018**, *8*, 32132.
[333] H. Shen, C. Cai, J. Guo, Z. Qian, N. Zhao, J. Xu, *RSC Adv.* **2016**, *6*, 16489.
[334] X. Hou, Y. Chen, L. Lv, W. Dai, S. Zhao, Z. Wang, L. Fu, C.-T. Lin, N. Jiang, J. Yu, *ACS Appl. Nano Mater.* **2019**, *2*, 360.
[335] D. Pan, J. Dong, G. Yang, F. Su, B. Chang, C. Liu, Y.-C. Zhu, Z. Guo, *Adv. Compos. Hybrid Mater.* **2021**, *5*, 58.
[336] D. Pan, G. Yang, H. M. Abo-Dief, J. Dong, F. Su, C. Liu, Y. Li, B. Bin Xu, V. Murugadoss, N. Naik, S. M. El-Bahy, Z. M. El-Bahy, M. Huang, Z. Guo, *Nano-Micro Lett.* **2022**, *14*, 118.
[337] Y. Lu, J. Cao, S. Ren, W. Gao, H. Chen, S. Chen, X. Yan, S. Xin, J. Li, Y. Bai, *Compos. Sci. Technol.* **2021**, *201*, 108536.
[338] Y. Li, W. Wei, Y. Wang, N. Kadhim, Y. Mei, Z. Zhou, *J. Mater. Chem. C* **2019**, *7*, 11783.
[339] Z. Li, J. Kong, D. Ju, Z. Cao, L. Han, L. Dong, *Compos. Sci. Technol.* **2017**, *149*, 185.
[340] J. Chen, X. Cui, Y. Zhu, W. Jiang, K. Sui, *Carbon* **2017**, *114*, 441.
[341] R. Wang, H. Cheng, Y. Gong, F. Wang, X. Ding, R. Hu, X. Zhang, J. He, X. Tian, *ACS Appl. Mater. Interfaces* **2019**, *11*, 42818.
[342] K. Kim, J. Kim, *Compos. Sci. Technol.* **2016**, *134*, 209.
[343] X. Zhang, K. Wu, Y. Liu, B. Yu, Q. Zhang, F. Chen, Q. Fu, *Compos. Sci. Technol.* **2019**, *175*, 135.
[344] X. Leng, C. Xiao, L. Chen, Z. Su, K. Zheng, X. Zhang, X. Tian, *High Perform. Polym.* **2019**, *31*, 350.
[345] B. Shan, G. Yuan, H. Li, J. Liu, *Jpn. J. Appl. Phys.* **2019**, *58*, SHHH01.
[346] X. Shen, Z. Wang, Y. Wu, X. Liu, Y.-B. He, Q. Zheng, Q.-H. Yang, F. Kang, J.-K. Kim, *Mater. Horiz.* **2018**, *5*, 275.
[347] T. Ji, Y. Feng, M. Qin, S. Li, F. Zhang, F. Lv, W. Feng, *Carbon* **2018**, *131*, 149.
[348] J. Chen, H. Wei, H. Bao, P. Jiang, X. Huang, *ACS Appl. Mater. Interfaces* **2019**, *11*, 31402.
[349] L. Bai, S. Zheng, R. Bao, Z. Liu, M. Yang, W. Yang, *ES Mater. Manuf.* **2019**, *3*, 66.
[350] Y. Guo, K. Ruan, X. Shi, X. Yang, J. Gu, *Compos. Sci. Technol.* **2020**, *193*, 108134.
[351] F. E. Alam, W. Dai, M. Yang, S. Du, X. Li, J. Yu, N. Jiang, C.-T. Lin, *J. Mater. Chem. A* **2017**, *5*, 6164.
[352] W. Dai, T. Ma, Q. Yan, J. Gao, X. Tan, L. Lv, H. Hou, Q. Wei, J. Yu, J. Wu, Y. Yao, S. Du, R. Sun, N. Jiang, Y. Wang, J. Kong, C. Wong, S. Maruyama, C. T. Lin, *ACS Nano* **2019**, *13*, 11561.
[353] M. Seong, I. Hwang, S. Park, H. Jang, G. Choi, J. Kim, S. K. Kim, G. H. Kim, J. Yeo, H. E. Jeong, *Adv. Funct. Mater.* **2021**, *31*, 2107023.
[354] C. Guo, Y. Li, J. Xu, Q. Zhang, K. Wu, Q. Fu, *Mater. Horiz.* **2022**, *9*, 1690.
[355] Q. Yan, F. E. Alam, J. Gao, W. Dai, X. Tan, L. Lv, J. Wang, H. Zhang, D. Chen, K. Nishimura, L. Wang, J. Yu, J. Lu, R. Sun, R. Xiang, S. Maruyama, H. Zhang, S. Wu, N. Jiang, C. T. Lin, *Adv. Funct. Mater.* **2021**, *31*, 2104062.
[356] L. Cai, J. Fan, S. Ding, D. He, X. Zeng, R. Sun, L. Ren, J. Xu, X. Zeng, *Adv. Funct. Mater.* **2023**, *33*, 2207143.
[357] X. Jing, Y. Li, J. Zhu, L. Chang, S. Maganti, N. Naik, B. B. Xu, V. Murugadoss, M. Huang, Z. Guo, *Adv. Compos. Hybrid Mater.* **2022**, *5*, 1090.
[358] J. Wang, Q. Li, D. Liu, C. Chen, Z. Chen, J. Hao, Y. Li, J. Zhang, M. Naebe, W. Lei, *Nanoscale* **2018**, *10*, 16868.
[359] T. Wang, M. Wang, L. Fu, Z. Duan, Y. Chen, X. Hou, Y. Wu, S. Li, L. Guo, R. Kang, N. Jiang, J. Yu, *Sci. Rep.* **2018**, *8*, 1557.
[360] M. Cao, C. Du, H. Guo, S. Song, X. Li, B. Li, *Compos. Sci. Technol.* **2019**, *173*, 33.
[361] L. Altay, M. Atagur, K. Sever, I. Sen, T. Uysalman, Y. Seki, M. Sarikanat, *Polym. Compos.* **2019**, *40*, 277.
[362] B. Wen, X. Zheng, *Compos. Sci. Technol.* **2019**, *174*, 68.
[363] H. S. Kim, H. S. Bae, J. Yu, S. Y. Kim, *Sci. Rep.* **2016**, *6*, 26825.
[364] Q. Chi, T. Ma, J. Dong, Y. Cui, Y. Zhang, C. Zhang, S. Xu, X. Wang, Q. Lei, *Sci. Rep.* **2017**, *7*, 3072.
[365] H. Oh, J. Kim, *Compos. Sci. Technol.* **2019**, *172*, 153.

© 2023 Wiley-VCH GmbH

16163028, 0, Downloaded from https://onlinelibrary.wiley.com/doi/10.1002/adfm.202301549 by University of California - Los Ange, Wiley Online Library on [16/06/2023]. See the Terms and Conditions (https://onlinelibrary.wiley.com/terms-and-conditions) on Wiley Online Library for rules of use; OA articles are governed by the applicable Creative Commons License

[366] S. Waheed, J. M. Cabot, P. Smejkal, S. Farajikhah, S. Sayyar, P. C. Innis, S. Beirne, G. Barnsley, T. W. Lewis, M. C. Breadmore, B. Paull, *ACS Appl. Mater. Interfaces* **2019**, *11*, 4353.
[367] H. Guo, H. Zhao, H. Niu, Y. Ren, H. Fang, X. Fang, R. Lv, M. Maqbool, S. Bai, *ACS Nano* **2021**, *15*, 6917.
[368] T.-B. Ma, H. Ma, K.-P. Ruan, X.-T. Shi, H. Qiu, S.-Y. Gao, J.-W. Gu, *Chin. J. Polym. Sci.* **2022**, *40*, 248.
[369] Y. Jia, H. He, Y. Geng, B. Huang, X. Peng, *Compos. Sci. Technol.* **2017**, *145*, 55.
[370] J. Chen, X. Huang, B. Sun, Y. Wang, Y. Zhu, P. Jiang, *ACS Appl. Mater. Interfaces* **2017**, *9*, 30909.
[371] Z. Li, Q. Yin, W. Hu, J. Zhang, J. Guo, J. Chen, T. Sun, C. Du, J. Shu, L. Yu, J. Zhang, *J. Mater. Sci.* **2019**, *54*, 9025.
[372] D.-L. Zhang, J.-W. Zha, W.-K. Li, C.-Q. Li, S.-J. Wang, Y. Wen, Z.-M. Dang, *Compos. Sci. Technol.* **2018**, *156*, 1.
[373] X. Yang, Y. Guo, Y. Han, Y. Li, T. Ma, M. Chen, J. Kong, J. Zhu, J. Gu, *Composites, Part B* **2019**, *175*, 107070.
[374] B. Lin, Z.-T. Li, Y. Yang, Y. Li, J.-C. Lin, X.-M. Zheng, F.-A. He, K.-H. Lam, *Compos. Sci. Technol.* **2019**, *172*, 58.
[375] Y. Guo, L. Pan, X. Yang, K. Ruan, Y. Han, J. Kong, J. Gu, *Composites, Part A* **2019**, *124*, 105484.
[376] D. Ding, H. Wang, Z. Wu, Y. Chen, Q. Zhang, *Macromol. Rapid Commun.* **2019**, *40*, 1800805.
[377] X. He, D. Ou, S. Wu, Y. Luo, Y. Ma, J. Sun, *Adv. Compos. Hybrid Mater.* **2021**, *5*, 21.
[378] Z.-G. Wang, Y.-F. Huang, G.-Q. Zhang, H.-Q. Wang, J.-Z. Xu, J. Lei, L. Zhu, F. Gong, Z.-M. Li, *Ind. Eng. Chem. Res.* **2018**, *57*, 10391.
[379] S. Uchida, T. Murakami, T. Iwamura, R. Ishige, S. Ando, *RSC Adv.* **2017**, *7*, 15492.
[380] A. Kotia, S. Borkakoti, P. Deval, S. K. Ghosh, *Heat Mass Transfer* **2017**, *53*, 2199.
[381] D. M. Panaitescu, R. A. Gabor, C. A. Nicolae, A. C. Parau, C. Vitelaru, V. Raditoiu, M. Chipara, *Polymers* **2018**, *10*, 46.
[382] J. Song, Y. Zhang, *Int. J. Heat Mass Transfer* **2019**, *141*, 1049.
[383] Y. Wen, C. Chen, Y. Ye, Z. Xue, H. Liu, X. Zhou, Y. Zhang, D. Li, X. Xie, Y. W. Mai, *Adv. Mater.* **2022**, *34*, 2201023.
[384] M. Ge, J. Zhang, C. Zhao, C. Lu, G. Du, *Mater. Des.* **2019**, *182*, 108028.
[385] F. Jiang, N. Song, R. Ouyang, P. Ding, *ACS Appl. Mater. Interfaces* **2021**, *13*, 7556.
[386] X. Huang, Y. Lin, G. Fang, *Sol. Energy* **2018**, *161*, 187.
[387] N. Kim, D. Kim, H. Kang, Y.-G. Park, *Energy* **2016**, *113*, 515.
[388] Y. Zhang, N. Hao, X. Lin, S. Nie, *Carbohydr. Polym.* **2020**, *234*, 115888.
[389] B. Lee, J. Z. Liu, B. Sun, C. Y. Shen, G. C. Dai, *eXPRESS Polym. Lett.* **2008**, *2*, 357.
[390] R. Huang, J. Xie, X. Wu, G. Zhang, X. Yang, *Energy Fuels* **2021**, *35*, 13466.
[391] J. Kim, J. Oh, H. Lee, *Appl. Therm. Eng.* **2019**, *149*, 192.
[392] J. Shi, D. Han, Z. Li, L. Yang, S.-G. Lu, Z. Zhong, J. Chen, Q. Zhang, X. Qian, *Joule* **2019**, *3*, 1200.
[393] G. Zhang, B. Fan, P. Zhao, Z. Hu, Y. Liu, F. Liu, S. Jiang, S. Zhang, H. Li, Q. Wang, *ACS Appl. Energy Mater.* **2018**, *1*, 1344.
[394] Y. Sargolzaeiaval, V. P. Ramesh, T. V. Neumann, V. Misra, D. Vashaee, M. D. Dickey, M. C. Öztürk, *Appl. Energy* **2020**, *262*, 114370.
[395] T. Gao, Z. Yang, C. Chen, Y. Li, K. Fu, J. Dai, E. M. Hitz, H. Xie, B. Liu, J. Song, *ACS Nano* **2017**, *11*, 11513.
[396] Y. Guo, C. Dun, J. Xu, J. Mu, P. Li, L. Gu, C. Hou, C. A. Hewitt, Q. Zhang, Y. Li, *Small* **2017**, *13*, 1702645.
[397] X. Zhang, X. Chao, L. Lou, J. Fan, Q. Chen, B. Li, L. Ye, D. Shou, *Compos. Commun.* **2021**, *23*, 100595.
[398] H.-Y. Zhao, M.-Y. Yu, J. Liu, X. Li, P. Min, Z.-Z. Yu, *Nano-Micro Lett.* **2022**, *14*, 129.
[399] H. Yu, C. Chen, J. Sun, H. Zhang, Y. Feng, M. Qin, W. Feng, *Nanomicro Lett.* **2022**, *14*, 135.
[400] H. Yu, Y. Feng, C. Chen, Z. Zhang, Y. Cai, M. Qin, W. Feng, *Carbon* **2021**, *179*, 348.

Zhengfang Wang is now pursuing a Master of Science degree at the School of Materials Science and Chemical Engineering at Harbin University of Science and Technology. She received her Bachelor of Science degree from Northwest Normal University in 2019. Her research focuses on polymer-based thermally conductive composites.

© 2023 Wiley-VCH GmbH

16163028, 0, Downloaded from https://onlinelibrary.wiley.com/doi/10.1002/adfm.202301549 by University of California - Los Ange, Wiley Online Library on [16/06/2023]. See the Terms and Conditions (https://onlinelibrary.wiley.com/terms-and-conditions) on Wiley Online Library for rules of use; OA articles are governed by the applicable Creative Commons License

Zijian Wu is an associate professor at Harbin University of Science and Technology. He obtained his Ph.D. degree in 2015 from Harbin Institute of Technology. He was a postdoc researcher in Key Laboratory of Engineering Dielectric and its Application Technology of Ministry of Education, Harbin University of Science and Technology, and a visiting student in General Motors Research-Development Center, United States. His researches focus on functional dielectric materials, polymer composites, and advanced electronic materials.

Shengbo Ge is currently an associate professor at the College of Materials Science and Engineering, Nanjing Forestry University. He received his Ph.D. in forestry engineering in 2020 at Central South University of Forestry and Technology. His current research interests include micro-nano structure regulation and recombination of wood cells, advanced biomass composite materials, and green and sustainable energy. Up to now, he has published more than 100 SCI papers.

Zhanhu Guo is a professor of mechanical & construction engineering at Northumbria University at Newcastle Upon Tyne in the UK. He held a professorship of chemical engineering at Lamar University (2008-2014) and the University of Tennessee at Knoxville (2015-2022) in USA. He has been actively doing research and education in the fields of composites and structural materials. His research outputs have generated broad impacts with a ranking of top 100 globally.

Ximin He is an associate professor of materials science and engineering at University of California, Los Angeles (UCLA) and the faculty of California Nanosystems Institute (CNSI). She was postdoctoral research fellow in the School of Engineering and Applied Science and the Wyss Institute of Bioinspired Engineering at Harvard University. She received her Ph,D. in chemistry at Melville Laboratory for Polymer Synthesis from the University of Cambridge. Her research focuses on bioinspired soft materials, structural polymers and their physical, mechanical, electrical and photothermal properties with broad applications in biomedicine, energy, environment, and robotics.

© 2023 Wiley-VCH GmbH

16163028, 0, Downloaded from https://onlinelibrary.wiley.com/doi/10.1002/adfm.202301549 by University of California - Los Ange, Wiley Online Library on [16/06/2023]. See the Terms and Conditions (https://onlinelibrary.wiley.com/terms-and-conditions) on Wiley Online Library for rules of use; OA articles are governed by the applicable Creative Commons License

Ben Bin Xu (FRSC, FIMMM, FRSA, FSCI) is a professor of materials and mechanics in the Department of Mechanical and Construction Engineering at Northumbria University, UK. Ben obtained his Ph.D. in mechanical engineering (2011) at Heriot-Watt University in Edinburgh, then moved to the University of Massachusetts, Amherst (US, 2011-2013) to work as postdoc. Since joining Northumbria in 2013, Ben has established a multidisciplinary research group with diverse interests in energy materials and technology, materials chemistry, responsive materials/surface, soft matter, mechanics, and micro-engineering.

© 2023 Wiley-VCH GmbH

16163028, 0, Downloaded from https://onlinelibrary.wiley.com/doi/10.1002/adfm.202301549 by University of California - Los Ange, Wiley Online Library on [16/06/2023]. See the Terms and Conditions (https://onlinelibrary.wiley.com/terms-and-conditions) on Wiley Online Library for rules of use; OA articles are governed by the applicable Creative Commons License